TAMPEREEN TEKNILLINEN YLIOPISTO

SONJA KALLIO

# MODELLING OF A COMBINED HEAT AND POWER SYSTEM

Master of Science Thesis

Examiner: Professor Risto Raiko
The examiner and topic approved at Faculty Council of the Faculty of Science and Environmental Engineering 15th August 2012

# TIIVISTELMÄ

TAMPEREEN TEKNILLINEN YLIOPISTO
Ympäristö- ja energiatekniikan koulutusohjelma
**KALLIO, SONJA**: Yhdistetyn sähkön- ja lämmöntuotanto yksikön mallintaminen
Diplomityö, 102 sivua, 7 liitesivua
Elokuu 2012
Pääaine: Voimalaitos- ja polttotekniikka
Tarkastaja: professori Risto Raiko
Avainsanat: Yhdistetty sähkön- ja lämmöntuotanto, pien- ja mikro-CHP, teknologia, sähköyhtiö, fysikaalinen malli, Matlab/Simulink, taloudelliset näkökulmat, lämmönkulutus, optimointi

Maailmanlaajuisesti kasvava energian kulutus johtaa ilmaston lämpenemiseen. Puhtailla ja tehokkailla energiantuotanto ratkaisuilla pyritän hidastamaan ilmastonmuutosta ja tehostamaan energiantuotantoa. Uusiutuvan energiantuotannon määrä kasvaa jatkuvasti ja on hyvin voimakkaasti riippuvainen vallitsevasta säätilasta. Tämän vuoksi uusiutuvaa energiantuotantoa tukevan ja nopean energiantuotannon tarve kasvaa. Sähkön kulutus kasvaa myös jatkuvasti, joka johtaa suurempiin huippukulutuksiin ja sähkönsiirto- ja jakelukapasiteetin supistumiseen. Tämä vaatii enemmän nopean varavoiman käyttöä sekä hajautettua energiantuotanto. Yhdistetty sähkön- ja lämmöntuotanto (CHP) on sähkön ja lämmön yhteistuotantoa yhdestä polttoainelähteestä erinomaisella kokonaishyötysuhteella. Suuri määrä pieniä ja hajautettuja polttomoottori teknologiaan perustuvia CHP yksiköitä voi tuottaa energiaa nopeasti tukemaan uusiutuvia energianlähteitä. Samanaikaisesti voidaan tuottaa lämpöä erilaisiin lämmönkulutuskohteisiin, kuten asuin- ja liikerakennuksiin. Mahdolliset lämmönkulutuskohteet ovat hajautuneet, joka johtaa hajautettuun energiantuotantoon. Tällöin pienvoimalat tuottavat energiaa jakeluverkkotasolla suurten siirtoverkkotasolla olevien voimaloiden sijaan. Tässä työssä mallinnetaan ja tutkitaan pienen CHP yksikön toimintaa uuden konseptin alla, jossa sähköyhtiö voi kauko-ohjata yksiköitä, jotka ovat sijoitettu lämmönkulutuskohteisiin. Näin voidaan saavuttaa taloudellinen hyöty monista kauko-ohjattavasti CHP yksiköistä ja energia voidaan tuottaa mahdollisemman lähellä kulutusta tukemaan uusiutuvia energianlähteitä.

Työ jakaantuu kahteen osaan. Kirjallisuustutkimusosassa tutustutaan yhdistettyyn sähkön- ja lämmöntuotantoon sekä käydään läpi potentiaaliset teknologiat pien- ja mikro-CHP yksiköille. Lopuksi esitellään tulokset markkinatutkimuksesta, jossa selvitettiin markkinoilta saatavia moottori teknologiaan perustuvia pien- ja micro-CHP yksiköitä. Työn toisessa osassa esitellään tutkimuksessa käytetyt menetelmät ja CHP yksikön mallinnusta Matlab/Simulink ympäristössä. Yksikön käyttäytymistä tutkittiin mallin avulla ja tulokset keskusteluineen käydään läpi. Lopuksi esitellään optimointiongelma, menetelmät ja tulokset.

Tulokset osoittivat, että pienen CHP yksikön toiminta vapailla sähkömarkkinoilla on taloudellisesti kannattavaa sähköyhtiölle. Tämä kuitenkin vaatii riittävän suuren lämpövaraston, joka mahdollistaa pitkän varastointiajan ja operoinnin vain korkean sähkönhinnan aikana. Tämä mahdollistaa myös nopean varavoiman tuotannon tukemaan uusiutuvia energiantuotanto menetelmiä ja sähköverkkoa. Suuren lämpövaraston avulla pystytään yhdistämään lämmön- ja sähkönkysyntää seuraava operointi. Tähän asti operointi on pääasiassa seurannut lämmönkysyntää ja sähkö on tuotettu sivutuotteena.

# ABSTRACT

TAMPERE UNIVERSITY OF TECHNOLOGY
Master's Degree Program in Environmental and Energy Technology
**KALLIO, SONJA**: Modelling of a combined heat and power system
Master of Science Thesis, 102 pages, 7 Appendix pages
August 2012
Major: Power Plant and Combustion Technology
Examiner: Professor Risto Raiko
Keywords: Combined heat and power, small- and micro CHP, prime movers, power- and heat-driven, thermal storage, electricity utility, physical model, economical aspects, heat demand, Matlab/Simulink, optimization

Due to rising global demands for energy and growing concerns about the accelerating greenhouse effect, efficient and clean energy generation is increasingly under a spotlight. At the moment and in the future the weather depending renewable energy production is increasing. This growth leads to higher demand for fast balancing energy production during unfavorable generation conditions. Additionally, overall electricity consumption is increasing which results in higher peak loads and decreasing transmission and distribution capacity in the electric grid. This requires more fast support for the grid and decentralized energy production. Combined heat and power (CHP) is the simultaneously generation of electricity and useful heat from a single fuel source at high efficiency. A high number of small internal combustion engine based CHP units can provide fast balancing energy, due to good dynamic behaviour, and simultaneously heat for heat sinks, such as residential and commercial buildings. The distributed structure of the heat sinks leads to a transformation towards a decentralized energy system in which small-scale distributed generation is connected to the distribution network instead of large central generators connected to the transmission network. This thesis models and examines a small CHP system operation under a new concept where the electricity utility can remote control a contracted CHP units within different heat sinks and gain a benefit by generating electricity during unfavourable weather conditions and peak loads. The main goal of this thesis was to construct a single CHP system model into the Matlab/Simulink and investigate the behaviour of the system.

The thesis is divided into two parts. In the literature study part, combined heat and power and different prime movers are introduced. Additionally, different CHP configurations and components are presented. Finally, the market research was conducted and market available internal combustion based small- and micro CHP units were introduced. In the second part, the model construction methodology was presented and results of two test cases were discussed. Finally, the optimization was performed using the model.

The result indicates that small CHP operation on the liberalized electricity market is profitable from the electricity utility point of view. In this case the CHP unit requires large thermal storage which enables long storage time and operation only during the high electricity price. This enables also to provide fast balancing energy for weather depending renewables energies and support for the grid during peak loads. The large storage decouples heat- and power driven CHP system because it can respond to both demand with the storage. Until now the heat-driven systems have been commonly used and electricity is produced as a by-product.

## ACKNOWLEDGEMENTS

I would like to show my gratitude to Professor Konstantinos Boulouchos for his advice on my thesis and for this possibility to conduct my Master Thesis in his Laboratory of Aerothermochemistry and Combustion Systems. I would like to thank my supervisor Philipp Vögelin for his support, guidance, and understanding and for his advice throughout the thesis. I would like to thank also Fabrizio Noembrini for his support to find interesting Master Thesis. I am also thankful to Niko Heeren, Institute of Construction and Infrastructure Management, for his time and advice.

I would like to show my gratitude also to Professor Risto Raiko for his valuable support to make it possible to conduct my Master Thesis at ETH Zurich, Switzerland. From this opportunity I have gained significant experience for my life and future.

Finally, I want to thank my family in Finland for continuous support provided during my Master Thesis. Without you this adventure would not have been possible. The last and greatest acknowledge I want to show to Jukka Vastaranta for his irreplaceable support during each day on this journey which has both taken and also given a lot.

# TABLE OF CONTENT

# NOMENCLATURE

| | |
|---|---|
| $A_{CHP}$ | External area of the CHP unit, $[m^2]$ |
| $A_{HS}$ | External area of the heat store, $[m^2]$ |
| $C_{Fuel}$ | Fuel costs, [CHF] |
| $c_{Main\_overhaul}$ | Specific main overhaul costs of the CHP unit, $[\frac{\text{CHF}}{kW_e}]$ |
| $C_{O\&M}$ | Operating & Maintenance costs, [CHF] |
| $c_{pEG}$ | Specific heat capacity of the exhaust gas, $\left[\frac{\text{J}}{kgK}\right]$ |
| $c_{pW}$ | Specific heat capacity of water, $\left[\frac{\text{J}}{kgK}\right]$ |
| $d_{TS}$ | Diameter of the thermal storage, [m] |
| $E_{charged}$ | Charger heat to the thermal storage by a CHP unit, [J] |
| $E_{demand\_charging}$ | Heat demand over charging time, [J] |
| $E_{demand\_storage\_time}$ | Heat demand over storage time, [J] |
| $E_{el}$ | Total generated electric energy over simulation time, [J] |
| $E_{fuel}$ | Total fuel energy input over simulation time, [J] |
| $E_{th}$ | Total generated thermal energy over simulation time, [J] |
| $E_{th_{DHW}}$ | Thermal energy demand for domestic hot water, [J] |
| $E_{th_{sp}}$ | Thermal energy demand for space heating, [J] |
| $E_{total\_heat\_demand}$ | Total heat demand of the heat sink over year, [kWh] |
| $Ex_{destroyed}$ | Exergy destroyed in the system, [kW] |
| $Ex_{EC\_in}$ | Exergy of engine cooling flow in, [kW] |
| $Ex_{EC\_out}$ | Exergy of engine cooling flow out, [kW] |
| $Ex_{EG}$ | Exergy of the exhaust gas flow, [kW] |
| $Ex_{TS}$ | Exergy content of the thermal storage, [kW] |
| $Ex_{in}$ | Exergy in the system, [kW] |
| $Ex_{out}$ | Exergy out of the system, [kW] |
| $\Delta Ex_{system}$ | Change in exergy of a system, [kW] |
| $e_{fuel}$ | Specific flow exergy of fuel, $\left[\frac{\text{kJ}}{\text{kg}}\right]$ |
| $h$ | Specific in, out and dead state enthalpy, $\left[\frac{\text{kJ}}{\text{kg}}\right]$ |
| $h_{c,i}$ | The convective heat transfer coefficient inside, $\left[\frac{\text{W}}{m^2K}\right]$ |
| $h_{c,o}$ | The convective heat transfer coefficient outside, $\left[\frac{\text{W}}{m^2K}\right]$ |
| $h_{op}$ | Operating hours of the CHP unit, [h] |
| $h_{r,o}$ | The radiation heat transfer coefficient, $\left[\frac{\text{W}}{m^2K}\right]$ |
| $h_{TS}$ | Height of the thermal storage, [m] |
| $I_{Electricity}$ | Incomes from electricity, [CHF] |
| $I_{Heat}$ | Incomes from heat, [CHF] |

| | |
|---|---|
| $k_{inside}$ | The conductivity coefficient inside, $[\frac{\mathrm{W}}{mK}]$ |
| $k_{insulation}$ | The conductivity coefficient insulation, $[\frac{\mathrm{W}}{mK}]$ |
| $k_{outside}$ | The conductivity coefficient outside, $[\frac{\mathrm{W}}{mK}]$ |
| $L_{inside}$ | Thickness of inside wall, [m] |
| $L_{insulation}$ | Thickness of insulation, [m] |
| $L_{outside}$ | Thickness of outside wall, [m] |
| $LHV$ | Lower heating value of fuel, $\left[\frac{\mathrm{J}}{\mathrm{kg}}\right]$ |
| $m_{DHW}$ | Required domestic hot water mass flow, $\left[\frac{\mathrm{l}}{\mathrm{h}}\right]$ |
| $m_{dot\_EG}$ | Mass flow of the exhaust gas, $\left[\frac{\mathrm{kg}}{\mathrm{h}}\right]$ |
| $m_{dot\_fuel}$ | Fuel mass flow, $\left[\frac{\mathrm{kg}}{\mathrm{h}}\right]$ |
| $m_{dot_{water}}$ | Mass flow through the CHP unit, $\left[\frac{\mathrm{kg}}{\mathrm{h}}\right]$ |
| $m_{TS}$ | Mass of water in the thermal storage, [kg] |
| $NPV$ | The net present value, [CHF] |
| $P_e$ | Electrical power the CHP unit, [ kW ] |
| $P_{Electricity}$ | Electricity price, $\left[\frac{\mathrm{CHF}}{kWh_{el}}\right]$ |
| $P_{fuel}$ | Fuel power, [kW ] |
| $Pr_{Fuel}$ | Fuel price, $\left[\frac{\mathrm{CHF}}{\mathrm{kWh\_fuel}}\right]$ |
| $Pr_{Heat}$ | Heat price, $\left[\frac{\mathrm{CHF}}{kWh_{th}}\right]$ |
| $P_{mech}$ | Mechanical power of the CHP unit, [ kW ] |
| $Pr_{O\&M}$ | Operating & Maintenance costs, $\left[\frac{\mathrm{CHF}}{kWh_{el}}\right]$ |
| $P_{yearly}$ | Yearly profit, [CHF] |
| $PES$ | Primary energy saving |
| $T_{TS}$ | Temperature in the thermal storage, [K] |
| $Q_{CHP}$ | Heat addition from the CHP unit, [ J] |
| $Q_{CHP\_losses}$ | Heat losses from the CHP unit, [ W ] |
| $Q_{DHW}$ | Charged heat for hot domestic water, [ J ] |
| $Q_{Engine\_cooling}$ | Heat removed from the engine cooling circuit, [ J ] |
| $Q_{Exhaust\_gas}$ | Heat removed from the exhaust gas, [ J] |
| $Q_{Heat\_demand}$ | Charged heat from the thermal storage: space heating and domestic hot water demand, [ J] |
| $Q_{Heat\_losses}$ | Heat losses from the thermal storage and CHP unit, [ W ] |
| $Q_{TS\_losses}$ | Heat losses from the thermal storage, [ W] |
| $r$ | Discount rate, [%] |
| $S$ | Investment, [CHF] |
| $s_{CHP\_unit}$ | Specific investment costs of the CHP unit, $[\frac{\mathrm{CHF}}{kW_e}]$ |

| | |
|---|---|
| $s_{TS}$ | Specific investment of the thermal storage, $[\frac{\text{CHF}}{m^3}]$ |
| $S_{gen}$ | Generate entropy, $\left[\frac{\text{kJ}}{\text{K}}\right]$ |
| $s$ | Specific in, out and dead state entropy, $\left[\frac{\text{kJ}}{\text{kgK}}\right]$ |
| $T_{ambient}$ | Ambient temperature around the system, [K] |
| $T_{CHP_{inside}}$ | Temperature inside a CHP unit, [K] |
| $T_{EC_{HX_{out}}}$ | Outlet temperature of the engine cooling heat exchanger, [K] |
| $T_{EG}$ | Temperature of the exhaust gas, [K] |
| $T_{EG_{HX_{out}}}$ | Outlet temperature of the exhaust gas heat exchanger, [K] |
| $T_i$ | Inlet temperature of domestic hot water, [K] |
| $T_m$ | The mean temperature, [K] |
| $T_w$ | Temperature of domestic hot water, [K] |
| $T_0$ | Dead state temperature, [K] |
| $\Delta T_{TS}$ | Maximum allowed temperature difference in the thermal storage, [K] |
| $t$ | A number of years |
| $U_{CHP}$ | U-value of the surface of a thermal storage, $\left[\frac{\text{W}}{m^2K}\right]$ |
| $U_{HS}$ | U-value of the surface of a CHP unit, $\left[\frac{\text{W}}{m^2K}\right]$ |
| $V_{TS}$ | Volume of the thermal storage, $[m^3]$ |
| $W_{dot_{net}}$ | Net electric power generated by the CHP unit, [kW] |
| $\varepsilon$ | Effectiveness of the exhaust gas heat exchanger |
| $\varepsilon_{surface}$ | The emittance of the surface |
| $\sigma$ | Stefan-Boltzmann constant, $\left[\frac{\text{W}}{m^2K^4}\right]$ |
| $\eta_{Ex\_CHP}$ | Exergy efficiency of the CHP unit |
| $\eta_{Ex\_EC\_HX}$ | Exergy efficiency of the engine cooling heat exchanger |
| $\eta_{Ex\_EG\_HX}$ | Exergy efficiency of the exhaust gas heat exchanger |
| $\eta_{Ex\_ICE}$ | Exergy efficiency of the internal combustion engine |
| $\eta_e$ | Electrical efficiency of the CHP unit |
| $\eta_g$ | Efficiency of the generator |
| $\eta_{Refe}$ | The harmonized electric efficiency reference value |
| $\eta_{Refth}$ | The harmonized thermal efficiency reference value |

# 1 INTRODUCTION

Due to rising global demands for energy and growing concerns about the accelerating greenhouse effect, efficient and clean energy generation and renewable energy sources are increasingly under a spotlight. At the moment and in the future the weather depending renewable energy production is increasing. This growth leads to higher demand for fast balancing energy production during unfavorable generation conditions. Furthermore, the manner and geographical location of the energy production have become more interesting from end users' point of view. Nowadays useful energy, in forms of electricity and heat, has to fulfill certain characteristics such as ecologic and high value. On the other hand, the location of the production has increasing importance in terms of the electric grid due to its restricted transmission capacity. This limitation and increasing energy consumption force the energy system to be transformed towards a decentralized energy system, in which small-scale distributed generation is connected to the distribution network instead of large central generators connected to the transmission network. Thus, energy is generated locally and more effectively. Additionally, the distributed generation provides local support for the electric grid during peak periods in order to increase power quality and electricity reliability.

Combined heat and power (CHP), or co-generation, is the simultaneously generation of electricity and useful heat from a single fuel source at high efficiency. In contrast to a conventional power plant, in which 60 % of primary energy is lost as heat to the environment, CHP is provided with heat recovery and 40 % of this waste heat can be utilized. [2] Furthermore, up to 40 % of the input energy is converted into electricity and the overall efficiency of 75–90 % can be reached. [4] Compared to the overall efficiency of a conventional power plant, the enhancement of 40 % and primary energy saving are significant. Additionally, a $CO_2$ emission reduction of 30 % in comparison with large coal-fired power plant and a 10 % reduction in comparison with central combined-cycle gas turbine power plant are possible. [10]

The CHP is widely used in large industrial applications, in which generated electricity is used on-site and heat is utilized in industrial processes or fed into a district-heating network. On the other hand, micro-scale CHP systems play an increasing role in the distribution network. Hence, the proximity of heat and electricity consumption is reached. The primary energy saving and the reduction of greenhouse gas emissions in the building sector have led to a growing interest in micro-CHP systems. This novel technology has led to a growth in research into the suitability of micro-CHP systems to provide on-site heating and electricity for residential and commercial buildings. In [34] a methodology for assessing the performance of building-integrated micro-cogeneration systems based fuel cells, Stirling engine and internal combustion engines are established and demonstrated in terms of primary energy demand and $CO_2$ emissions. Finally the maximum reduction of 14 % was reached with the internal combustion based system in the single-family house. [34] Tri-generation is the combined cooling, heat and power generation when cooling device utilizes waste heat of cogeneration unit in order to produce required cooling. A simple performance assessment of micro-scale tri-generation system in an office building was made in [35].

Micro-CHP systems are powered by different prime movers of which the most advanced are fuel cells, Stirling engine and internal combustion engine. In [36] the performance of fuel cell micro-CHP systems for residential buildings was assessed. On the other hand, a building-integrated Stirling engine micro-CHP unit has been studied [37]. The performance of small-scale tri-generation systems based on internal combustion engine for building applications was analysed in [19]. Additionally, the Organic Rankine Cycle is an interesting prime mover technology under development. In [38] research of a novel biomass fired Organic Rankine Cycle system was carried out.

Small- and micro-CHP systems are typically used as an individual unit in order to provide heat for a building or a building complex. On the other hand, a high number of decentralized small- and micro-CHP units could perform as a cluster and be remote controlled by an electricity utility in order to support fluctuating renewable energies and the electric grid during peak loads. Furthermore, in the previous research the main interest has been in heat-driven systems in which the main interest has been to cover heat demand. However, a combination of power- and heat-driven systems will become more important in the near future. Furthermore, additional electricity and cooling generation devices, such as a piston steam engine and absorption chiller, could be inserted in configurations of small- and micro-CHP systems in order to enhance an overall efficiency. Hence, the previous research should be extended in order to have knowledge of the CHP cluster's performance.

The first step towards a simulation and performance analysis of the CHP cluster is to model a single CHP unit performing in single-, multi-family or small office buildings. The aim of this thesis is to construct a model of the internal combustion engine based CHP unit using the Matlab/Simulink environment and investigate its performance under different operating strategies. Furthermore, techno-economical aspects of the model are investigated. The second chapter of the thesis introduces the concept of the combined heat and power system and tri-generation. Next the most advanced prime movers for micro-CHP systems are presented and the argument for choosing an internal combustion engine based CHP-system as a main object of this thesis. Heat recovery is discussed further in the fourth chapter. Finally, existing micro-CHP systems are introduced. In the second part of the thesis the model and numerical study are presented. Next the operational result and sensitivity analysis for two test cases are presented and discussed. Finally, the optimization is conducted and the result analysed.

# 2 COMBINED HEAT AND POWER

Combined heat and power (CHP) is the simultaneously generation of electricity and useful heat from a single fuel source at high efficiency and with reduced operating costs. Additionally, this cogeneration takes place in the vicinity of end users. The electricity and useful heat can be generated using different energy conversion technologies and fuels. The fuel is converted into heat and mechanical energy in order to drive a generator for electricity production. In Figure 1 several possibilities of implementations a combined heat and power system are presented.

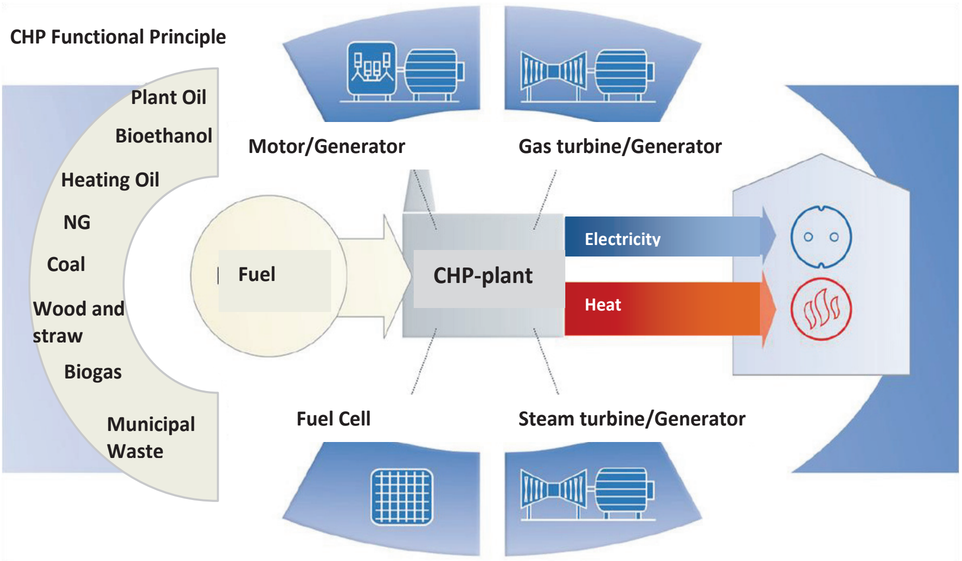


***Figure 1.*** *Alternative means of implementing [1]*

The main advantages of using CHP in power generation are an enhanced overall efficiency of the input energy and reduced operation costs. In a conventional power plant utilizing fossil fuels up to 40 % of the energy input is converted into electrical energy and the remaining 60 % of the input is released to the environment as waste heat in the form of exhaust gases and irreversible energy losses such as radiation and convection [2]. Other typical characteristic of the conventional power plant is a far-away location in the view of the end users. This distance between the generation and end users leads to transmission losses up to 10 % of the generated electricity reducing the overall efficiency of the plant [3]. In contrast to this conventional concept 40 % of released waste heat can be recovered in a CHP-plant and utilized to produce hot water or steam, which are consumed on-site or delivered into a distinct heating system. Thus, only 20 % of the energy input is lost as heat to the environment. Furthermore, due to the proximity of the generation, the transmission losses are negligible and the overall efficiency of 75–90 % can be achieved within the CHP system. At the same time the simultaneously generation of electricity and heat from the single fuel reduces the operation costs of the plant compared to the conventional separated generation [2; 4].

## 2.1 Small- and micro-CHP

The size of a CHP system can vary from micro- to large-scale applications within the electrical output of 1 kW to over 1 GW. The definition of a large-scale combined heat and power system consists of capacities over 2 $MW_e$ and simultaneously produced heat is fed to a district heating system or used on-site. [5] Thus, all CHP systems below this definition belong to scale of small- and micro-CHP. A definition of the micro-CHP in the EU cogeneration directive instead consists of units with maximum capacity below 50 $kW_e$. [6] However, the micro-CHP systems are meant to use in single- or multiple family houses, office buildings, small hotels and small industrial buildings. Furthermore, the micro-CHP systems do not supply heat to a district heating system or neighbourhood. Thus, the definition of the micro-CHP can be restricted to systems below 15 $kW_e$. [7] A typical configuration of micro-CHP system within a building is showed in Figure 2. [2]

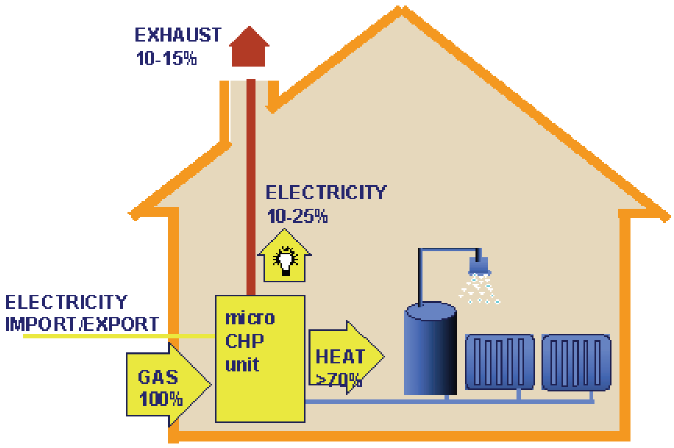


***Figure 2.*** *A typical configuration of micro-CHP within a building [10]*

Different energy conversion devices called prime movers can power a combined heat and power system. Thus, gas turbines, steam turbines and reciprocating engines are commonly used prime movers in large-scale CHP systems. The gas turbines can be effectively scaled down for small-CHP system as a micro-turbine with the capacity of 30 $kW_e$–250 $kW_e$. [5] However, in terms of the micro-CHP definition internal combustion engines are the most successful technology scaled down. Thus, the electrical output even below 5 kW is effectively reached. Additionally Stirling engines and fuel cells are common technologies in the micro-CHP systems. These three different prime mover technologies dominate in the micro-CHP systems and are discussed in the following chapter. [5]

Operating a CHP system at small- and micro scale provides many benefits compered to large-CHP system. An ability to match a building heat load with heat capacities increases due to the on-site micro-CHP system in a basement of the building. Thus, a thermal output of the system can be easily matched with the thermal load of the building and simultaneously generate electricity as a by-product to be fed into the electric grid. This accurate load fitting is the most energy and cost effective manner to produce heat and electricity. Furthermore, a smaller system size requires less initial capital investment which fits better into smaller budgets of residential and commercial building owners. The small- and micro-scale leads to a smaller single dose of a fuel than the large CHP-systems due to the size of the system. Hence, renewable fuel sources, which are not available in large quantities, are suitable to use in the small- and micro-CHP units. For instance, biogas can replace natural gas in gas-fired prime movers, which makes the CHP-unit renewable energy source with zero emissions. [2]

In terms of the electric grid connection, an installation of a small and micro-CHP system in the distribution grid improves electric reliability and power quality. Thus, the building has two sources of electricity. On the other hand, the CHP system can support the grid during peak loads and possible voltage sags. This grid support allows maintaining proper voltage requirement in the grid and facilities. [2] Furthermore, the grid connection allows selling the electricity to the grid and getting incomes in order to cover operating costs of the CHP system. Especially in the micro-CHP systems, which are typically heat demand controlled and the electricity is a by-product, selling electricity back to the grid is reasonable under certain grid policy conditions. [5] These appropriate policy conditions leads to increasing interest in power driven small- and micro-CHP systems with heat production as a by-product. Simultaneously, power driven CHP systems act as an incentive to grow a usage of renewable energy sources and improve the grid policy conditions towards favouring micro generation.

## 2.2 Tri-generation

Tri-generation is the simultaneous generation of heating, cooling and electrical or mechanical power using a single fuel source. [5] As a result hot water or steam, chilled water and electricity are produced in this combined cooling, heat and power (CCHP) system. In contrast to a CHP system the CCHP system is coupled with a heat-activated cooling device or compression in order to provide either space cooling or refrigeration. In the first waste heat recovered from cogeneration is utilized to create chilled water and in the latter generated electricity is used to drive compressors in refrigeration system. [4] Hence, recovered heat can be utilized also in the summertime to produce cooling. Consequently, the thermal power is requested throughout the whole year which makes cogeneration profitable. This extension of the system leads also to higher flexibility, the increased overall efficiency of the input energy, and maximized running hours of the system at averagely higher load. Additionally, shorter investment payback times are reached. [4; 5; 9]

Tri-generation is widely used in large- and small-scale due to available knowledge of typical industrial installations and high initial capital costs. Thus, the utilization of heat-activated cooling devices, like absorption chillers, has been limited to large commercial and industrial applications. However, micro-scale CCHP systems are not so advanced due to their unique properties, requirements, and challenges. Consequently, only little information and few cooling devices are available for the micro-CCHP systems. On the other hand, in recent year the market of the micro-CHP systems has growth and smaller more efficient and less expensive absorption chillers have been developed. [2; 5]

# 3 PRIME MOVERS FOR CHP SYSTEMS

An energy conversion device is used to generate electricity and heat in a micro-CHP system called a prime mover. If the conversion process is based on combustion, the prime mover first converts the chemical energy of fuel into the mechanical and thermal energy of the system. The produced mechanical energy drives a generator for electricity production. Such a prime mover can be an internal combustion engine, micro turbine, Stirling engine, the water based Rankine cycle, or the organic Rankine cycle (ORC). Alternatively, a fuel cell can be used as a prime mover converting the chemical energy of fuel directly into the electrical energy and heat. Of the mentioned prime movers the Rankine cycle and Stirling engine operate with external combustion and thus own high fuel flexibility. Hence, an external burner provides heat from the desired fuel, for example natural gas or biomass, in order to drive the prime mover. In the Rankine cycle the working gas, water or organic liquid depending on the temperature level, undergoes a phase change from liquid to gas followed by expansion and pressure on a piston of steam engine or turbine rotor in, for example, wood fired boilers. Hence, useful work is produced. [7; 10]

However, the Rankine cycle for micro-CHP systems in residential buildings is still under the development while the internal combustion engine, Stirling engine, and fuel cells are the most promising technologies for the commercial systems today. The micro turbines are small size turbines and thus a plant consists of a turbine, compressor, combustion chamber and generator which are connected by a shaft. Anyway, the micro turbines instead have been developed with an electric output from 25 kW to 250 kW and are thus not in micro-CHP category defined in this context to be the systems below 15 $kW_e$. [7; 16]

Since the internal combustion engine, the Stirling engine, and the fuel cells are the most advanced and commercially available prime movers for micro-CHP systems they are introduced in this chapter. First the operating principle of the prime mover is presented and the most important features related to the micro-CHP system are discussed. Finally, advantages and disadvantages of these conversion devices based micro-CHP systems are compered.

## 3.1 Internal combustion engine

The internal combustion engine is based on a conventional piston-driven combustion process. Basically this conversion device consists of a cylinder, piston, inlet port and exhaust port. The inlet port allows air or mixture to enter the cylinder. In this combustion chamber the chemical energy of the fuel is converted into heat, and therefore into pressure rise, and the mechanical energy of the moving piston which is connected with a crankshaft mechanism. Consequently, hot exhaust gases pass through the exhaust port and the thermodynamic cycle can start again. The most advanced use of internal combustion engine technology is in automobile applications, stationary power generation, and combined heat and power systems. [7]

The internal combustion engines are generally divided in Diesel and Otto engines, which are distinguished from each other by the ignition principle. In the diesel engine the compression ignition is utilized to ignite fuel. Thus, the piston first compresses the intake air when the fuel is directly injected to the cylinder at high pressure and temperature in order to self-ignite and to combust. An Otto engine is instead a spark ignition engine in which fuel is premixed and charged into the cylinder and a spark plug is used to ignite the charge after compression. [5]

The internal combustion engine can operate in a lean mode or stoichiometrically. In the lean mode, with air-to-fuel ratio $\lambda = 1.7$, the combustion takes place with excess air and as a result the flame temperatures are lower than in stoichiometric combustion, with $\lambda = 1$. The lean mode results also in low $NO_x$ emissions but facing the future more strict emission regulations $NO_x$ emissions are not low enough. A three-way catalyst is used to mitigate $NO_x$ production when operating stoichiometrically and simultaneously, the other main emission hydrocarbons (HC) and carbon monoxide (CO) is reduced. In order to have effective operation of the three-way catalyst, excess oxygen in the exhaust gas has to be avoided and thus stoichiometric engine operation is required. Furthermore, an exhaust gas recirculation (EGR) can be used to reduce temperatures and hence raw $NO_x$ emissions while still operating stoichiometrically. The operation with $\lambda = 1$, EGR and three-way catalyst leads to even lower emissions than the lean mode. [5; 7; 39]

For micro-CHP applications, the four stroke spark ignition engines are typically used which are fuelled by natural gas. The chemical energy of the fuel is converted in different proportions into other forms of energy. Accordingly, approximately one-third of the fuel energy supplied into the engine is converted into mechanical work. Furthermore, the rest of the fuel energy is lost as heat in the exhaust gases at temperature 300–600 °C and as friction and heat losses within the engine. [5] Most of the latter is recovered from the engine cooling circulation using heat exchanger but a part is lost due to irreversible energy losses such as radiation and convection to the environment. Eventually domestic hot water and space heating is supplied by recovered heat from the exhaust gases and the engine cooling circulation. In general commercially available internal combustion engine-based micro-CHP systems provide the electrical efficiency of 24–30 % and the thermal efficiency of 60–70 %. Thus, the overall efficiency 85–90 %

can be reached. Commercially available micro-CHP systems based on the internal combustion engine are introduced further.

## 3.2 Stirling engine

The Stirling engine is an external combustion engine in which heat is generated externally and continuously in a separate combustion chamber. Heat can be generated by means of a gas burner and transferred through the Stirling engine's working gas to the central heating flow of the building instead of a conventional heat exchanger. Simultaneously, the engine generates the electricity when the heated working gas undergoes pressure fluctuations and thus does useful work. [5]

The simplest configuration of the Stirling engine consists of a cylinder, working piston, displacer and regenerator. One end of the cylinder is maintained at high temperature by the external heat resource while the other end is cooled by a flow of cooling water. The working gas is moved between the hot and cold ends by the loose fit and non-working displacer which is 90° in front of the working piston on the same shaft and within the same cylinder. A fixed volume of the working gas is heated in the hot end and increased pressure acts on the working piston generating reciprocal piston motion in order to drive a generator through the crankshaft mechanism. The working gas is shuttled from the hot end to the cold end via the regenerator in order to enhance thermal efficiency. Hence, heat of the hot and expanded working gas is stored in a heavy matrix of fine tubes during the cooling pass to be regenerated during the heating pass of the working gas from the cold end. [5; 7]

The working gas releases heat to the cooling water in the cold end. Helium, hydrogen and nitrogen are well suited to use as a working gas due to their low specific heat. Considering the small molecular size of these gases they can leak easily and thus, helium is the most used working gas in the Stirling engines. [5; 7]

The Stirling engine can have different configurations that differ from each other by the number and position of cylinders and pistons. [7] The presented configuration of the Stirling engine is called a beta type and it is inherently the most efficient configuration of the displacer and working pistons. [5] Other configurations are alpaha which has two pistons without displacer and gamma type in which the working piston and displacer are placed in separated cylinders.

The Stirling engine based micro-CHP system produce simultaneously hot water for a domestic heating system and the electricity used onsite or fed to the electric grid. An external heat resource can heat up the hot end as high as 800 °C and the temperature of the cold end is around 80 °C. The flow of cooling water removes useful heat from the cold end to a domestic heating system. Simultaneously, the Stirling engine generates electricity. A seasonal average electrical efficiency of 20 % has been achieved in larger Stirling engine systems and the efficiency of over 24 % is predicted for future models. However, the much lower electrical efficiency of around 10 to 15 % is achieved in small Stirling engines used in micro-combined heat and power systems. [5; 7]

## 3.3 Fuel cells

A fuel cell is an electrochemical device that converts the chemical energy of a fuel directly into electrical energy and heat by means of the chemical reaction between a fuel and oxygen. The effectively used fuel is hydrogen, which reacts with oxygen producing water with the overall reaction

$$H_2 + \frac{1}{2} O_2 = H_2O \tag{1}$$

The reaction energy is transformed into electrical energy and heat. [5]

The individual fuel cell consists of different layers in which an electrolyte is between an anode and cathode. Furthermore, the farthest layers of the fuel cell are electrically conductive bipolar plates of which function is feed the reactants to the anode and cathode, conduct the reaction heat and collect the electrons. The central electrolyte separates reactants, the hydrogen and the oxygen, in order to avoid an uncontrolled reaction. [7] The delivered fuel is oxidized at the anode when electrons are stripped from the hydrogen and ions are formed. The electrons pass to the external circuit and produce an electric current while the hydrogen ions pass through the electrolyte to the cathode in order to combine with oxygen. In order to increase the capacity of the fuel cell, several single fuel cells can be electrically connected in series as a fuel cell stack by means of the bipolar plates. [5; 7]

In practice the pure hydrogen, as a fuel is not suitable for domestic use due to currently lack of general hydrogen generation and distribution infrastructure. Natural gas $CH_4$, which mainly consists of hydrogen-containing methane, instead has both extensive infrastructure and low costs. Thus, it is typically used as a fuel in commercial available fuel cell micro-CHP systems. Before feeding natural gas to the fuel cell stack methane is converted into hydrogen by means of a reforming reaction in a reformer or inside the stack as an internal reforming. [5; 7]

In terms of domestic micro-CHP systems, two types of existing fuel cell stack technologies have been applied which are a polymer electrolyte fuel cell (PEFC), also called as a proton exchange membrane fuel cell (PEMFC), and a solid oxide fuel cell (SOFC). The types use the same operating principles outlined above but used materials, operating temperatures and the ability to tolerate the fuels differ them from each other. PEFC technologies use solid polymer as the electrolyte and graphite or steels as the bipolar plates. The operating temperature of PEFC is 30–100 °C and the used fuel is the hydrogen which is converted from natural gas in an external reformer device. In contrast the SOFC technologies use ceramics and steels or chromium alloys due to high operating temperatures of 500–1000 °C. In addition to the hydrogen SOFCs are fuel tolerant for carbon monoxide, CO and instead of the external reformer the internal reforming is used. [5]

Heat recovery from the fuel cell stacks differs between PEFC and SOFC technologies. PEFCs are operated at low temperature and a liquid cooling circulation is used to cool the stack that pass through a liquid-liquid heat exchanger in order to remove waste heat to a domestic heating system at temperature of 60–65 °C. Heat recovery of high temperature SOFCs is instead more complicated. Heat in the exhaust gas is firstly employed to pre-heat the gas inlets and maintain reforming temperature followed by a condensing heat exchanger to provide hot water for the domestic heating system. [5]

Fuel cells can have the electrical efficiency as high as 45–55 % [16] but the overall efficiency suffers from low thermal efficiency due to difficulties in recovering low-grade waste heat. The fuel cell stack generates a low voltage and direct current output that leads to a requirement of an inverter and power-conditioning unit in order to convert the output into a stabilized alternating current. [5] Generally SOFC systems have higher electrical efficiency than PEFC systems. The average electrical efficiency of 35 % and overall efficiency of 71–74 % has been achieved during residential demonstrations in Japan. In PEFC systems the electrical efficiency is reduced to 27–32 % due to greater losses in fuel processing. [5]

However, the German company Baxi Innotech has the low temperature PEM fuel cell GAMMA 1.0 for single-family houses on the market. Its electrical output is 1.0 kW with electrical efficiency of 32 %. The thermal output is 1.8 kW and the achieved overall efficiency is 91 %. [11] Furthermore, the Swiss company Hexis has developed a SOFC technology based fuel cell called Galileo of which outputs are same than GAMMA 1.0 has. The electrical efficiency of 30–35 % is achieved and the overall efficiency of 95 %. [12]

## 3.4 Advantages and disadvantages

All mentioned prime movers have the key characteristics that make them suitable for micro-CHP applications. These key features in residential and commercial building environment are high efficiency, dynamic behavior, low emissions, low noise level, long lifetime, long service intervals and low initial investment cost. [5] The advantages and disadvantages of different prime mover technologies in the micro-CHP application are created from differences between these key features.

The ability to convert a fuel into desirable energy forms is described by the efficiency. The electric efficiency has important role when assessing different prime mover technologies because electricity, as a form of energy, has a high value. In terms of an internal combustion engine, the electrical efficiency of 24–30 % can be reached in commercially available units whereas the significantly lower electrical efficiency of 10 to 15 % is achieved in small Stirling engines. Conversely, the fuel cells have higher electrical efficiency than the engine based micro-CHP. As a disadvantage of the fuel cells, the operation temperature can be substantially higher than in the engines even up to 1000 °C but it does not, however, relatively increase electrical efficiency and there are difficulties to recover waste heat effectively. Furthermore, the fuel cells have a drop in efficiency between 0 and 5 % per thousand operating hours depending on the used materials and design. [5]

The operating environment of the micro-CHP system has the dynamic nature of energy demand and requires thus a prompt response to a changing power and heat demand. Thus, a significant advantage of the internal combustion engine is the dynamic behavior. In contrast to the fuel cells this combustion engine has a fast start-up and shutdown time and there is no a time delay between the fuel input and the power output such as in the Stirling engine. In terms of dynamic behavior a remarkable disadvantage of the fuel cells is required pre-heating time being an hour in PEFC systems and even 12 hours in SOFC systems. Additionally, a changing behavior of the fuel cell, especially in high temperature SOFCs, causes the materials degradation due to thermal cycling. These constraints lead to a requirement of continuously operation in order to avoid decrease of the predicted lifetime. [5]

The low emission level of the micro-CHP system is required in residential and commercial buildings due to the legislation and the operating environment. The Stirling engine has high fuel flexibility due to the external combustion chamber and instead of the chamber a concentrated solar irradiation can be used as an external heat source in which case the emission free system is achieved. [7] Anyway, the low emissions level of the Stirling engine is achieved by means of continuous combustion process and exhaust gas recirculation when a catalytic converter is not required like in internal combustion engines. [5] Actually, low emission level is achieved in the spark ignition internal combustion engine as well. Stoichiometric operation of the engine fitted with a three-way catalyst and operating at steady state leads to the lowest emission level. [5] In the fuel cells the main reaction between hydrogen and oxygen produces water and the useful energy production is in itself carbon-neutral but the reforming process of natural gas or other fossil fuel release emissions.

Depending on the noise level the micro-CHP system can be installed in a basement or living area of the building. The fuel cell stack, in itself, does not consist of moving parts and hence has a quiet operation. However, this energy generation system is not totally quit due to auxiliary devices, for instance the blower, burner or pumps, which generate a similar noise level than a conventional condensing boiler. [5] In reciprocating engines the noise level is higher and they are typically installed to the basement of the building.

Reliability of the heating system can be measured by long lifetime and service intervals. Expected lifetime for a conventional central heating boiler is around 20 000–30 000 hours. [5] In terms of micro-CHP systems, the lifetime of the fuel cells is shorter than the engines due to mechanical deterioration of the cells during the lifecycle. Although the heat engines have much moving parts and they require a regular maintenance, the Stirling and internal combustion engine have a long lifetime and service intervals due to the external combustion of the Stirling engine and well-established internal combustion engine technology.

Eventually, the initial investment cost of the micro-CHP unit is the most remarkable feature and the internal combustion engine achieves relatively the lowest costs due to well-developed and established technology. The fuel cells are novel micro scale technology and this novelty has an effect on economic viability creating relatively high initial capital cost. [5] All main features regarding micro-CHP technologies, which affect strongly to decision-making between different CHP technologies, are presented in Table 1.

***Table 1.*** *Qualitative characterization/assessment of prime mover technology with relative judging expressions [5; 7; 14; 16]*

| Prime mover / Key feature | ICE | Stirling engine | Fuel cells | Micro turbine | The Rankine cycle |
|---|---|---|---|---|---|
| **Electrical efficiency** | High | Low | High | Low | Low |
| **Dynamic behavior** | Good | Bad | Bad | Bad | Bad |
| **Emissions** | Low | Low | Low | Low | Low |
| **Noise level** | Rather low | Low | Low | Low | |
| **Fuel flexibility** | Good | Good | Bad | Good | Good |
| **Maintenance interval** | Long | Long | | Long | |
| **Initial investment and maintenance cost** | Lower | High | High | High | Not well-known |
| **Availability of technology** | Good | Good | Bad | | Bad |

In terms of the high electrical efficiency, good dynamic behavior, low emissions, long lifetime and maintenance interval, and lower initial investment cost, the internal combustion engine based micro-CHP system is most suitable for desired residential and commercial building environment. Due to this it has been selected for the main subject in this thesis. In this environment a suitable building range is older and equipped with heat distribution systems, such as water-based radiators or convectors, or floor heating. Hence, outgoing temperature level of the CHP system is 40–70 °C. The newer building range with the better insulation level has been generally started to construct after 1990 and is more ecological with air heating system when CHP is not reasonable heating system.

# 4 HEAT RECOVERY AND CHP COMPONENTS

Heat recovery is a manner to utilize the bigger portion of the fuel energy and to enhance the overall efficiency of a combined heat and power system. The chemical energy of a fuel is converted into mechanical energy in the internal combustion based combined heat and power system in order to generate electricity. However, the electrical efficiency of the engine-based system is limited and all of the available energy cannot be used to generate electricity. The rest of energy is released as waste heat within the exhaust gases and, as convection and radiation loses from the engine and generator to the environment. On the other hand, waste heat can be utilized using a heat recovery device. [13]

Depending on temperature level heat can be recovered within different categories. In the engine-based CHP systems up to 30 % of the energy input is recovered as heat from the engine cooling circulation at low-temperature category when the temperature is less than 230 °C. Furthermore 30–50 % of the energy input is recovered as heat from the exhaust gas either at low- or medium-temperature category when in the latter the temperature is 230–650 °C. The third category is high-temperature when greater than 650 °C is reached. Eventually heat recovery can enhance the overall efficiency of the CHP system up to 90 % depending on the used application. [13; 14]

In the residential and commercial building environment a basic configuration of an internal combustion engine based CHP system consists of an internal combustion engine (ICE) with liquid-to-liquid and gas-to-liquid heat exchangers and thermal storage. The basic configuration can be extended with different components in order to achieve the higher electrical efficiency and to response to cooling demand during low heating demand. Thus, thermal energy from engine cooling is utilized to produce hot water and hot exhaust gas is utilized in a thermally activated component. The internal combustion engine can be provided with the exhaust gas recirculation (EGR) when an additional heat exchanger is required to cool down the exhaust gas after a heat recuperation device. This EGR heat exchanger takes cooling water directly from the storage before the other exchangers because of the low temperature. In this chapter different CHP components and configurations are presented.

## 4.1 Heat exchanger

A heat exchanger is a device used to facilitate heat recovery from a hotter fluid to a colder fluid. Generally, the heat exchanger can be a recuperator, regenerator or direct contact heat exchanger. Most of used heat exchangers are recuperators, in which separated steady flows and steady temperatures exist and heat is transferred directly from one fluid to another through the wall. In the regenerator heat from the hotter fluid is firstly stored in a matrix of a thermal mass having a substantial heat store capacity. Next the colder fluid runs through the mass and regenerates stored heat. Conversely in direct-contact heat exchangers the two fluids are completely mixed like in a water heater in which steam is bubbled through the water when it condenses and increases the amount of water. Due to this the direct contact exchanger is more used in mass transfer and simultaneous heat and mass transfer applications. The fluids in the heat exchanger can have the different physical states, phases like liquid and gas. A single-phase flow refers to gas-to-gas or liquid-to-liquid heat exchangers while two-phase refers to gas-to-liquid exchangers like evaporator or condenser. Both single- and two-phase heat transfers are occurred in combined heat and power system. Heat is transferred from the hot exhaust gas to water and from water to water in the engine's cooling circuit. [14; 15]

Furthermore the heat exchangers can vary a lot according to a heat recovery application by changing the type of heat transfer surface, the materials of construction and the geometry of the flow configuration. The type of heat transfer surface can vary through different heat exchangers and have different forms. Nevertheless, the most common form is a plain circular straight tube, which can be bent or coiled. If the heat transfer resistance on the other side of tube is much larger, the finned surface of the tube is commonly used on the other side surface in order to increase the effective heat transfer area. In the following section different geometric flow configurations are presented. [15]

***Geometric flow configurations***

A geometric flow configuration describes how two fluids, in relation to each other, move through the heat exchanger. The most common geometric flow configurations are a single-stream, counter-, cross-flow- and parallel-flow configurations that are employed in the recuperators as well as in the regenerators. The configurations are presented in Figure 3. In the single-stream configuration the direction of the flow is irrelevant because the temperature of only one stream varies due to the phase transition of the other stream. In the counter-flow two-stream configuration the two separated and parallel fluids flow in opposite directions. The temperature difference of the flows is the same at the inlet and outlet of the heat exchanger. Conversely the cross-flow two-stream configuration has the two fluids encountering each other at right angle such that the hot flow runs inside tubes arranged in a bank while the cold flow runs through the bank in perpendicular to the tubes. In the parallel flow configuration the two parallel flows enter the heat exchanger with the vast temperature difference and run in the same direction in order to have a much smaller temperature difference at the outlet of the heat exchanger. [15]

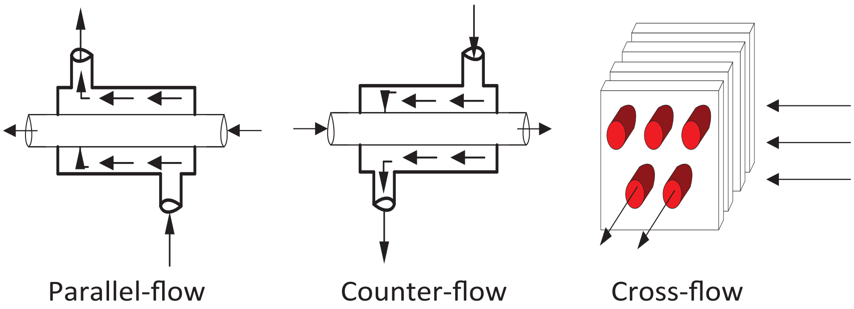


***Figure 3.*** *Different flow configurations [14]*

The suitable configuration depends strongly on the application. The single-stream configuration is utilized particularly in condensers and evaporator for power plants and refrigeration systems. While the counter-flow two-stream configuration is commonly employed in feed water preheaters for boilers and in cooling circulations. In this case a heat exchanger is called a shell-and-tube exchanger which consists of several tubes located in a shell and is most often used for liquids and high pressures [15]. Furthermore, plate exchanger is other option that consists of several plates separated by gaskets and is more suitable for gases at low pressure [15]. These two heat exchanger types are presented in Figure 4. The parallel-flow configuration is also employed in both the shell-and-tube exchanger and the plate exchanger but it has the lower effectiveness than the counter-flow configuration that has the highest effectiveness. In contrast to the other configurations the cross-flow is simple to realize and is usually used in the automobile radiator. [15]

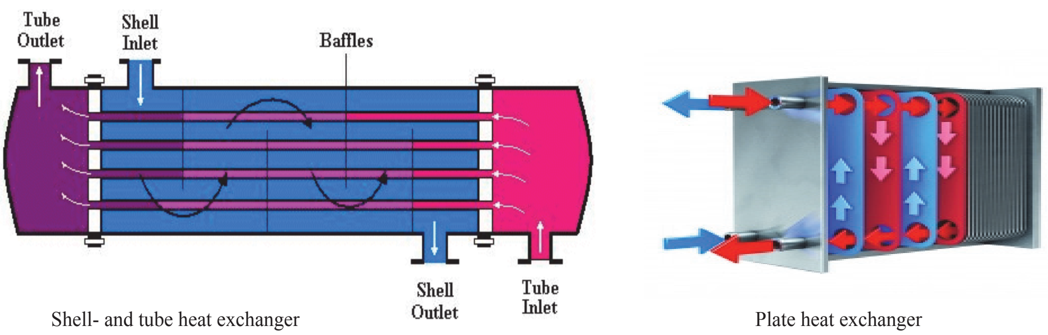


***Figure 4.*** *Principle of a shell- and tube heat exchanger and plate heat exchanger [17; 18]*

However, in internal combustion based CHP systems the plate heat exchanger are used to recover heat from the engine cooling circuit and the shell and tube exchanger recovers heat from the exhaust gases.

***Effectiveness***
The effectiveness of the heat exchanger depends on the rate of transferred heat between two fluids. In theory the maximum possible temperature decrease of the hot fluid could be obtained in an infinitely long heat exchanger when the outlet temperature of the hot fluid is the saturation temperature. However, in practice the exchanger is not infinitely long and the maximum possible temperature decrease is not obtained. The actual heat transfer from the hot fluid to the cold fluid is

$$Q = m_H c_{pH}(T_{H,in} - T_{H,out}) \tag{2}$$

where $m_H$ is the mass flow of the hot fluid, $c_{pH}$ is the specific heat capacity, $T_{H,in}$ and $T_{H,out}$ are the inlet and outlet temperatures of the hot fluid. The effectiveness of the heat exchanger can be described as the actual heat transfer divided by the maximum heat transfer obtained

$$\varepsilon = \frac{Q_{actual}}{Q_{max}} = \frac{C_H(T_{H,in}-T_{H,out})}{C_{min}(T_{H,in}-T_{C,in})} = \frac{C_C(T_{C,out}-T_{C,in})}{C_{min}(T_{H,in}-T_{C,in})} \tag{3}$$

where C is the flow thermal capacity of the flow and the smaller limits the amount of heat that can be transferred. In practice the effectiveness of the heat exchanger varies between values of 0.6 and 0.9. [15]

## 4.2 Thermal storage

A CHP unit generates heat and thermal buffering is used in the system to improve the thermal efficiency and performance. [8] The lack of appropriate buffering between the CHP unit and the building leads to increasing duty cycling, a reduced lifecycle of the unit and a reduction in fuel efficiency. [8] Usually, thermal buffering is implemented as insulated water tank of which maximum temperature is limited below 100 °C, such as in Figure 5. This limited temperature controls the cycling of the CHP unit if heat is not desired to waste. Thus, the space heating and domestic hot water circuits run from the tank by means of heat exchangers. In addition to water an energy storage medium can be combination of water and phase change material (PCM). Thus, more efficient heat storage can be achieved in a limited volume.

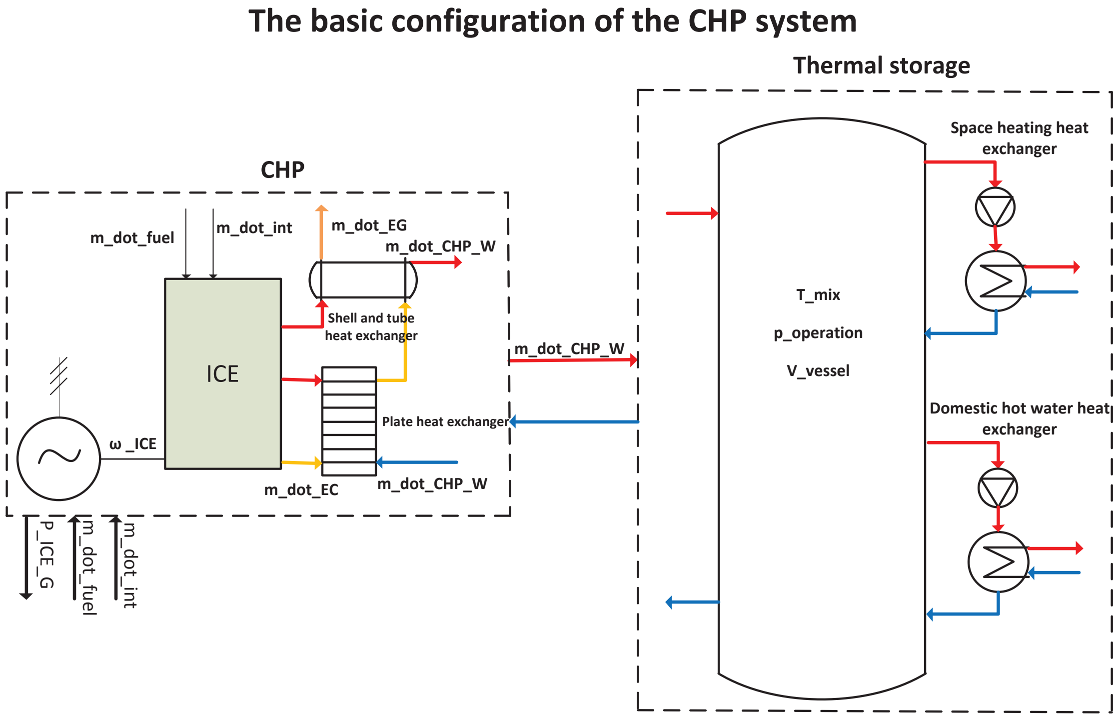


***Figure 5.*** *The basic configuration of the CHP system*

In this basic configuration a direct integrated thermal storage is used between the CHP unit and thermal consumer in order to store primary hot water from the CHP unit and to provide indirectly domestic hot water and space heating by means of external forced convection heat exchangers. The mains water at temperature 10 °C flows through the domestic hot water heat exchanger and heat is transferred in order to achieve desired domestic hot water temperature 50–55 °C. At the same time outgoing temperature of the space heating circuit is 40–50 °C for floor heating system and 60–70 °C for radiator heating system. [20]

## 4.3 The Rankine cycle

The Rankine cycle can be added to a basic CHP configuration as bottoming cycle in order to increase the electrical efficiency of a system. The Rankine cycle converts externally to a closed loop supplied heat into useful work and consists of a heat recovery steam generator, expander, condenser and feed water pump. An extended configuration with the Rankine cycle is presented in Figure 6.

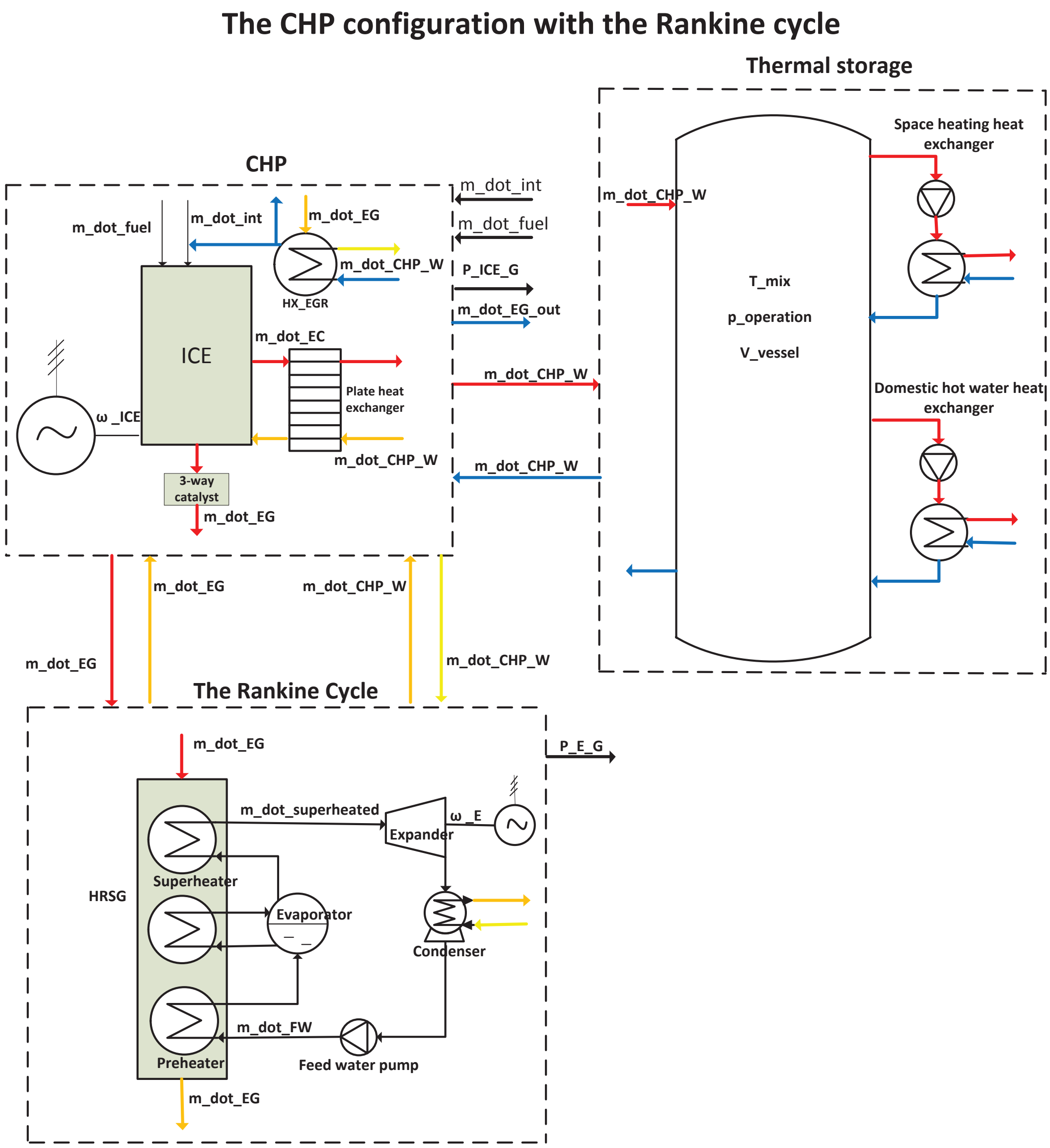


***Figure 6.*** *The configuration of the CHP system with the Rankine cycle*

A working fluid in the closed loop can be water or organic fluid, which undergoes a phase change from liquid to gas. The heat recovery steam generator is a shell-and tube heat exchanger and recovers waste heat from hot exhaust gases to produce steam in the cycle. The expander can be, for example, a steam engine or turbine in which steam expansion causes useful work of expander and electricity can be generated. After the expansion low-pressure steam is cooled in the condenser and remained heat is removed into cold-water flow from a thermal storage. Hence, the feed water pump is used to increase again the working liquid pressure. [2; 19]

## 4.4 Thermoelectric element

Thermal energy of hot exhaust gas can be converted directly into electricity in terms of thermoelectric element. The energy conversion is based on a phenomenon of the Seebeck effect in which a temperature difference between two different electrical conductors or semiconductors generate voltage difference. In this case hot exhaust gas heat up the one side of thermoelectric element whereas the other side stays cooler. Heated electrons of conductor material flow towards the cooler side generating voltage difference. The thermoelectric element is connected to an electrical circuit and thus direct current (DC) is generated. The advantages of the thermoelectric element are quiet operation, no moving parts, environment friendliness and compact structure. The main disadvantages of this generator are a low electrical efficiency of 3–5 % in commercial available elements and the operation temperature is limited rather low. However, the thermoelectric generator can be used in a CHP system to raise the overall efficiency by means of waste heat recovery. [21] The configuration is presented in Figure 7.

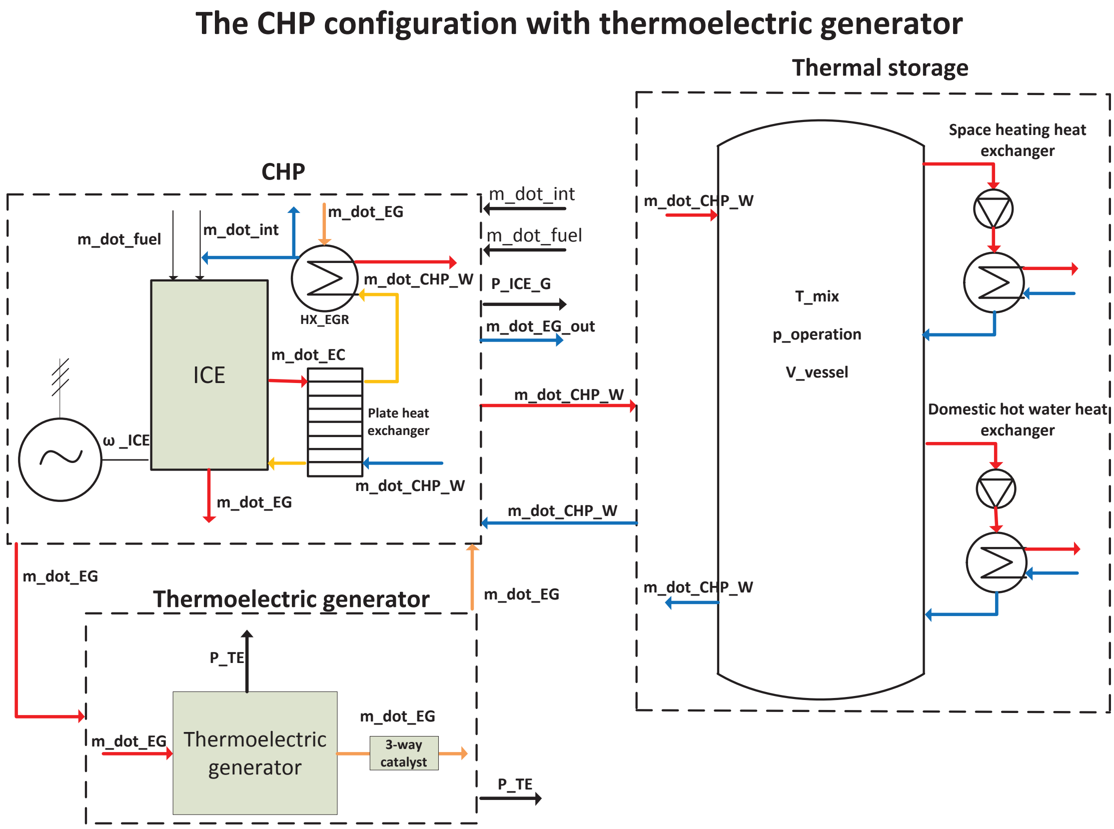


***Figure 7.*** *The configuration of the CHP system with the thermoelectric generator*

In a CHP configuration the thermoelectric element with a power inverter is placed in the exhaust gas part of the system.

## 4.5 Absorption chiller

A combined heat and power system can be extended to a combined cooling, heat and power (CCHP) by means of heat-activated cooling devices. Thus, the produced thermal power is requested throughout the whole year which makes cogeneration more profitable in terms of increasing operating hours and fuel efficiency. An absorption chiller is a cooling device which uses hot water or steam to create chilled water for an air conditioning system. This device recovers heat from an exhaust gas part. The most used absorption chiller utilizes a single-effect water/lithium bromide (water/LiBr) cycle which is driven with hot water at temperature 70–120 °C [22]. With this absorption cycle cooling temperature as low as 5 °C can be achieved. In the water/LiBr cycle pure water acts as a refrigerant and water/LiBr solution as an absorbent. Lower temperatures are achieved with different working pair such as ammonia/water in which a freezing point of refrigerant is not a limiting factor. A CCHP configuration with the absorption chiller is presented in Figure 8. [22]

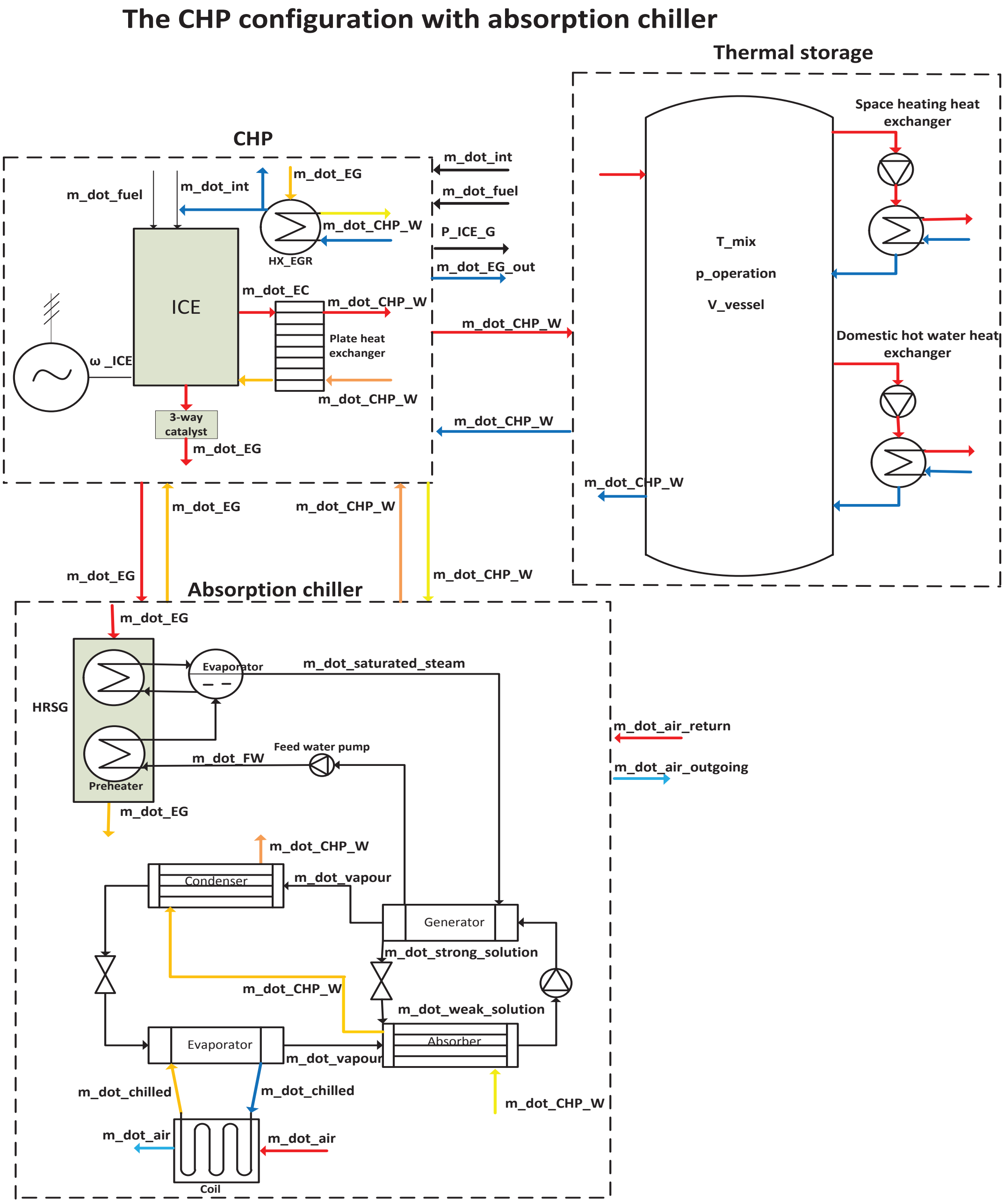


*__Figure 8.__ The configuration of the CHP system with the absorption chiller*

The absorption chiller consists of four main heat exchangers: an evaporator, absorber, generator and condenser where the main processes of the absorption cycle take place. In addition to the heat exchangers two valves are used to separate the cycle's high-pressure side from low-pressure side. A pump is used to increase a pressure of water/LiBr solution. In order to have a working absorption cycle at least three external streams in different temperatures are required. In the evaporator water of the cycle is at low pressure and heat of return stream of chilled water is transferred to water which evaporates. Chilled water is produced and vapour flows to the absorber in which the vapour is absorbed into the water/LiBr solution due to higher pressure of the vapour than the vapour pressure of the solution. This process is exothermic and an external cooling stream is needed to move released heat. The weak water/LiBr solution is pumped to the evaporator at high pressure where water is vaporized by recovered heat from the exhaust gas part. The vapour flows to the condenser and strong water/LiBr solution is circulated through the valve back to the absorber at low pressure. The external cooling stream from the absorber is used to condense the vapour to liquid in the condenser. Hence, the liquid flows through the valve in order to reach lower pressure again. The external cooling stream can flow from a separate cooling tower or heat store. [22]

The absorption chiller thermal COP is used to assess the performance of the chiller and is defined as

$$COP_{th} = \frac{Q_c}{Q_{th}} \tag{4}$$

where $Q_c$ is reached cooling power at the evaporator and $Q_{th}$ is the heat input required in the generator. [22] For single effect absorption chillers the driving temperatures are around 75–80 °C with COP values of 0.7–0.8. On the other hand double effect chillers have a driving temperatures higher than 180 °C and COP values of 1.2–1.3. [23] The absorption chillers are well established in a large scale and in recent years also small-capacity single-effect chillers with cooling power from 5 to 30 kW have been developed and available on the market. [23] However, the disadvantages of heat activated cooling for small-scale CHP systems are the increasing initial capital cost due to adding expensive components and increasing system complexity. Additionally, a lack of commercially available small-scale heat activated cooling technologies with well-proven reliability and long term performance is seen as a disadvantage. [5]

## 4.6 Steam jet ejector cooling

A steam jet ejector cooling device utilizes steam in order to produce chilled water. The device is mechanically simple with no moving parts and consists of a heat recovery steam generator, feed water pump, ejector, condenser and expansion valve. Its advantages are high reliability, simplicity and a tolerance to a range of working fluids. On the other hand the disadvantage as a cooling device is low performance which is lower than absorption chiller has. Due to this there is not commercially available steam jet ejector cooling devices on the market. On the other hand there is much on-going research into steam ejector cycle. In Figure 9 a fundamental CCHP configuration with steam ejector cycle is presented. [5; 24]

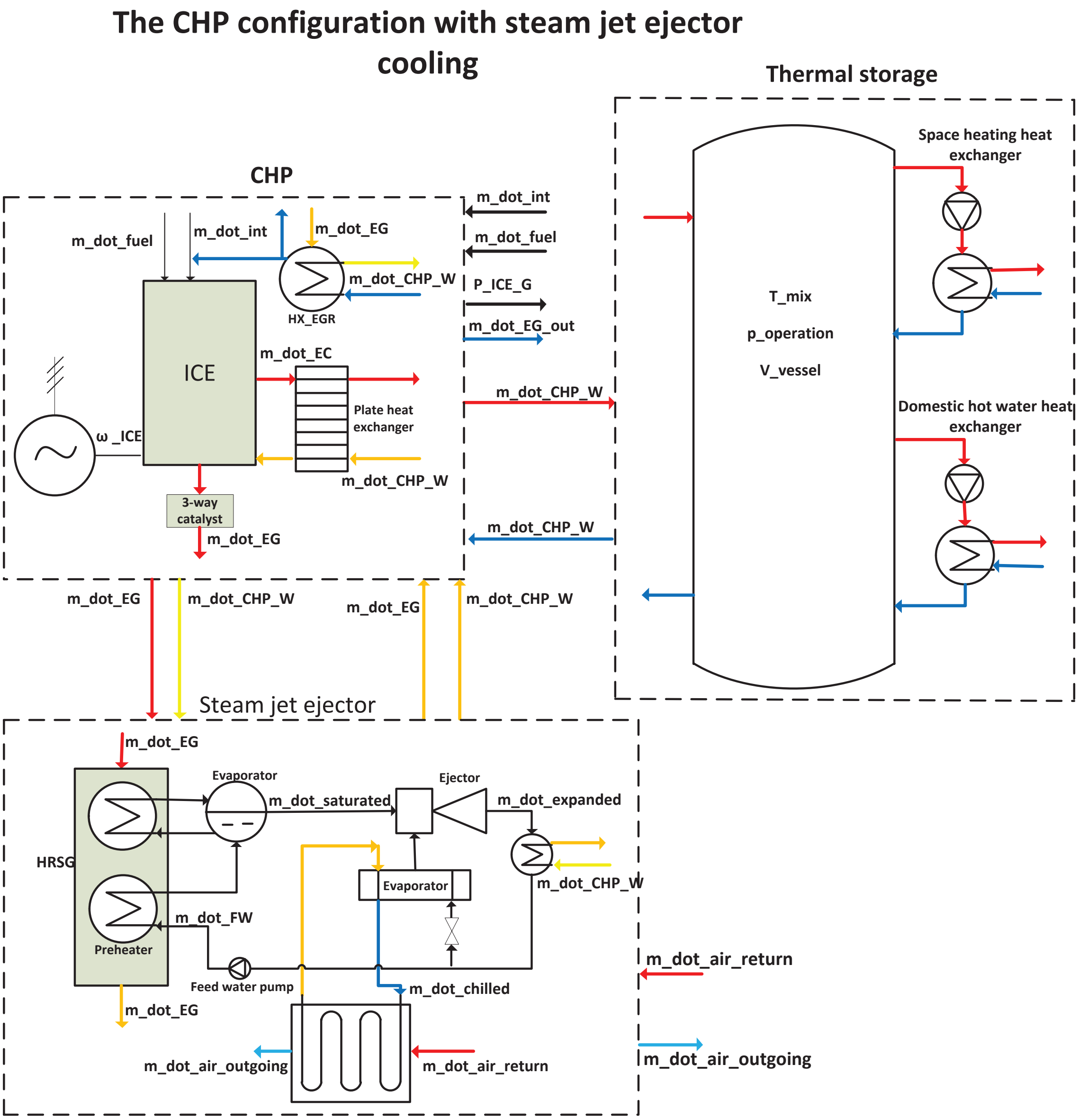


***Figure 9.*** *The configuration of the CHP system with the steam jet ejector*

Water is used as working fluid in the cycle and the ejector produces the compression effect. The feed water pump generates a desirable pressure to operate the steam ejector cycle. The working fluid of a steam ejector cycle is evaporated in the heat recovery steam generator by means of hot exhaust gases. This generated vapour flows to the ejector and through its converging-diverging nozzle which accelerated the flow. Thus, the vapour enthalpy is converted into kinetic energy of the flow and the temperature and pressure decrease. At the same time the low pressure at the exit of the nozzle leads to drawing vapour flow from the evaporator. Water evaporates in the evaporator due to low pressure and transferred heat in the refrigerant return stream which is chilled again in the evaporator. The vapour flows of the generator and evaporator are mixed in the ejector and the mixture undergoes a compression shock. In the condenser heat of the flow from the ejector is transformed to an external cooling circuit from a cooling tower or heat store. Finally the flow is divided into two streams of which one undergoes pressure reduction in the expansion valve and enters the evaporator. The other stream flows back to the generator through the feed water pump. [24]

# 5 EXISTING INTERNAL COMBUSTION BASED MICRO-CHP SYSTEMS

In this chapter commercially available small- and micro-CHP systems based on an internal combustion engine are introduced. The core of a combined heat and power unit is the purpose-developed or from other applications converted engine. Purpose-developed engines Honda GE160EV, the Dachs and the Marathon Engine are used in micro-CHP units in the USA, Japan and European market. On the other hand, German Volkswagen uses in cogeneration the gas engine from its car applications. These cogeneration units are suitable to produce required heat demand of residential and commercial buildings and generate electricity as by-product. During this chapter the engine models and their features are presented. Subsequently, the CHP systems powered by the engine are presented. Finally, all system features are collected to a table for a comparison purpose.

## 5.1 Honda GE160EV

Honda Motor Co. has developed the gas-fired four-stroke single-cylinder GE160EV engine for household combined heat and power systems. The engine operates on stoichiometric conditions and uses a three-way catalytic converter in order to reduce $NO_x$, HC and CO emissions. Waste heat of this energy conversion device is recovered from exhaust gas and engine cooling circuit and the heat recovery rate of 65.7 % can be reached. The mechanical energy instead is converted into electricity using Honda's multipolar sine wave inverter power generation technology reaching electric efficiency of 26.3 %. Simultaneously, the engine has 1.0 kW electrical and 2.5 kW thermal outputs. [2]

A special feature of Honda's engine is its longer expansion stroke than intake/compression stroke. An extended expansion stroke is achieved by Honda's unique multi-link expansion linkage mechanism EXlink (Extended Expansion Linkage Engine) which enables increased thermal and fuel efficiency. The shorter compression stroke leads to smaller quantity of compressed fuel and air while EXlink makes possible to expand combustion gas to a greater volume resulting in a high expansion ratio. The achieved expansion ratio is 1.4 times greater than the compression ratio, which leads to maximize power output from the heat energy released by combustion. Additionally, the energy lost caused by moving air into a cylinder is reduced because of the shorter intake stroke. [1]

### 5.1.1 ECOWILL, freewatt and ecoPOWER 1.0

ECOWILL, freewatt and ecoPOWER 1.0 are the micro-CHP systems based on Honda GE160EV engine. These smallest internal combustion engine based cogeneration systems are suitable for single-family residential applications. Considering 1 kW electrical and 2.5 kW thermal outputs 70 % of a typical single-family house electricity demand can be supplied by the ECOWILL, freewatt and ecoPOWER 1.0. [4] Due to this supplementary components are required and different system configurations distinguish the systems from each other. In addition to the energy conversion device the ECOWILL includes a hot water storage of which capacity is 90 liter at high temperature 75 °C and a supplementary boiler. [1] The Freewatt instead combines a gas-fired engine-generator with an advanced boiler or warm air furnace while the EcoPOWER 1.0 a 300-litre multi-function storage cylinder and a wall-hung gas-fired condensing boiler in order to supplement heat output of the engine and meet a current heat demand. [3; 5] In each system generated and stored heat is utilized as hot water supply and space heating in a residential building whereas the electricity generated by the engine is transferred into the building and the rest of the electricity demand is supplied from the national grid. Additionally, Freewatt provides a possibility to use the system as backup power in a situation of a power failure. [1]

The three micro-CHP systems are available in different market area. The ECOWILL is the world’s first internal combustion based micro-CHP system and it was launched on the Japanese market in 2003. During the next years it had been improved until 2011 when the latest model was revealed. ECOWILL has met great success on the Japanese market by installed number of 108 000 cogeneration units in 2011. [1; 2] Freewatt instead is available on the American market. [3] The Europe’s first 1 kW micro-CHP system EcoPOWER 1.0 was launched in 2011 and was developed by the large boiler manufacturer Vaillant in cooperation with Honda. [4]

## 5.2 SenerTec Dachs

The purpose-developed Dachs gas-fired four-stroke internal combustion engine is used as an energy conversion device in the micro-CHP system and was developed by the European market leader German company Senertec. In contrast to Honda’s engine the combustion process is lean burn and therefore, it is provided with an oxidation catalyst in order to reduce exhaust gas emissions. Thermal output of the Dachs is 12.5 kW which can be reached with a combined engine cooling and exhaust gas heat exchanger. The engine is connected to an asynchronous generator of which nominal electrical power is 5.5 kW. This energy conversion device can reach the electrical efficiency of 27 % and the overall efficiency of 88 %. A natural gas running model of the Dachs is the most sold but the engine can run on propane, biodiesel, rapeseed oil and heating oil as well. [6; 7]

The Dachs micro-CHP system is suitable for both small and large residential and commercial buildings. In addition to the engine the system includes supplementary devices and thus it is connected with a 750 liters buffer vessel and 30 liters domestic hot water module at temperature 45 °C in order to enable continuous running of the unit when the heat demand is varying. Furthermore, an external exhaust heat exchanger can be added in order to recover heat from exhaust gas leaving the Dachs at temperature 150 °C. This additional condensing heat exchanger can provide 1.4–2.5 kW thermal output by cooling the exhaust gas to 55 °C which enhances the overall efficiency up to 99 %. The Dach unit can be used also to generate backup power in case of power failure. Moreover an integrated peak load boiler can be added and several micro-CHP units can operate in parallel if additional heat and electricity generation is required. [6; 7]

The Dachs micro-CHP unit is available on the European market especially in German, Austria, Switzerland, Belgium, Denmark, the Netherlands, Portugal, Spain, Italy and the U.K via the SenerTec partner network consisting of more than 350 SenerTec partners. In 1996 the serial production of the Dachs started in SenerTec's own facilities and within the first year 450 units were sold with continuously growing amount of sold units. Thus, in 2009 more than 20,000 Dachs micro-CHP units were sold. [6]

## 5.3 Marathon engine

The gas-fired four-stroke Marathon Engine was developed by the company Marathon engine systems in the USA. The engine operate at stoichiometric conditions and runs on natural gas or propane. In order to reduce exhaust gas emissions the engine is provided with a three-way catalyst that results in very low emission level at steady state operation. In contrast to Honda's engine and the Dachs the marathon engine can operate under varying speed 1200–3600 rpm achieving the part load electrical efficiency of above 20 % all the time. Meanwhile, time speed depending electric output can vary from 1.3 kW to 4.7 kW. [7; 8]

### 5.3.1 ecoPOWER 3.0/4.7

The Marathon Engine is used as core unit in ecoPOWER 3.0 and 4.7 micro-CHP systems developed by Vaillant's subsidiary PowerPlus Technologies. The systems can have the varying electrical output between 1.5 kW and 4.7 kW due to the engines ability to operate efficiently under varying speed conditions. Thus, the electric efficiency is all the time above 20 % and at full load the efficiency of 25 % is achieved. Generated electricity can be used within a building or supplied to the national grid using a frequency converter. In contrast to the Dachs a condensing heat exchanger is already included in the ecoPOWER 3.0 and 4.7 standard versions. Considering this combination the systems' thermal outputs are from 4.7 kW up to 8.0 and 12.5 kW when the overall efficiency of 88.9 % can be reached. [7; 9]

Different auxiliary devices are combined with the core unit. Thus, EcoPOWER 3.0/4.7 can include a gas boiler in order to compensate peak loads and different sizes of buffer vessels in order to compensate peak loads and provide heat storage capacity. EcoPOWER 3.0 and 4.7 are proper for residential and commercial buildings of which energy demands are at least 25 000 kWh/year and 45 000 kWh/year. In case of increasing energy demand a cascade use of ecoPOWER 4.7 units enables to meet energy requirements. [10]

## 5.4 Yanmar

The lean-burn 3-cylinder Miller Cycle gas engine was developed by the small diesel engine producer Yanmar in the USA in order to have a core unit in a combined heat and power system. The engine can run on natural gas or propane and the optimal ignition timing and amount of excess intake air reduce $NO_x$ emissions and fuel consumption. The engine's thermal energy is recovered at temperature 158 °C which gains heating water at temperature 70 °C. Thus, the thermal output of 16.8 kW is provided and produced hot water is used directly or stored into a system combined heat store. Simultaneously the electrical output of 10 kW is generated by the electrical power generator and inverter and thus can be used on-site or fed to the electric grid. The system is suitable for applications with greater energy demand like fitness centers, restaurants, hotels and multi-family houses. In addition to the American market a clean tech solutions provider ENER-G offers the combined heat and power system powered by Yanmar in the U.K. Hence, the system is also available with electrical outputs of 4 kW and 25 kW. [11; 12]

## 5.5 Volkswagen 2.0l CNG-EcoFuel

A state-of-the-art natural gas-fired engine CNG 2.0 was developed by Volkswagen and is similar with engines of Volkswagen's car models Caddy and Touran. The system's electrical output of 19 kW is generated via an asynchronous alternator and fed into the electric grid. Meanwhile, the engine's waste heat is recovered, stored and utilized in the house as hot water and heating. Thus, the thermal output of 32 kW and the overall efficiency of 90 % are achieved. Low CO and $NO_x$ are achieved CO < 125 mg/Nm$^3$ and NOx < 100 mg/Nm$^3$. In addition to natural gas the engine can run on biogas, which make it renewable energy source with zero emissions. [13]

### 5.5.1 'Zuhausekraftwerk'

The 'ZuhauseKraftwerk' or "home power plant" is an innovative and reliable combined heat and power system of which main purpose is to generate heat for a building and electricity for the electric grid. Volkswagen CNG 2.0 engine called EcoBlue powers this

CHP-system that includes different sizes and number of the buffer vessels depending on the application. The domestic fresh water station and the heater circuit distributor instead are integrated in the ‘ZuhauseKraftwerk’ unit. Compared with conventional heat and power generation the natural-gas-fired ‘ZuhauseKraftwerk’ can reduce $CO_2$ emissions up to 60 %. [15; 17]

The ‘ZuhauseKraftwerk’ differs from other combined heat and power systems presented in this chapter due to its purpose not only to be a single and separate cogeneration unit but to be a part of a CHP cluster. Hence, the power company Lichtblick and Volkswagen started cooperation in 2009 and are working towards decentralized intelligent energy supply. Lichtblick is German’s biggest independent green energy provider and has over 590 000 customers and 400 employs in Hamburg. The power company aims to build a network of 100 000 ‘ZuhauseKraftwerk’ units in order to have the large virtual power plant intelligently controlled by LichtBlick via the mobile phone network. Thus, the virtual power plant has a capacity of 2 000 MW that corresponds to two nuclear power plants. As a virtual power plant the cluster of the ‘ZuhausKraftwerk’ units can provide a quickly compensation for weather dependent and fluctuating solar and wind power supply. For example, if wind power is not available and the electricity price is high, LichtBlick can by means of a remote control to adjust activity of the ‘ZuhauseKraftwerk’ units in order to feed the electric grid. The key feature of the cluster is fast start-ups and shutdowns that are impossible to implement with conventional base-load power plants. [13; 14; 16]

## 5.6 Conclusion

The main purpose of this chapter was to demonstrate different kind of combined heat and power systems based on internal combustion engine suitable for residential and commercial buildings and available on the market. As can be seen most of the systems are used as single and separate heat-driven systems in order to cover a proportion of the hot domestic water and space heating demand of the building and thus, the electricity is generated as by-product to utilize in the house or to feed into the grid. Typically, the systems include an additional boiler and heat store in order to meet peak loads and run the cogeneration unit continuously. However, the ‘ZuhauseKraftwerk’ can be sad to be heat- and power-driven system because it has to cover heat demand and generate electricity to the grid when necessary. The specifications of the presented natural gas-fired CHP systems are enumerated in table 2.

**Table 2:** CHP-unit design and operational data [1; 2; 6; 7; 8; 9; 11; 12; 13; 17]

| **CHP unit** | **ECOWILL, freewatt, ecoPOWER 1.0** | **ecoPOWER 3.0/4.7** | **SenerTec Dachs** | **Zuhause-Kraftwerk** | **Yanmar** |
|---|---|---|---|---|---|
| **Engine** | Honda GE160EV | Marathon engine | Dachs | Volkswagen CNG 2.0 | Miller Cycle gas engine |
| **Cylinders** | 1-cylinder | 1-cylinder | 1-cylinder | 4-cylinder | 3-cylinder |
| **Displacement** | 110/163 $cm^3$ | 272 $cm^3$ | 578 $cm^3$ | 2000 $cm^3$ | |
| **Electrical efficiency** | 26.3% | 24.7% | 27% | 33.5% | 31.5% |
| **Thermal efficiency** | 65.7% | 65.7% | 61% (72%) | 56.4% | 53.5% |
| **Overall efficiency** | 92.0% | 88.9% | 88% (99%) | 90% | 85% |
| **Electrical/ Thermal output** | 1.0 kW/2.5 kW | 1.3–4.7 kW/4.0-12.5 kW | 5.5 kW/ 12.5 kW (14.8kW) | 19 kW/32 kW | 10 kW/16.8 kW |
| **Voltage** | 230 V, 50/60 Hz, single phase | 400 V, 50 Hz, 3 ~ | 230/400 V, 50 Hz, 3 ~ | 400 V / 50 Hz, 3 ~ | 240/120 ACV, 60 Hz, single phase |
| **Transmission method** | Inverter | Frequency converter | Asynchronous generator | Asynchronous alternator | Inverter |
| **Sound level** | < 52 dB (A) | < 56 dB (A) | 52–56 dB (A) | < 50 dB (A) | 56 dB (A) |
| **Operating speed** | 1950 rpm | 1400–3600 rpm | 2450 rpm | 1500 rpm | 1700 rpm |
| **Maintenance interval** | 6000 hours | 4000 hours | 3500 hours | 5000 hours | 10000 hours |

**Table 2.** CHP-unit design and operational data [1; 2; 6; 7; 8; 9; 11; 12; 13; 17]

| | | | | | |
|---|---|---|---|---|---|
| **Dimensions** | ECOWILL: W: 58 cm, L: 29.8 cm, H: 75 cm<br>ecoPOWER 1.0: W: 118 cm, L: 113.2 cm, H: 113.2 cm | W: 76.2 cm, L: 137.0 cm, H: 108.5 cm | W: 72 cm, L: 107 cm, H: 100 cm | W: 85.5 cm, L: 116.5 cm, H: 170.0 cm | W: 147 cm, L: 90 cm, H: 179 cm |
| **Weight** | ECOWILL: 71 kg<br>ecoPOWER 1.0: 100 kg | 395 kg | 530 kg | 700 kg | 756 kg |
| **Price** | | 6666 €/$kW_{el}$ / 4255 €/$kW_{el}$ | 3818 €/$kW_{el}$ – 4181 €/$kW_{el}$ | Installation: 5 000 € (not ownership) | |

The electrical efficiencies of the systems are around 24–33 % and the overall efficiencies up to 92 % are achieved. Usually, the engine is four-stroke and single cylinder but the number of cylinders can be higher like in Volkswagen CNG 2.0 and Miller cycle gas engine. The electrical and thermal outputs of the systems vary up to 19 kW and 32 kW. Within the definition of micro-scale CHP systems are ECOWILL, freewatt, ecoPOWER 1.0/3.0/4.7, SenerTec Dachs and Yanmar. In terms of residential and commercial buildings the important specification is the required maintenance interval of the unit. Yanmar requires maintenance only in the intervals of 10 000 hours whereas the other units require maintenance within the intervals below 6000 hours. However, the main interest is moving towards heat- and power-driven systems in near future and units, like the 'ZuhauseKraftwerk', will be more interesting. Furthermore, increasing amount of fluctuating renewable energy in the grid makes it necessary to have fast balancing energy.

## 5.7 Sources


[1] Hiroki Tanaka. New Ecowill- a new generation gas engine micro-CHP. 2011, Osaka gas co., LTD.

[2] Honda Motor Co., Ltd. Honda to Begin Sales through Gas Utilities of All-New Ultra-Efficient Household Gas Engine Cogeneration Unit Featuring World's Most Compact Design. May 23, 2011, [referred 26.3.2012]. Available: http://world.honda.com/news/2011/p110523Gas-Engine-Cogeneration/index.html

[3] freewatt. Products. 2008, [referred 26.3.2012]. Available: http://freewatt.com/products.asp

[4] Energy Efficiency News. Vaillant and Honda launch micro-CHP systems for homes. 9 February 2011, [referred 26.3.2012]. Available: http://www.energyefficiencynews.com/articles/i/3789/

[5] Honda Motor Co., Ltd. Vaillant and Honda Present Micro-Combined Heat and Power System for Home Use. 3 February 2011, [referred 26.3.2012]. Available: http://world.honda.com/news/2011/c110203Micro-Combined-Heat_power-System/index.html

[6] SenerTec. Dachs. [referred 26.3.2012]. Available: http://www.senertec.de/index.php?id=3&L=1

[7] Robert Beith. Small- and micro combined heat and power (CHP) systems: advanced design, performance, materials and applications. 2011, Woodhead Publishing. 528 pgs.

[8] Marathon engine systems. Cogeneration. [referred 31.3.2012]. Available: http://www.marathonengine.com

[9] Vaillant. Kraft-Wärme-Kopplung. 2012, [referred 31.3.2012]. Available: http://www.vaillant.de/Produkte/Kraft-Waerme-Kopplung/

[10] Vaillant. Mini-KWK-Systeme ecoPOWER 3.0/4.7. 2012, [referred 31.3.2012]. Available: http://www.vaillant.de/Produkte/Kraft-Waerme-Kopplung/Blockheizkraftwerke/produkt_vaillant/mini-KWK-System_ecoPOWER_3.0_und_4.7.html

[11] Ener-G. Micro CHP operation and maintenance. 2010, [referred 2.4.2012]. Available: http://www.energ.co.uk/index896.aspx

[12] Yanmar. Energy Systems. [referred 2.4.2012]. Available: http://us.yanmar.com/products/energy-systems/

[13] Volkswagen Powersystems. Volkswagen EcoBlue – The drive for your energy. 2011, [referred 31.3.2012]. Available: http://www.volkswagen-antriebssysteme.com/en/produkte/blockheizkraftwerk.html

[14] LichtBlick. ZuhauseKraftwerk. [referred 31.3.2012]. Available: http://www.lichtblick.de/h/english_information_395.php

[15] Green Car Congress. Volkswagen and LichtBlick Partner on Home Combined Heat and Power Systems; LichtBlick Plans a “SchwarmStrom” for 2,000 MW of Decentralized Power. 9 September 2009, [referred 31.3.2012]. Available: http://www.greencarcongress.com/2009/09/volkswagen-lichtblick-20090909.html

[16] ARGION Global network for energy. 2011, [referred 1.4.2012]. Available: http://www.agrion.org/first_mover_advantage/agrion-en-Miniature_power_plants_to_create_swarm_power_.htm

[17] LichtBlick. Technisches datenblatt. ZuhauseKraftWerk. 28 March 2012, [referred 3.4.2012]. Available: http://www.lichtblick.de/pdf/zhkw/info/zhkw_technische_daten.pdf

# 6 METHODOLOGY

## 6.1 Overview

In Chapter 5, internal combustion engine based micro-combined heat and power systems on the market were presented. With the exception of the 'ZuhauseKraftwerk', all presented systems are meant to be individual heat-driven units in its owner's building. However, an electricity utility can be an owner and controller of a high number of small- and decentralized CHP systems within different heat sinks, such as residential and commercial buildings. These remote controlled systems provide heat as space heating and domestic hot water and support for the electric grid during peak loads, such as lunch- and dinnertime. Additionally, fluctuating renewable energy production can be supported during undesirable generation conditions. Hence, an interest in valuable and profitable electricity generation of decentralized micro- and small CHP-systems is increasing. These systems are becoming more important meanwhile a proportion of renewable energy and overall energy consumption is increasing.

In Chapter 3, three different CHP technologies were presented and assessed. Compering of the CHP technologies' key features led to the selection of the internal combustion engine based CHP technology to be most suitable for desired residential and commercial building environment and for power-driven system considering its good dynamic behaviour.

The interdisciplinary model of a single internal combustion engine based CHP system was constructed in order to make a step towards modelling of a CHP cluster in the future work. The framework of the CHP model is presented in Figure 10. It consists of three main fields:

- Physical model of cogeneration unit and thermal storage
- Techno-economic analysis
- Outputs

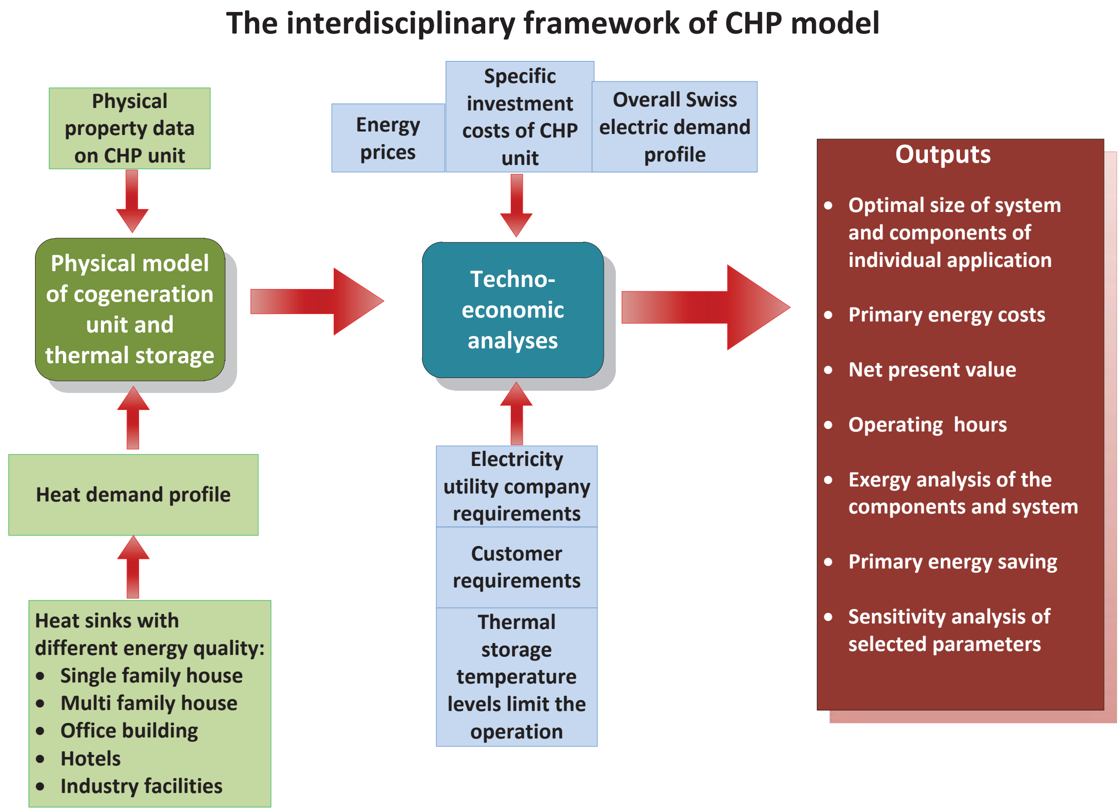


***Figure 10.*** *Interdisciplinary framework*

The first field is mainly influenced by the physical property data on the CHP unit. Secondly, heat demand profile of a heat sink and occupant distributions have an influence to the physical model. In addition to this physical model the latter field is influenced by prices of energy forms, specific investment costs of the CHP system and the overall Swiss electric demand profile which influences to the electricity market price. On the other hand, the customer, electricity utility and temperature limits in the thermal storage have an impact to operation strategies of the CHP system and thus, they influence to the techno-economic analysis field.

Finally, the main outputs of the CHP model are collected together on the third field. The optimal size of the cogeneration unit and thermal storage depends on heat demand profiles and cost minimization from the electricity utility point of view. Primary energy costs are related to operating hours and they present fuel costs. An assessment of payback time evaluates a time period in which the initial investment costs are covered by annual revenue. The exergy analysis of the CHP system calculates exergy content of a thermal storage and exergy efficiencies of a CHP unit, engine cooling and exhaust gas heat exchanger, and internal combustion engine. The concept of the primary energy saving evaluates energetic performance of a combined heat and power generation in terms of saved primary energy compered to generating heat and power separately in two different technologies. The sensitivity analysis presents influences to the model if some parameter is systematically varied.

The impact factors of the CHP system's operating strategy are presented in Figure 11. Three parties with their main criteria influence to the operation of a CHP system:

- Electricity utility
- Customer
- Thermal storage

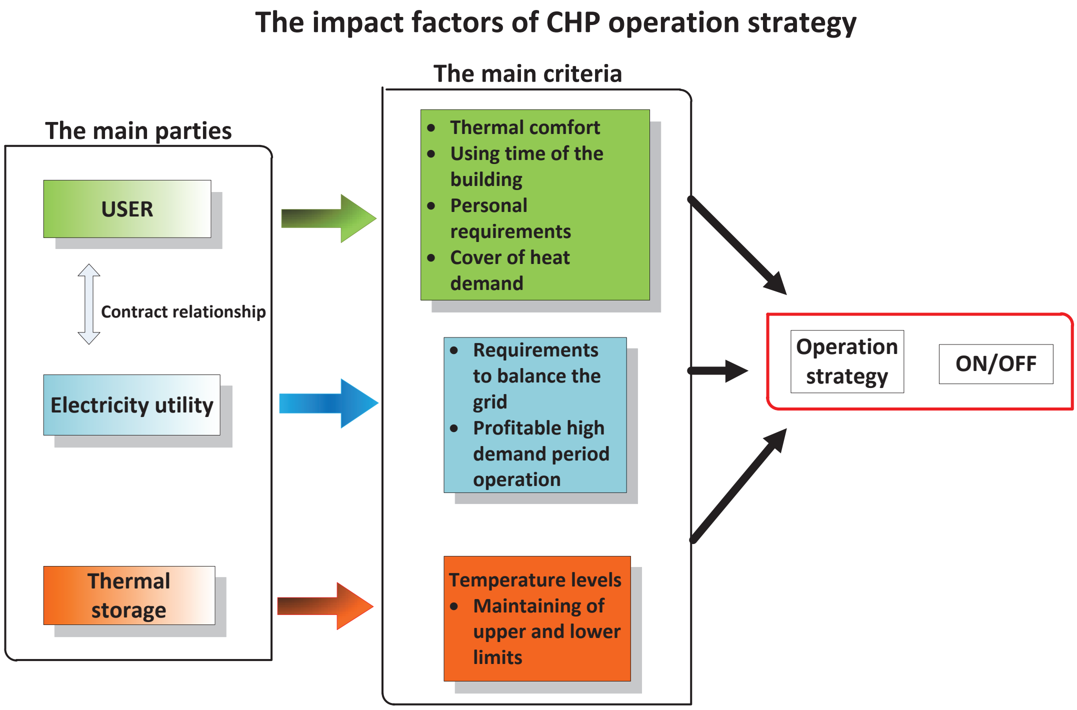


***Figure 11.*** *Operation strategy*

The electricity utility has the criteria to generate balancing energy to the electric grid during peak loads and to support fluctuating renewable energy production. These important criteria define the CHP system operation period due to the high electricity price and valuable balancing energy. On the other hand, the customer, as a heat sink owner, has a heat supply contract with the electricity utility and requires thermal comfort in the building. Thus, the heat demand of the building has to be covered during the operation hours. On the other hand, the CHP system is within the customer's building and thus he can have personal requirements concerning timing of CHP operation, such as a night time operation is not allowed. Finally, the operation strategy has to fulfil the criteria of the maintaining desired temperature level in the thermal storage in order to provide space heating and domestic hot water, or industrial process heat at required temperature. The operation strategy concerns a single CHP unit and differs also within a cluster operation in the future. Thus, depending on criteria some units can be switched off whereas some are switched on.

## 6.2 The influence relations in the CHP model

The scheme of the influence relations in the CHP model was constructed in order to explain relations and the approach of modeling a CHP system. This scheme is presented in Figure 12 and the details of all blocks are explained. At the beginning two main parties of the model are a heat sink and electricity utility which have an impact on power and performance of a CHP unit. From the heat sink's point of view heat demand profile has to be covered over a year and on the other hand, the electricity utility wants to maximize a benefit of running the unit during a specific time period. The overall Swiss electric demand profile has an impact on high demand periods and the electricity price in the liberalized electricity market. In Switzerland electricity is sold to a customer with a low and high tariff depending on time of a day and a date of a week. The transition towards the liberalized electricity market is expected in the future.

The power and performance of the CHP system and high demand periods have an impact on system parameters in the "CHP" block. Additionally, the economic parameters are strongly influenced by the power and performance of the system and the "CHP" block parameters. The electricity price is determined by the overall Swiss electric demand profile and influences to the "Prices" block. Finally, these three blocks have an impact to the "Economic analysis" block where the seasonal profitability, net present value and payback period of the system are assessed.

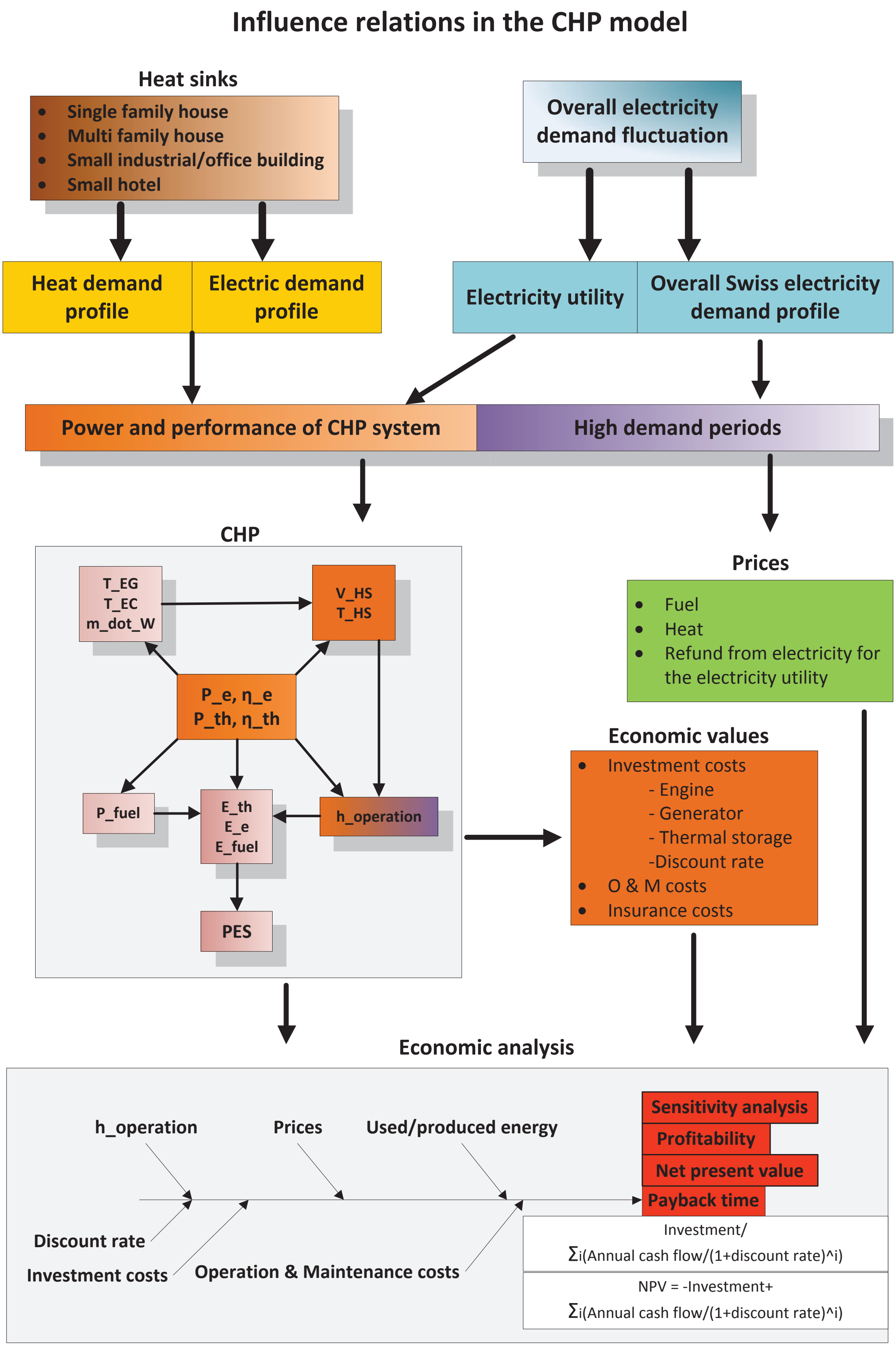


*Figure 12.* *Influence relations in the CHP model*

### *Heat sink*

The heat sink presents a residential or commercial building with high annual heat demand, such as a single- and multifamily house, small office and industrial building or hotel. The heat sink can be also a cooling demand if a CHP system is extended to a

CCHP system. In addition to a type, the heat sinks can differ from each other by construction year and material which influences strongly to the heating demand profile.

***Heat demand profile***

The heat demand profile consists of space heating and domestic hot water consumption. The space heating demand is strongly influenced by the type and construction year of a building whereas domestic hot water demand depends on an occupant distribution in a building.

***Electric demand profile***

The electric demand profile presents annual electrical demand of a heat sink. A part or total demand can be covered by generated electricity of a CHP unit. On the other hand, a surplus or all generated electricity can be sold to the grid and electricity demand is covered from the grid.

***Overall electricity demand fluctuation***

Overall electricity demand fluctuation presents a behavior of the electric grid in Switzerland. This fluctuation influences to the overall Swiss electric demand profile and to the behavior of an electricity utility.

***Electricity utility***

The electricity utility has a contract with a heat sink owner. The company can run a CHP unit by remote control during peak loads in order to gain a benefit of electricity generation to balance the grid and get the high electricity price. Due to this the electricity utility has a strong influence to the power and performance of a CHP system because the larger engine can run less time and gain the high electricity price during the peak loads. The smaller engine has to run longer time in order to cover same heat demand.

***Overall Swiss electric demand profile***

The overall Swiss electric demand profile has an impact on high demand periods and electricity price. The electricity market price for the electricity utility fluctuates depending on the overall electricity demand profile. During the high demand periods, such as lunch- and dinnertime, the price is higher and vice versa. This fluctuation defines the most profitable time to operate the CHP unit.

***Power and performance of the CHP system***

The power and performance of a CHP system is defined by the heat demand profile of a heat sink and by the criteria of an electricity utility. This block influences strongly to parameters in the “CHP” and the “Economic parameters” block.

### *High demand periods*

High demand periods are influenced by the overall Swiss electric demand profile. These periods influence to timing of a CHP unit operation due to profitability to run the unit during the high electricity price and during timing of the grid-balancing requirement.

### *Prices*

The “Prices” block includes all unit prices of energy forms. These prices have a strong impact on the “Economic analysis” block and profitability of a CHP system for an electricity utility. The current prices of exported electricity, fuel, and heat are presented in the “Prices” block. The fuel and heat prices are influenced by a current market situation. The electricity price as a refund for the electricity utility varies depending on the overall electric demand profile. This variation leads to the assumption of the liberalized electricity market, which is a market place for electricity generators and buyers, and the system is competitive. Thus, the electricity price follows electricity demand and production.

However, in Switzerland the electricity price consists of a low and high tariff depending on time and an overall variation of electricity demand. From Monday to Friday the high tariff is 25 rp/kWh from 7:00 until 20:00 and the low tariff is 15 rp/kWh from 20:00 until 7:00. On Saturdays the high tariff is valid from 7:00 until 13:00 and the low tariff is the rest of the day. On Sundays only the low tariff is used.

### *CHP*

The main variables of a CHP system are presented in the “CHP” block. The power of an internal combustion engine, as a CHP unit, has the strongest influence to all other system variables. The electrical and thermal power of the unit are, in contrast, influenced by a heat sink and electricity utility in order to cover heat demand and maximize a benefit during high electricity price periods. The smaller engine size leads to longer operation time (h_operation) in order to cover the heat demand and less electricity generation during the profitable peak demands. On the other hand, the larger engine size results in a higher amount of generated electricity during the high price periods.

The temperatures of an engine exhaust gas (T_EG) and engine cooling circuit outlet (T_EC) together with water mass flow (m_dot_W) between a CHP unit and thermal storage are influenced by the power of the engine. Those four parameters affect to a volume (V_HS) and current temperature level (T_HS) of the thermal storage. The maximum temperature of the thermal storage depends on the engine cooling circuit outlet temperature and has to be lower in order to ensure heat transfer from the engine. On the other hand, the minimum temperature depends on the required domestic hot water temperature or the outgoing temperature for space heating.

The higher electric power of an engine the higher a required fuel power (P_fuel) but the increased electrical efficiency, in turn, decreases the required fuel power. These powers influence to seasonally generated heat and electric energy and required primary energy. Hence, the amount of generated and required energies affect to primary energy saving (PES).

***Economic parameters***

The block of the economic parameters is strongly influenced by the power and performance of a CHP system. The initial investment costs of a CHP system include installed costs and the investment of each system component. The discount rate of the investment is used to discount a sum of future annual cash flow to present value. The higher the discount rate the higher risk the investment has and the investment is expected to get back faster. The discount rate is used to calculate the net present value of the investment after certain time period, such as the lifetime of the system. The operation and maintenance costs are influenced by a number of the operating hours and the electric power of the CHP unit. The smaller the engine the higher operation and maintenance costs due to more operating hours.

***Economic analysis***

The block of the economic analysis is used to assess economic viability of a CHP system. The main influences to the economic viability come from the "CHP", the "Prices" and the "Economic parameters" block. In case of an electricity utility as an owner of a CHP system a payback time, net present value and seasonal earnings before interest, taxes, depreciation and amortization (EBITDA) can be calculated. The CHP unit generates electricity to the electric grid and heat for a heat sink. The owner of the heat sink is a customer of the electricity utility and pays the installation costs of the CHP system and heat price according to a contract between the utility and customer.

Profitability of the system can be assessed from the electricity utility company's point of view. The revenue of the system comes from sold heat and generated electricity. Total costs are influenced by the operation and maintenance costs and the fuel price. These total revenues and costs with discount rate are used to assess the payback time and net present value.

## 6.3 Physical model

The physical model of a combined heat and power system was constructed into Matlab/Simulink environment. In chapter 4 the different CHP components and configurations were introduced and the basic configuration in Figure 5 with the cogeneration unit and thermal storage was selected in order to construct the physical model. In order to develop a simplified thermal model of a combined heat and power system only the main components: an engine cooling heat exchanger, exhaust gas heat exchanger and thermal storage were taken into account. With information of the heat demand profile of a heat sink and physical property data on the CHP system, the mathematical equations can be solved simultaneously for simplified model over desired time period in order to assess thermal performance of the model with varying input data. In addition to the thermal model generated electricity and the fuel mass flow were taken into account in the physical model. Thermal masses of the system components were not taken into account expect the thermal storage. Additionally, steady state was assumed and start up dynamic was not taken into account.

***Matlab/Simulink***

The Matlab is a programming environment for numerical computation and data analysis where Matlab code is typed to the Command Window or text files can be created containing functions and Matlab code. The Simulink environment is integrated with the Matlab software environment for modeling and simulating dynamic time-varying systems. The main idea in the Simulink is to convert mathematical equations, which describe the behavior of a model, into graphical form with different blocks from customized set of block libraries. The interactive graphical environment of the Simulink helps to create understandable models. Due to integration with the Matlab input data can be exported to the Simulink model from the Matlab Workspace or ‘m’-file. In contrast, the output data of the Simulink model can be exported to the Workspace.

### 6.3.1 Mathematical equations

The cause and effect diagram in Figure 13 for the physical model was generated in order to find mathematical equations to describe the thermal behavior of the model. A control volume approach was applied to the components mentioned above in order to separate them. The energy balance of the thermal storage is fulfilled when the rate of change of energy inside the storage is equal to the rate of in- and output of energy to the control volume. The current temperature of the thermal storage has an influence to the outlet temperature of the engine cooling heat exchanger which has again an effect on the outlet temperature of the exhaust gas heat exchanger. A difference between the current temperature of the thermal storage and the outlet temperature of the exhaust gas heat exchanger affects to the thermal output of the CHP unit. On the other hand, the current thermal storage temperature has an influence on the rate of heat losses from the storage. The other part of the heat losses in the system is generated in the running CHP unit.

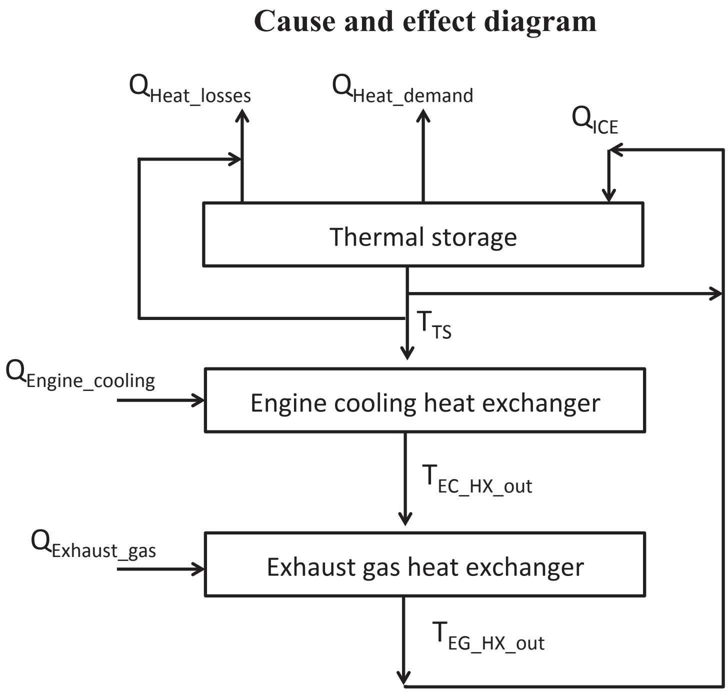


***Figure 13.*** *Cause and effect diagram*

In order to have a simplified thermal model of the CHP system, the thermal storage was modeled as a single node model and the thermal stratification in the store was not taking into account. By considering the First law of thermodynamics

$$m_{TS}c_{pW}\frac{dT_{TS}}{dt} = Q_{CHP} - Q_{Heat\_demand} - Q_{Heat\_losses} \tag{5}$$

The heat addition from the CHP unit consists of heat removed from the engine cooling and exhaust gas heat exchangers.

$$Q_{CHP} = Q_{engine\_cooling} + Q_{exhaust\_gas} \tag{6}$$

The engine cooling heat exchanger was modeled with the following equation.

$$Q_{engine\_cooling} = m_{dot\_water}c_{pw}\left(T_{EC\_HX\_out} - T_{TS}\right) \tag{7}$$

The definition of the heat exchanger effectiveness was used to model the exhaust gas heat exchanger.

$$\varepsilon = \frac{C_C\left(T_{C,out}-T_{C,in}\right)}{C_{min}\left(T_{H,in}-T_{C,in}\right)} = \frac{C_W\left(T_{EG\_HX\_out}-T_{EC\_HX\_out}\right)}{C_{EG}\left(T_{EG}-T_{EC\_HX\_out}\right)} \tag{8}$$

The outlet temperature of the exhaust gas heat exchanger was derived from the equation (8).

$$T_{EG\_HX\_out} = \frac{\varepsilon m_{dot\_EG} c_{pEG}\left(T_{EG} - T_{EC_{HX_{out}}}\right)}{m_{dot\_W} c_{pW}} + T_{EC\_HX\_out} \tag{9}$$

The modeled heat losses consist of the losses from the thermal storage and the CHP unit and are described with following equations.

$$Q_{HS\_losses} = U_{HS} A_{HS} (T_{TS} - T_{ambient}) \tag{10}$$

$$Q_{CHP\_losses} = U_{CHP} A_{CHP} \left(T_{CHP_{inside}} - T_{ambient}\right) \tag{11}$$

The overall heat transfer coefficient U is given by

$$\frac{1}{U} = \frac{1}{h_{c,i}} + \frac{L_{inside}}{k_{inside}} + \frac{L_{insulation}}{k_{insulation}} + \frac{L_{outside}}{k_{outside}} + \frac{1}{(h_{c,o} + h_{r,o})} \tag{12}$$

Where,

$$h_{r,o} = 4\varepsilon\sigma T_m^3 \tag{13}$$

The convective heat transfer coefficients for the thermal storage were taken as free convection in water and air. For the CHP unit these coefficients were taken as forced and free convection in air. The forced convection heat transfer coefficient inside the CHP unit was used due to forced air-cooling inside the unit. In addition to the convective heat transfer coefficient the conductivity coefficient were used for different materials from the table in [15].

Mechanical power of the CHP unit is converted into electrical power using a generator with certain efficiency $\eta_g$.

$$P_e = \eta_g P_{mech} \tag{14}$$

The fuel power is derived from the electrical power of the unit when the fuel mass flow can be calculated by following equations:

$$P_{fuel} = \frac{P_e}{\eta_e} \tag{15}$$

$$m_{dot\_fuel} = \frac{P_{fuel}}{LHV} \tag{16}$$

These mathematical equations were implemented in the Matlab/Simulink in order to have the physical model of the cogeneration unit and the thermal storage.

### 6.3.2 CHP-model operation control

The ON/OFF control strategy was implemented in the Simulink in order to control behavior of the physical model considering all criteria of each party in Figure 10. In order to keep the temperature in the thermal storage within the desired range a relay block and defined set point was used to control the current temperature level. The customer and electricity utility has own operation criteria when the CHP unit is allowed to run and when it has to run in order to generate benefit for the utility. These criteria were implemented as a pulse generator blocks that generates positive pulse when the CHP unit should run. The priority levels of the control strategy were defined in order to show who has the strongest and weakest impact on the control. These levels are presented in the Figure 14.

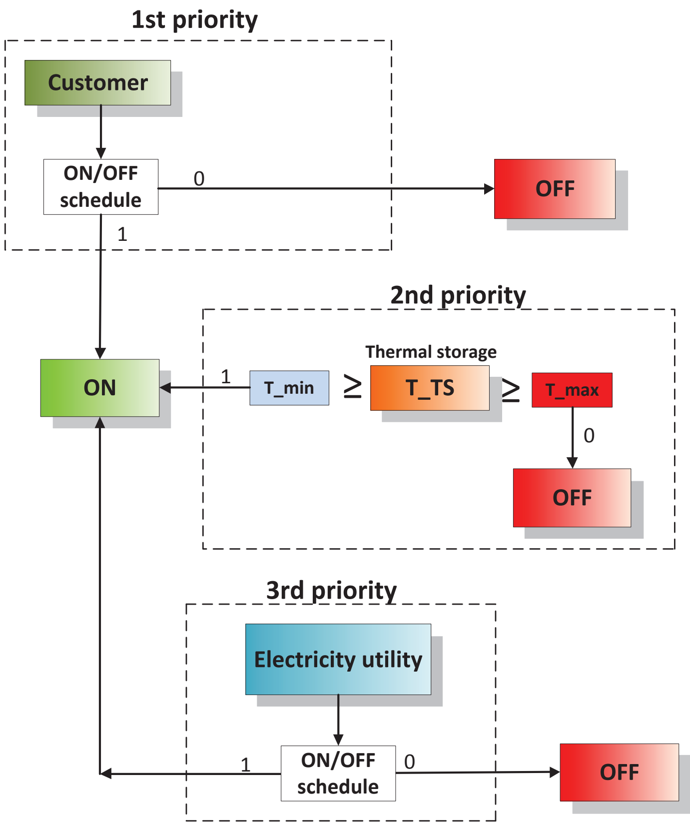


***Figure 14.*** *The priority levels of the CHP control*

The customer has the first priority to influence to the ON/OFF control and he decides which time of day the CHP unit is allowed to run. If the output is off, the other priority levels do not have any influence to the control. In case of the positive output from the first priority level, the second priority level can turn the unit on or off if the temperature (T_TS) in the thermal storage undercut or exceeds the determined minimum and maximum temperatures (T_min, T_max). If the output is positive from the first and second priority level, the electricity utility, on the third level, can allow the unit run during an desired time period, such as lunch- and dinnertime.

On the other hand, there could be only two priority levels which are the thermal storage temperature level and electricity utility. Thus, the CHP control can follow the electricity price on the market and the electricity utility set an electricity price threshold. This threshold allows the CHP run if the electricity price on the market is equal or higher than the threshold and the temperature in the thermal storage is between upper and lower limit. Thus, the electricity utility can maximize the benefit of the operation and the operation during the low electricity price is avoided.

### 6.3.3 Thermal storage volume

The thermal storage volume has a significant role in the model. The large volume enables longer storage time and operation of the CHP unit is more independent on heat demand. The larger volume enables also usage of the larger unit with the higher electrical power when the benefit of electricity generation during the high electricity price is higher. The smaller volume leads to higher duty cycle of the engine if the engine is too large. On the other hand, increasing external area of the storage results in the higher heat losses. If thermal power of a CHP unit and daily operation time is defined, appropriate thermal storage volume has to fulfill energy balance at least over the coldest day. The energy balance is described as:

$$c_{pW} m_{TS} \Delta T_{TS} = E_{demand\_storage\_time} + (E_{charged} - E_{demand\_charging}) \tag{17}$$

The model was simulated with the energy balance defined volume in order to see how temperature in the storage behaves when the heat losses are taken into account. Finally, the simulation result defines the most appropriate volume.

Heat losses from the cylindrical thermal storage can be minimized when the external surface area of the thermal storage is minimized. The area is a function of volume, height and diameter.

$$A_{TS} = f(V_{TS}, h_{TS}, d_{TS}) \tag{18}$$

On the other hand, the volume is described as:

$$V_{TS} = \pi \frac{d_{TS}^2}{4} h_{TS} \tag{19}$$

While,

$$d_{TS} = \sqrt{\frac{4V_{TS}}{h_{TS}\pi}} \tag{20}$$

Now, the area $A_{TS}$ can be described with one variable, which has to be minimized, in order to minimize the area.

### 6.3.4 Exergy analysis

The exergy analysis is used to analyse the exergy performance of a system and is based on the Second law of thermodynamics. This new approach differs from the First law of thermodynamics analysis by taking into account the irreversible production of entropy in the system. The traditional First law based energy analysis has been used to calculate the energy losses and to define the loss of efficiency in any system or process. However, the traditional method has been seen to generate an insufficient analysis from an energy performance point of view. [27]

The exergy approach takes into account quality of energy forms. For example, heat has a lower quality than electricity due to the irreversible entropy production which destroys exergy. The losses in energy quality result in the loss of efficiency. With the exergy analysis the magnitudes and locations of exergy losses can be defined in order to find subject for improvements in the system.

The overall exergy balance of a system is based on the equals of the change in exergy of the system and the total transfer of exergy and exergy destroyed within the system boundaries. [27]

$$Ex_{in} - Ex_{out} - Ex_{destroyed} = \Delta Ex_{system} \tag{21}$$

$$Ex_{destroyed} = T_0 S_{gen} \tag{22}$$

Where $T_0$ is the temperature of exergy reference environment. If the system reaches the temperature of $T_0$, it is in balance with its environment and work cannot be produced anymore. $S_{gen}$ represent irreversible entropy production. Exergy can be transferred over the system boundaries as heat, work or mass flow. In the case of the CHP system exergy is transferred in heat, water and exhaust gas mass flow, and electricity.

The exergy analysis of the basic CHP configuration was constructed into the physical model in order to assess performance of the individual system components. In the model exergy content of the thermal store was calculated and exergy efficiencies of the heat exchangers, internal combustion engine and CHP unit were determined simultaneously with the simulation of the physical model. The exergy efficiencies are derived from products, such as heated water mass flow, and from fuels, such as natural gas or hot engine cooling flow. Only physical and mechanical exergies were taken into account and potential and chemical exergies were neglected. In the Figure 15 the control volumes and exergy flows used in the analysis are presented.

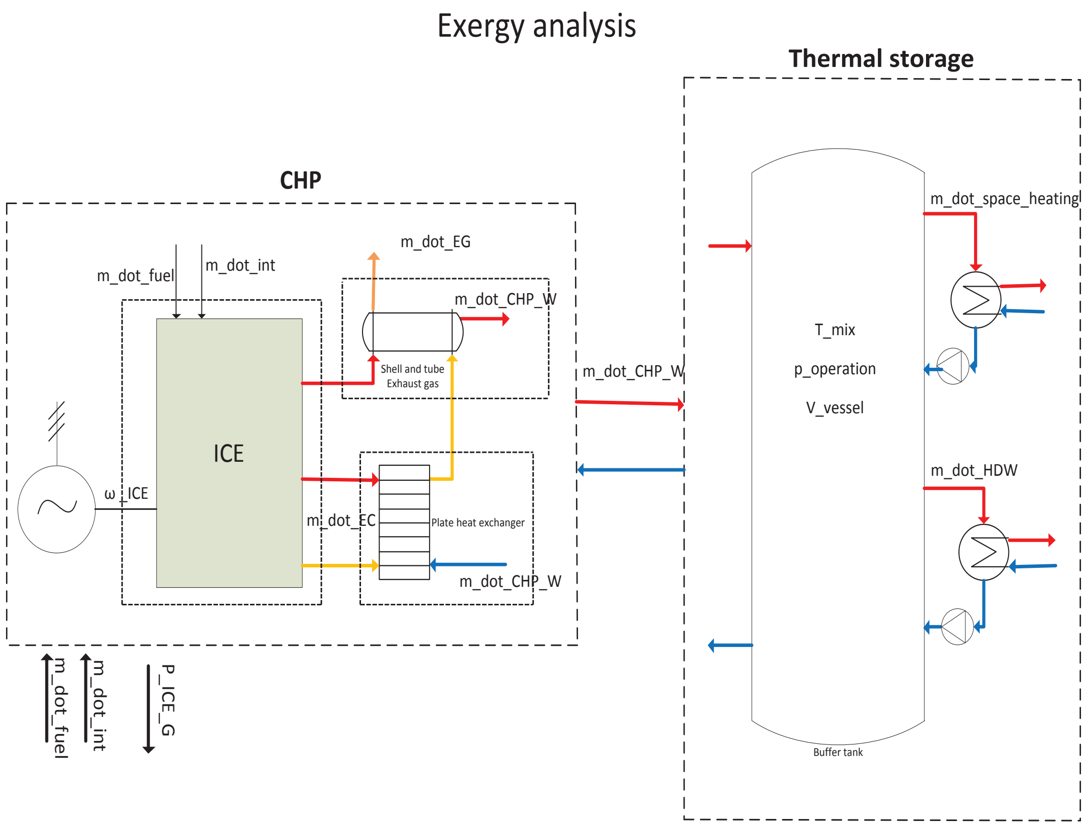


***Figure 15.*** *The CHP configuration with the control volumes and the mass flows*

The exergy content of the thermal storage is followed and varies over time depending on the temperature in the thermal storage. This content is described as:

$$Ex_{HS} = m_{TS}c_{pw}[(T_{TS} - T_{ambient}) - T_{ambient}\ln\left(\frac{T_{TS}}{T_{ambient}}\right)] \qquad (23)$$

The following exergy efficiency equations were presented in [19] and used in the Simulink model. The exergy efficiency of the natural gas fired CHP unit is expressed as:

$$\eta_{Ex\_CHP} = \frac{W_{dot_{net}} + m_{dot\_W}[(h_{out}-h_{in}) - T_0(s_{out}-s_{in})]}{m_{dot\_fuel}e_{fuel}} \qquad (24)$$

The exergy efficiency of the engine cooling heat exchanger is derived from the mass flows of heated water and cooled engine cooling fluid.

$$\eta_{Ex\_EC\_HX} = \frac{m_{dot\_W}[(h_{out}-h_{in}) - T_0(s_{out}-s_{in})]}{m_{EC}[(h_{out}-h_{in}) - T_0(s_{out}-s_{in})]} \qquad (25)$$

The exergy efficiency of the exhaust gas heat exchanger is derived similarly from exergy content of the water and exhaust gas mass flows.

$$\eta_{Ex\_EG\_HX} = \frac{m_{dot\_W}[(h_{out}-h_{in})-T_0(s_{out}-s_{in})]}{m_{EG}c_{pEG}[(T_{EG}-T_0)-T_0\ln(\frac{T_{EG}}{T_0})]} \tag{26}$$

The exergy efficiency of the internal combustion engine is described as:

$$\eta_{Ex\_ICE} = \frac{W_{dot_{net}}+Ex_{EG}+Ex_{EC\_in}}{m_{dot\_fuel}e_{fuel}+Ex_{EC\_out}} \tag{27}$$

Where,

$$Ex_{EG} = m_{dot_{EG}}c_{pEG}T_{EG}(1-\frac{T_0}{T_{EG}}) \tag{28}$$

$$Ex_{EC\_in} = m_c[(h_{EC_{in}}-h_0)-T_0(s_{EC_{in}}-s_0)] \tag{29}$$

$$Ex_{EC\_out} = m_c[(h_{EC_{in}}-h_0)-T_0(s_{EC_{in}}-s_0)] \tag{30}$$

$Ex_{EG}$ and $Ex_{EC\_in}$ describe exergy content of the exhaust gas and engine cooling circuit. They are as products of the internal combustion engine. On the other hand, the $Ex_{EC\_out}$ is described as fuel.

### 6.3.5 Primary energy saving

A method to assess primary energy saving (PES) is introduced in the Directive 2004/8/EC of the European Commission [6]. The PES indicator evaluates energetic performance of combined heat and power generation in terms of saved primary energy compered to generating heat and power separately in two different technologies. The PES indicator is defined as:

$$PES = 1-\frac{E_{fuel}}{\frac{E_{el}}{\eta_{Refe}}+\frac{E_{th}}{\eta_{Refth}}} \tag{31}$$

In order to perform the comparison between the combined heat and power and separated generation, reference values for electric and thermal efficiency of separate generation are required. These harmonized efficiency reference values are presented in the Directive 2004/8/EC [6]. The directive defines the thresholds for high efficiency CHP. If the CHP system size is 1 $MW_{el}$ or more, at least 10% PES value makes it high efficiency CHP unit. On the other hand, the CHP unit with electric power below 1 $MW_{el}$ is high efficiency when PES is at least 0 %. [6]

The harmonized efficiency reference values for natural gas and biogas were added into the lookup tables in the Matlab/Simulink model in order to calculate PES value over simulation time. These efficiency values differ from each other also depending on the construction year of a CHP plant. Additionally, the grid loss correction factors were added into the lookup table. By adding information of the voltage level of a CHP connection, on-site use and export proportion of electricity, fuel type, CHP construction year and type of used heat to the ‘m’-file the simulation model calculates PES value based on used and generated energy of the physical model.

## 6.4 Economical aspect

The economical values of the model were calculated in the Simulink using the simulation results of the physical model and economical parameters. The seasonal economical profitability or seasonal earnings before interest, taxes, depreciation and amortization (EBITDA) takes into account seasonal revenue and costs.

$$Profitability = Revenue - Costs \tag{32}$$

The revenue consist of seasonal incomes from heat and electricity which are described as:

$$I_{Heat} = Pr_{Heat}(E_{th_{sp}} + E_{th_{DHW}}) \tag{33}$$

$$I_{Electricity} = Pr_{Electricity}E_{el} \tag{34}$$

The costs consist of seasonal costs from operation and maintenance, and fuel consumption. These values are presented as:

$$C_{O\&M} = Pr_{O\&M}E_{el} \tag{35}$$

$$C_{Fuel} = Pr_{Fuel}m_{dot\_fuel} \tag{36}$$

The seasonal profitability can be calculated over year in order to have a yearly profit for combined heat and power generation. Hence, the net present value (NPV) of the initial investment S can be calculated over the lifetime of the CHP system by assuming the same yearly profit for each year. The NPV is described as

$$NPV = -S + \sum_t \frac{P_{yearly}}{(1-r)^t} \tag{37}$$

Where the yearly profit is presented as sum of the yearly revenue and costs that depend on yearly operating hours of the CHP unit, electrical power and electrical efficiency, yearly heat demand and energy prices.

$$P_{yearly} = h_{op}P_e Pr_{Electricity} + E_{total\_heat\_demand} Pr_{th} - h_{op}P_e(Pr_{O\&M} + \frac{Pr_{Fuel}}{\eta_e}) \qquad (38)$$

The net present value is used to analyze the acceptability of the initial investment. It takes into account inflation by discounting future cash flow to the present value over certain time period. If the NPV is positive over examined period, the investment is acceptable and there is economic potential. On the other hand, the negative NPV indicates unviable project and some modifications are required in order to have the positive NPV.

## 6.5 Heating demand profile

A single-family house was selected to present a heat sink in the model due to highly fluctuating heat demand over time. In order to have an hourly heating demand profile as input to the physical model of the CHP system, building simulations were set up into the building simulation software Lesosai 7. These simulations were based on the defined sample buildings from two different construction periods which led to difference in building construction materials.

### 6.5.1 Software Lesosai 7

The Lesosai software was developed in 1984 and runs under Windows. This building certification and thermal balance calculation software is developed by E4tech. [28] With the software an hourly heating demand profile can be generated for a specific building. In a demand profile calculation one or more heated or cooled zones can be taken into account. The Lesosai 7 includes a special version of the global weather database of Meteonorm, which enables to simulate buildings all over the world. The Meteonorm database contains average calculations of a long term overall radiation, temperature, wind and dew point. Thus, weather in a typical year is considered. The Lesosai 7 is integrated with the software USai which enables the calculation of the overall heat transfer coefficient (U-value) of external walls and is connected to the database of several materials producers. The Lesosai performs heat balances and certification calculation according to several standard methods based on Switzerland, Luxembourg, France, Italy and the global calculation methodologies. In order to generate hourly heating demand profile the global methodology EN ISO 13790 was used. [29]

The Lesosai 7 has a user-friendly interface where a building structure for a project can be determined from outside to inside. First a separation into heated zones and unheated zones is made. One heated zone includes areas inside the building which are at the same temperature. In contrast, unheated zone refers to zones, such as basements and garages. Next the envelopes, such as external walls, roofs and floors, and rooms are defined. In defining envelopes a specific construction of the envelopes can be determined and U-values calculated by using the included USai software. Finally, the envelope elements, such as windows and doors are defined. Each element can be modified to response a desired building construction. [29]

After simulation an hourly result data can be imported into other software, such as Exel. Monthly and yearly heating energy demand as global results can be seen directly from a results tab. Additionally, results related to the defined zones, rooms and windows are presented. The exported data includes hourly information, among other things, of solar and occupation gains, external, mass and operating temperature and demand for heat energy. Finally, the generated heating demand profile of the defined building can be used as input for the CHP model.

### 6.5.2 Reference buildings

Reference Buildings Description of the IEA SHC Task 44/HPP Annex 38 [30] was used as reference to define sample buildings for the CHP model. Two non-renovated single-family houses from the construction periods of 1946–1960 and 1971–1980 were defined and simulated to be the test cases for the CHP model. Both buildings are located in Zurich, Switzerland and have the same inner geometry. Hence, their main difference lies in construction year, which leads to a difference between heat loads. The construction periods were selected based on the historical data of high heating demand in buildings within these periods. However, the demand decreases towards the period of 1971–1980 due to the used construction materials. The data of different building construction materials within the time periods in Switzerland is investigated in the PhD Thesis of Jérôme Kämpf [31]. Two simplified reference buildings were simulated as one common thermal zone in order to have hourly heating demand profiles. The thermal capacity of the building was taken into account by adding internal walls. Additional thermal bridges were not considered. As simplification the buildings were presented as a living room in the simulation. Due to this the standard occupation distribution of living room was taken into account.

***Geometry***

The inside measurement were fixed to be same for both single-family houses. Different external materials, according to the data of the construction references in Switzerland [31], were added into the envelope definition in the simulation set-up and U-values were calculated. In Figure 16 the building’s structure is presented.

Single-family house

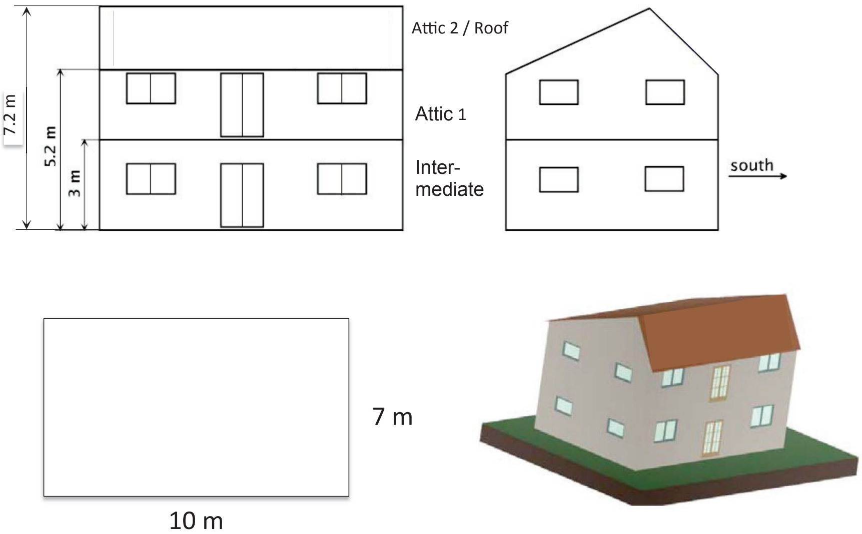


***Figure 16.*** *Geometry of reference buildings [33]*

The buildings have a first and second floor called intermediate and attic 1. The heated net surface area of the building is 140 $m^2$. The attic 2 is an unheated zone. In Figure 17 the walls, roof and floor, which present an active role in the simulation in terms of heat losses, are presented from the East to West and from the North to South sections. In the simulation the roof and floor are taken into account as U-value from the construction reference data [31]. In contrast, each layer of the external walls is considered and U-values are calculated. In Table 3 the used independent dimensions of the buildings are presented. The orientation and number of windows has a strong influence to the amount of solar gains and heating demand. In Table 4 the dimensions, the window area of the specific facade and a number of windows are presented. U-values of the windows were expected to be 2.8 $W/m^2K$ in both buildings.

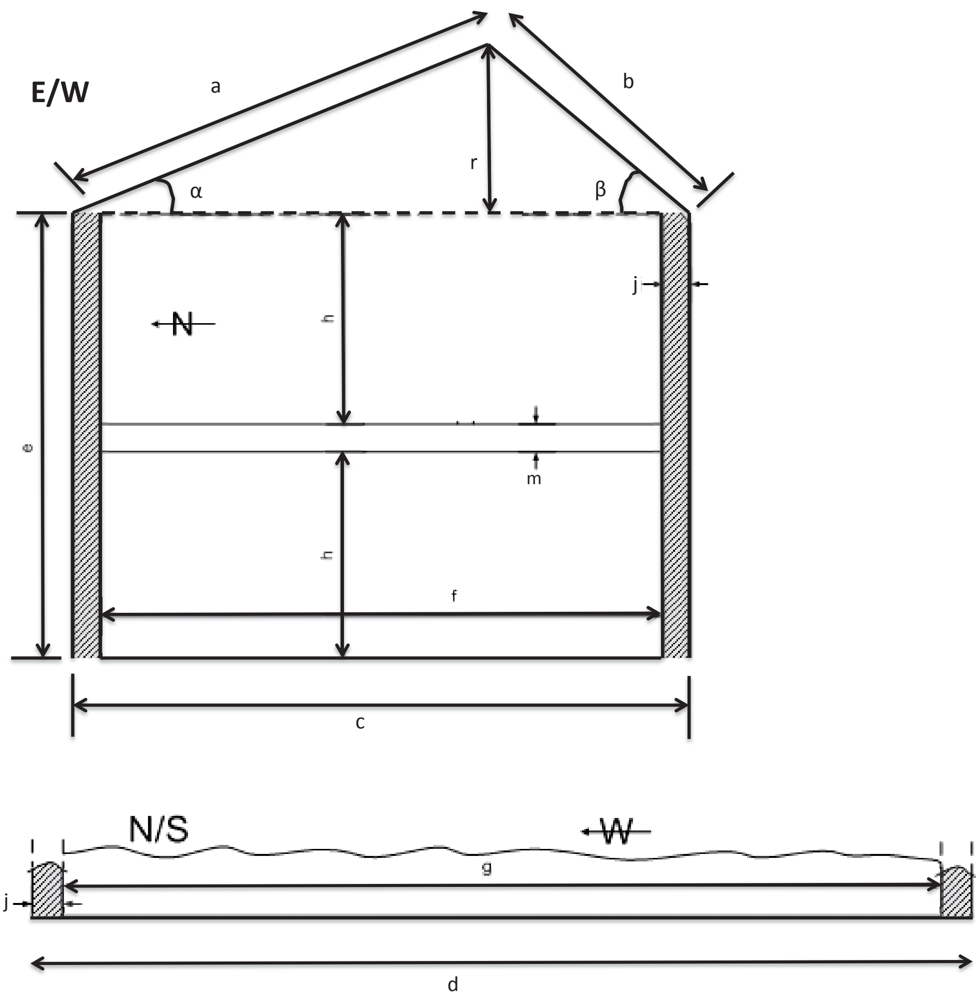


*Figure 17. View of the E/W and N/S sections of the building. [30]*

**Table 3.** The independent dimensions of the reference single-family house

| part | a | b | f | g | h | m | r | α | β |
|---|---|---|---|---|---|---|---|---|---|
| Measure [m] | 5.32 | 2.83 | 7 | 10 | 2.6/2.2 | 0.4 | 2 | 20° | 45° |

**Table 4.** Window areas [m$^2$] of each facade, dimensions and a number

| | East | West | North | South |
|---|---|---|---|---|
| Total area of windows, [m$^2$] | 4 | 4 | 3 | 12 |
| Dimensions and a number of windows | 4* 1m x 1m | 4* 1m x 1m | 1* 1m x 1m + 1* 1m x 2m | 6* 1m x 2m |

The building was separated into different envelope parts presented in Figure 18 in order to make summary tables of areas, volumes, U-values, external walls and measures according to the construction references in Switzerland. Finally, this information was used in the building simulations. The summary Tables 5, 6, 7, 8, 9 and 10 are presented under the topics “Construction period: 1946–1960” and “Construction period: 1971–1980”.

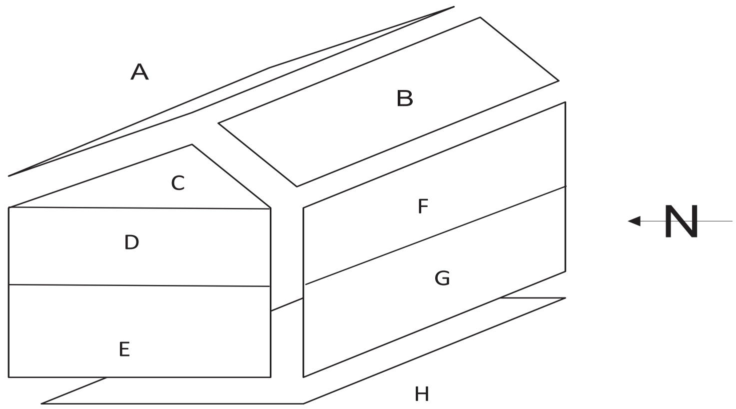


***Figure 18.*** *The envelope parts of the reference building [30]*

## ***Construction period: 1946–1960***

**Table 5.** External dimensions of the reference building corresponding to the independent dimensions and the construction period 1946–1960

| **part** | **d** | **c** | **j** |
|---|---|---|---|
| **Measure [m]** | 10.66 | 7.66 | 0.33 |

**Table 6.** Dimensions, floor areas and gross volume of the reference building from the construction period 1946–1960

| | | | | **Floor gross area [$m^2$]** | **Floor net area [$m^2$]** | **Facade N/S [$m^2$]** | **Facade E/W [$m^2$]** | **Gross volume [$m^3$]** |
|---|---|---|---|---|---|---|---|---|
| **External dimen-sions** | **L [m]** | **W [m]** | **H [m]** | | | | | |
| **Attic 1** | 10.66 | 7.66 | 2.2 | 81.7 | 70 | F=23.45 | D=16.85 | 179.7 |
| **Interme-diate** | 10.66 | 7.66 | 3 | 81.7 | 70 | G=31.98 | E=22.98 | 245.1 |
| **Attic 2** | 10.66 | 7.66 | 2 | | | A/B=55.8 /30.2 | C=7.66 | |
| **Sum** | | | | 163.4 | 140 | | | 424.8 |

**Table 7.** Wall materials, the layer thicknesses, U-values, G-value and infiltration rate according to the construction references in Switzerland

| **Wall inside to outside** | **Material** | **Thickness [m]** | **U-value [W/(m²K)]** | **G-value** | **Infiltration rate [1/h]** |
|---|---|---|---|---|---|
| | Plaster | 0.01 | | | |
| | Solid Brick | 0.04 | | | |
| | Air gap | 0.06 | | | |
| | Solid Brick | 0.20 | | | |
| | Render | 0.02 | | | |
| **Windows** | | | 2.8 | 0.7 | |
| **Roofs** | | | 1.0 | | |
| | | | | | 1.8 |

### *Construction period: 1971–1980*

**Table 8.** External dimensions of the reference building from the construction period 1971–1980

| **part** | **d** | **c** | **j** |
|---|---|---|---|
| **measure** | 10.48 | 7.48 | 0.24 |

**Table 9.** Dimensions, floor areas and gross volume of the reference building from the construction period 1971–1980

| | | | | **Floor gross area [m²]** | **Floor net area [m²]** | **Façade N/S [m²]** | **Façade E/W [m²]** | **Gross volume [m³]** |
|---|---|---|---|---|---|---|---|---|
| **External dimensions** | **L [m]** | **W [m]** | **H [m]** | | | | | |
| **Attic 1** | 10.48 | 7.48 | 2.2 | 78.39 | 70 | F=23.06 | D=16.46 | 172.46 |
| **Intermedi-ate** | 10.48 | 7.48 | 3 | 78.39 | 70 | G=31.44 | E=22.44 | 235.17 |
| **Attic 2** | 10.48 | 7.48 | 2 | | | A/B=55.75 /29.66 | C=7.48 | |
| **Sum** | | | | 157 | 140 | | | 407.6 |

**Table 10.** Wall materials, the layer thicknesses, U-values, G-value and infiltration rate according to the construction references in Switzerland

| **Wall inside to outside** | **Material** | **Thickness [m]** | **U-value [W/(m$^2$K)]** | **G-value** | **Infiltration rate [1/h]** |
|---|---|---|---|---|---|
| | Plaster | 0.01 | | | |
| | Hollow Brick | 0.08 | | | |
| | Polystyrene insulation | 0.06 | | | |
| | Hollow Brick | 0.8 | | | |
| | Render | 0.01 | | | |
| **Windows** | | | 2.8 | 0.7 | |
| **Roofs** | | | 0.6 | | |
| | | | | | 1.4 |

The parameters in the summary Tables were used in the building simulations that calculate heat balance of the building taken into account weather data, gains and losses through the envelope.

## 6.6 Domestic hot water profile

Two different domestic hot water (DHW) profiles were used as input to the CHP model. These profiles were used in the Annex 42 "The Simulation of Building-Integrated Fuel Cell and Other Cogeneration Systems" of the International Energy Agency [25] which has established an Implementing Agreement on Energy Conservation in Buildings & Community Systems (ECBCS). The ECBCS undertakes research and provides an international focus for building energy efficiency [25]. The profiles were developed by Annex 26 to produce domestic hot water profiles for residential housing and were downloaded in the Exel from [25].

The downloaded data file contains hot water consumption in every 1-minute, 5-minute and 15-minute with consumption peaks. Additionally, the data is separated in consumption of 100, 200 and 300 l/day and the assumed temperature lift from the domestic hot water inlet feed temperature is 35 Kelvin degrees. The 15-minute data of 100 and 200 l/day consumption was converted into hourly data in the MatLab and used as input for the CHP model. According to [26] daily domestic hot water consumption per person is 30–50 liters in a single-family house. Heat demand for domestic hot water is described as:

$$Q_{DHW} = m_{DHW} c_{pw} (T_w - T_i) \tag{39}$$

In order to have two different test cases the consumption profile of 100 liters per day was used with the reference building from the construction period 1971–1980. In contrast, the profile of 200 liter per day was used with the reference building from the construction period 1946–1960.

## 6.7 Test bench

The Laboratory of Aerothermochemistry and Combustion Systems (LAV) has been operated a single cylinder gasoline engine with 3-way catalyst for investigation towards a later combined heat and power application, such as single family houses and small industry buildings. The later unit will run on biogas and is provided with exhaust gas recirculation. Under the current investigation are heat and power balance, combustion process, warm-up characteristics and emissions. In Table 11 the laboratory data is presented.

**Table 11.** The laboratory data on the engine

| | |
|---|---|
| $\boldsymbol{P_{mech}}$ | 9.5 kW |
| $\boldsymbol{P_{th}}$ | 16.8 kW |
| $\boldsymbol{\eta_{mech}}$ | 0.36 |
| $\boldsymbol{\eta_{g}}$ | 0.95 |
| $\boldsymbol{\eta_{e}}$ | 0.342 |
| $\boldsymbol{P_{th\_engine\_cooling}}$ | 6 kW |
| $\mathbf{T_{EG}}$ | 780 °C |
| $\mathbf{m_{dot\_EG}}$ | 52 kg/h |

The specifications and data on the single cylinder engine for the physical model were taken from the test bench measurements in order to simulate the test cases.

# 7 RESULTS AND DISCUSSION

The behavior of a CHP system in two single-family houses with different heat demand profiles was investigated. For the both cases the same physical property data on the CHP unit in Table 11 was used. This leads in the CHP unit with 9 kW electrical power and 16.8 kW thermal power with losses. The first case includes a single-family house constructed in 1971–80 and is called a low demand case due to lower space heating demand and domestic hot water consumption. On the other hand, the second case is the same kind of single-family house which is constructed in 1946–60. Due to the earlier construction time period the second case has higher space heating demand and is called a high demand case. Additionally, the higher domestic hot water consumption was assumed in the second case.

From the electricity utility point of view an estimation of daily operating hours over year is important information in order to maximize the benefit of the operation. Finally, a sensitivity analysis of the net present value of initial investment costs was investigated in order to see how different economical parameters influence to the economical viability of the CHP unit. The used simulation parameters are presented in Appendix A as a Matlab 'm'-file with the overview of the Simulink model.

## 7.1 Low heat demand case

A single-family house presented in Section 6.5.2 was simulated with Lesosai 7.2 in order to get an hourly heating demand profile over year. In Table 12 the monthly results of the simulation are presented.

**Table 12:** Heating load, solar gains and domestic hot water load

| Month | Heating load [kWh/m$^2$] | Solar gains [kWh/m$^2$] | Domestic hot water load [kWh/m$^2$] |
|---|---|---|---|
| **January** | 27.2 | 1.8 | 3.5 |
| **February** | 22.2 | 2.4 | 4.3 |
| **March** | 17.4 | 3.2 | 4.5 |
| **April** | 12.6 | 3.4 | 3.3 |
| **May** | 6.9 | 3.8 | 3.4 |
| **June** | 2.3 | 3.8 | 3.2 |
| **July** | 1.4 | 4.3 | 3.3 |
| **August** | 1.8 | 4.1 | 2.0 |
| **September** | 5.7 | 3.6 | 3.0 |
| **October** | 13.4 | 2.7 | 3.5 |
| **November** | 21.6 | 1.5 | 3.9 |
| **December** | 26.8 | 1.3 | 4.0 |
| **Total** | **159.4** | **35.7** | **41.7** |

In Table 12 heat load for space heating and domestic hot water are represented. Additionally, solar gains over the simulation year are presented since weather has a strong influence on heating demand. The heating load was highest during the coldest months in winter whereas during the summer month the heat load was significantly reduced. This reduction is influenced by weather, for example, increased external temperature and the solar gains. On the other hand, the monthly averaged heat load of domestic hot water stayed almost constant over year. The domestic hot water consumption is influenced by a number of occupants and in August lower number of occupants can be assumed due to the lower domestic hot water load.

The highest total heat demand was in December 30.8 kWh/m2. In order to cover this peak load of the year with defined thermal power of the CHP unit estimation for daily operation hours in December was done. In Figure 19 daily operating hours over the peak load month with increasing thermal power are presented.

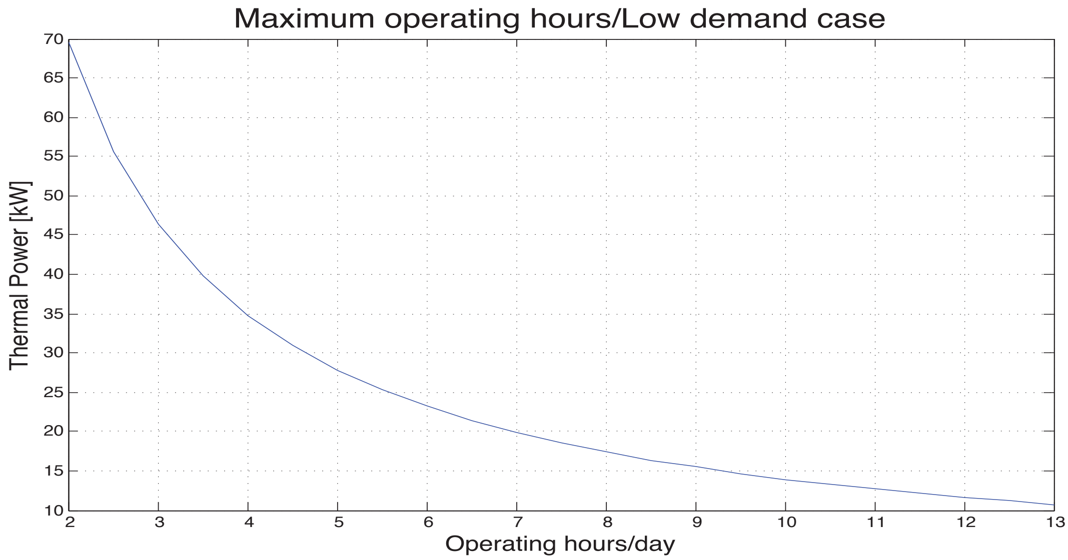


***Figure 19.*** *Required operation hours in peak load month depending on thermal power of a CHP unit*

In Figure 19 was seen that eight hours daily operation was required in order to cover heat demand in December with defined 16.8 kW thermal power. If the daily operation hours are reduced, the thermal power of the unit has to be increased.

The optimal volume for the cylindrical thermal storage, in order to minimize losses, was estimated using the peak load day in December and energy balance described in Section 6.3.3. Finally, the decision was made with a test simulation. In Table 13 geometry of the thermal storage is presented.

**Table 13.** The optimal geometry of the thermal storage

| | |
|---|---|
| **Volume [m$^3$]** | 4 |
| **Outer surface [m$^2$]** | 13.95 |
| **Height [m]** | 1.72 |
| **Diameter [m]** | 1.72 |

The height to diameter ratio of the optimal thermal storage geometry is 1. However, in the practice this ratio is typically 2 in order to have the better geometry in terms of the used environment. Monthly operation hours taken into account heat losses were simulated and divided for days in order to find required daily operating hours for each month. Finally, a number of yearly operating hours were 1863. The desired operation schedule from the electricity utility point of view was defined to be following in Table 14.

**Table 14.** The daily operation schedule

| Month | Starting time |
|---|---|
| **January** | 10 |
| **February** | 10 |
| **March** | 15 |
| **April** | 17 |
| **May** | 17 |
| **June** | 18 |
| **July** | 18 |
| **August** | 18 |
| **September** | 17 |
| **October** | 16 |
| **November** | 10 |
| **December** | 10 |

In order to maximize a benefit for the electricity utility operation of the CHP unit should take place during peak loads, such as lunch- and dinnertime. Due to this the CHP unit operates over lunch- and dinnertime during wintertime and over dinnertime during summer time when solar power generation can be assumed to be highest at lunchtime in the future.

The daily operation hours for each month were found with simulation and are presented in Figure 20.

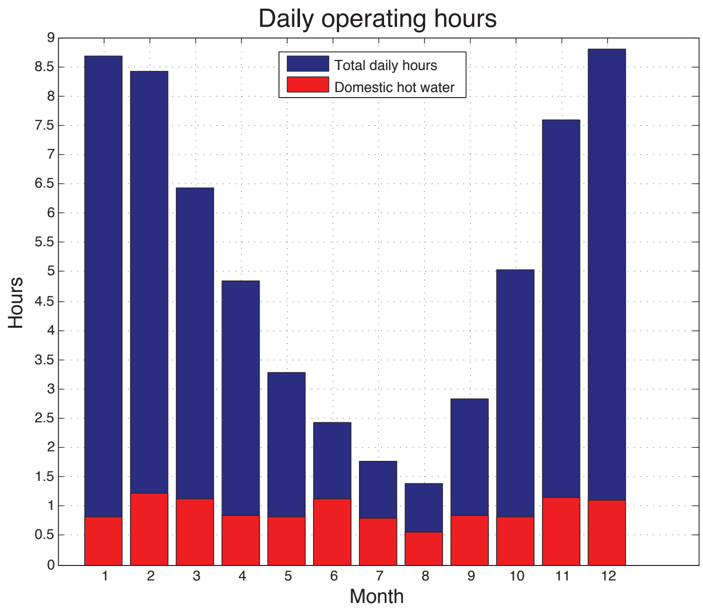


***Figure 20.*** *Daily required operation hours for each month*

It was found out that timing of operation has a small impact on overall monthly operation hours. The operating hours also increased few hours in month with schedule operation if compered to free operation when the maximum and minimum temperatures of the heat store are only constraints. In Figure 20 can be seen that during the coldest month the required daily operating hours are around eight and half hours whereas during the summer months the minimum daily operating hours are around one and half hours. From Figure 20 can be also seen that the operating hours are strongly influenced by space heating demand whereas the operating hours to cover domestic hot water heat load are almost constant over year. On the other hand, a proportion of the operating hours to cover domestic hot water heat load to total operation hours is much higher in the summer months than winter months. For example, in August the proportion is almost 50 % and in January only 10 %.

The relation of heat losses to the thermal production of a CHP unit was investigated. The heat losses consist of losses from the thermal storage and the CHP unit and were almost constant over year. However, thermal production differs over year due to varying space heating demand. The system was assumed to be in the basement of a building at temperature of 15 Celsius degree. In Figure 21 the percentage of the heat losses from the monthly thermal production is presented.

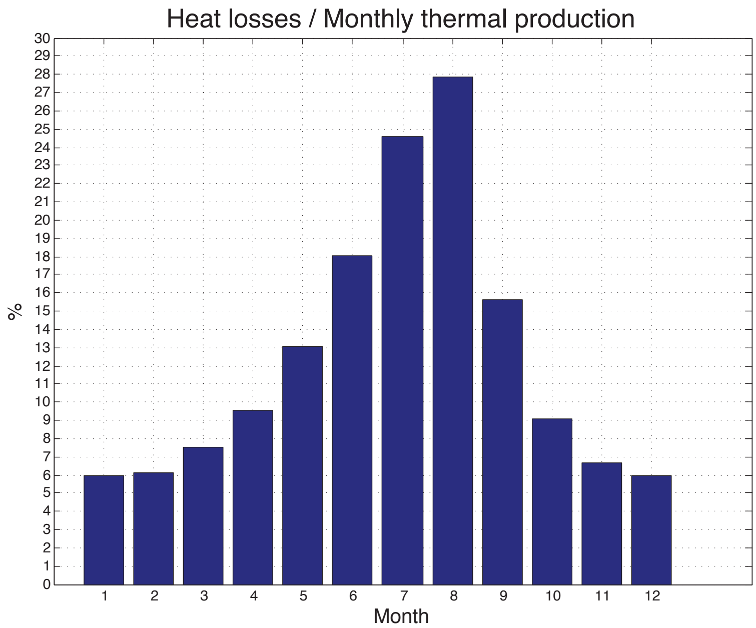


***Figure 21.*** *A percentage of heat losses from thermal production*

During the winter months a proportion of the heat losses to the thermal production was only six percent whereas the same relation was 28 % in August. The proportion was increased significantly when thermal production decreased.

The critical months for operating a CHP system are the months with the highest and lowest heat demand. In the low demand case these months were December and August. Thus, a week in December and August was investigated with the model in order to see the behavior of the temperature in the thermal storage considering and not considering the heat losses. Additionally, the corresponding data of the heat demand and the outside temperature during the week were investigated. In Figure 22 14th -20th December is presented.

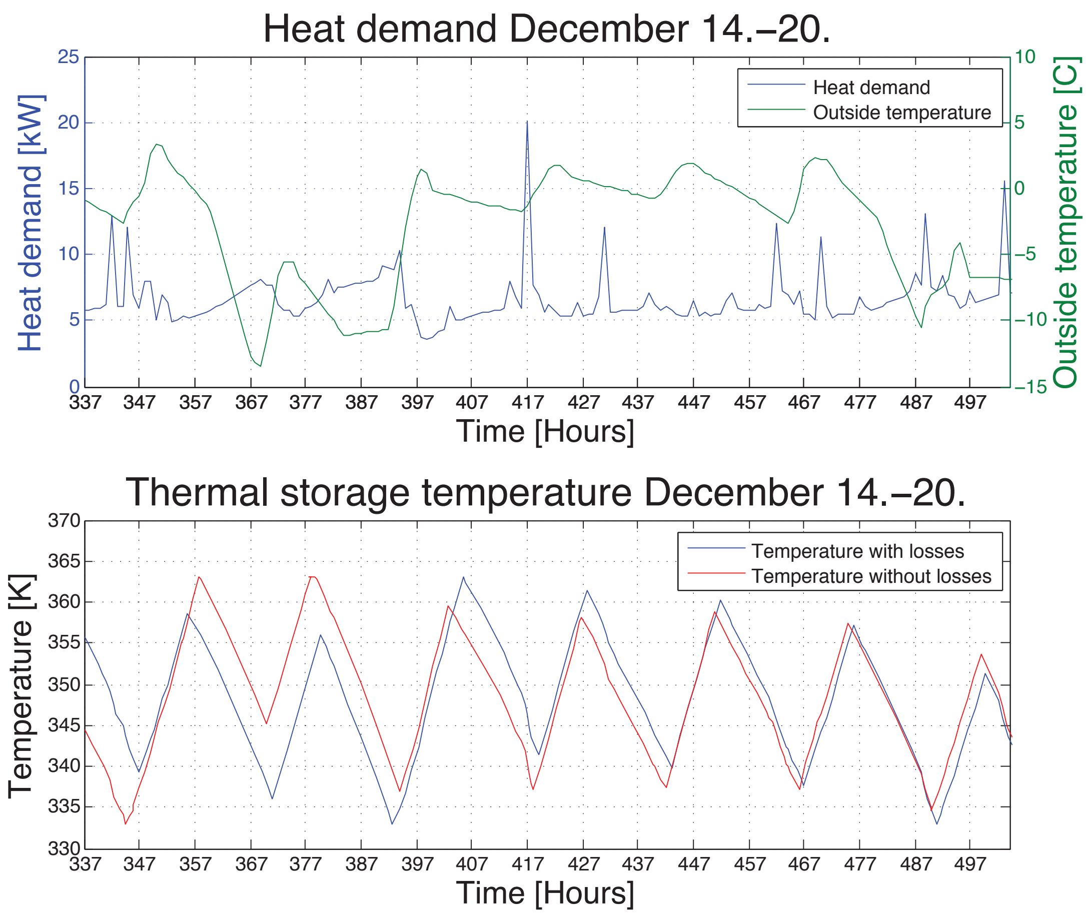


***Figure 22.*** *A week in December*

As can be seen in Figure 22 when the outside temperature decreases below -10 Celsius degrees the heat demand of the building increases gradually. In turn, when the outside temperature is varying around zero the heat demand is quite stable 5 kW excluding the peak demands due to domestic hot water consumption. On the other hand, the temperature in the thermal storage follows the heat demand. Thus, the temperature decreases when the CHP unit is off due to continuously heat demand. Scheduled charging at ten o'clock causes a strong temperature rise in the storage which can be seen in Figure 20. The minimum temperature of the thermal storage is reached between hours 387 and 397. At this point the CHP unit is switched on automatically by the control and the storage is charged until the maximum temperature is reached. If the losses are not taken into account the behavior of the temperature in the thermal storage has a same shape than with losses but different temperatures are reached between charging times. For example, between hours 387 and 397 the minimum temperature is reached if the losses are taken into account whereas without the losses the minimum temperature was not reached at that point.

Generally, an appropriate heating system for a light construction building is defined at least to cover the coldest period, such as four days. Between hours 367 and 397 the outside temperature is between -5 and -15 Celsius degrees. At the end of this cold period the thermal storage temperature reach the minimum. However, the used CHP unit and the thermal storage is an appropriate heating system for this building.

The lowest heat demand was in August due to slight space heating requirements. In Figure 23 14th –20th August is presented.

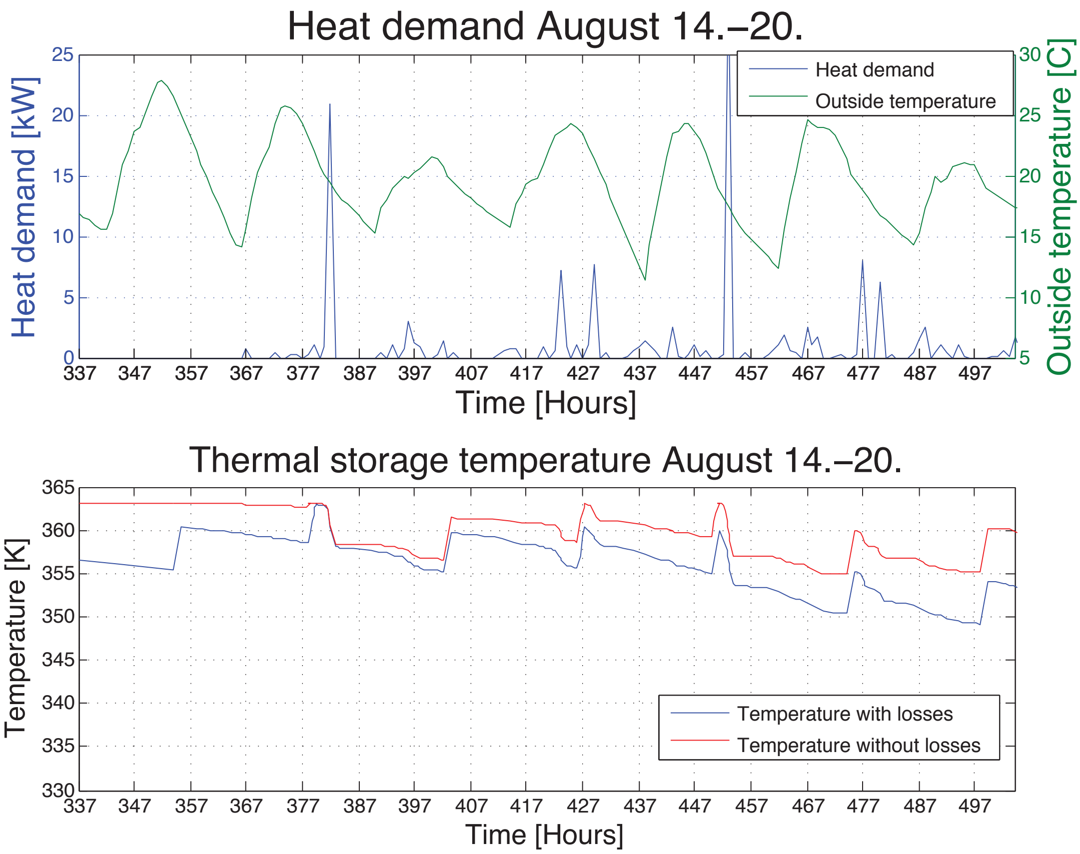


***Figure 23.*** *One week in August*

In August the outside temperature is significantly higher than in December but there is more fluctuation between the day and night temperatures. The peak loads in the heat demand are caused by domestic hot water demand. In August the thermal storage temperature has not have so big fluctuation than in December due to the lower heat demand. Additionally, the required charging time is much smaller as can be seen in Figure 23. The temperature level in the storage stays high which causes higher heat losses from the storage due to the higher temperature in relation to the environment. If the heat losses are not taken into account, the temperature stays long time at maximum due to the insignificant heat demand.

The primary energy saving according to [6] was calculated in the model and were introduced in Section 6.3.5. The yearly operation with natural gas resulted in 32 % primary energy saving in the low and high heat demand cases. With biogas as a fuel the primary energy saving 42 % was reached due to different efficiency reference values that the model calculates according to [6]. These primary energy saving results prove the benefit of combined heat and power generation in energy production.

## 7.2 High heat demand case

A single-family house with construction material from the time period of 1946–1960 was simulated in order to have a different heating demand profile than in the first case. Additionally, a higher number of occupants were assumed which leads to the higher domestic hot water consumption. The monthly simulation results of space heating demand and solar gains, and the data of the domestic hot water load are presented in Table 15.

**Table 15.** Heating load, solar gains and domestic hot water load

| Month | Heating load [kWh/m$^2$] | Solar gains [kWh/m$^2$] | Domestic hot water load [kWh/m$^2$] |
|---|---|---|---|
| **January** | 34.2 | 1.9 | 7.5 |
| **February** | 28.2 | 2.5 | 7.0 |
| **March** | 22.7 | 3.4 | 8.2 |
| **April** | 16.6 | 3.6 | 8.1 |
| **May** | 9.4 | 4.0 | 7.3 |
| **June** | 3.2 | 4.1 | 6.3 |
| **July** | 2.2 | 4.6 | 5.6 |
| **August** | 2.6 | 4.4 | 5.5 |
| **September** | 8.0 | 3.9 | 7.2 |
| **October** | 17.4 | 2.8 | 6.9 |
| **November** | 27.3 | 1.6 | 7.4 |
| **December** | 33.6 | 1.4 | 7.8 |
| **Total** | **205.3** | **38.2** | **84.6** |

In this second case the highest heat demand was in January and the lowest in July. The yearly heat demand was now 88.9 kWh/m$^2$ higher than in the low demand case. However, the trend of the heating requirements is same. Thus, the space heating demand decreases in summertime and increases in wintertime. The total domestic hot water consumption in year was almost double but has a same trend than in the low demand case. In August the demand was lowest and during the spring months the demand was the highest.

In Figure 24 the first estimation of daily operation hours in January was made in order to cover the heat demand.

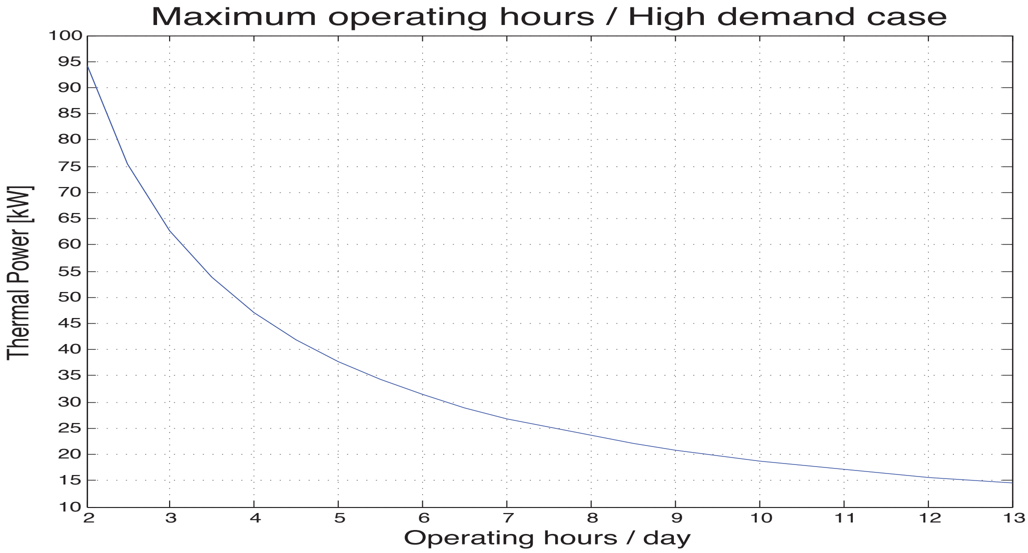


***Figure 24.*** *Required operation hours in the peak load month depending on thermal power of a CHP unit*

The same CHP unit was used in both cases which led to three hours longer daily operation in the peak load month than in the low demand case.

The optimal thermal storage volume was defined using the same method than in the low demand case. Finally, the volume of four cubic meters and geometry in Table 13 were determined to be appropriate also for the high demand case due to the smaller storage period and higher demand during the charging time.

Next the monthly operating hours were found with simulations in order to define required daily operating hours for each month. Eventually, the yearly operation of 2606 hours was required to cover total heat demand. The operation schedule, in Table 16, differs slightly from the low demand case due to the higher amount of daily operating hours.

**Table 16.** The daily operation schedule

| Month | Starting time |
|---|---|
| **January** | 10 |
| **February** | 10 |
| **March** | 10 |
| **April** | 10 |
| **May** | 16 |
| **June** | 17 |
| **July** | 18 |
| **August** | 17 |
| **September** | 17 |
| **October** | 10 |
| **November** | 10 |
| **December** | 10 |

In contrast to the low demand case there is only one month when operation was started at six o'clock. The daily operation hours in each month is presented in Figure 25.

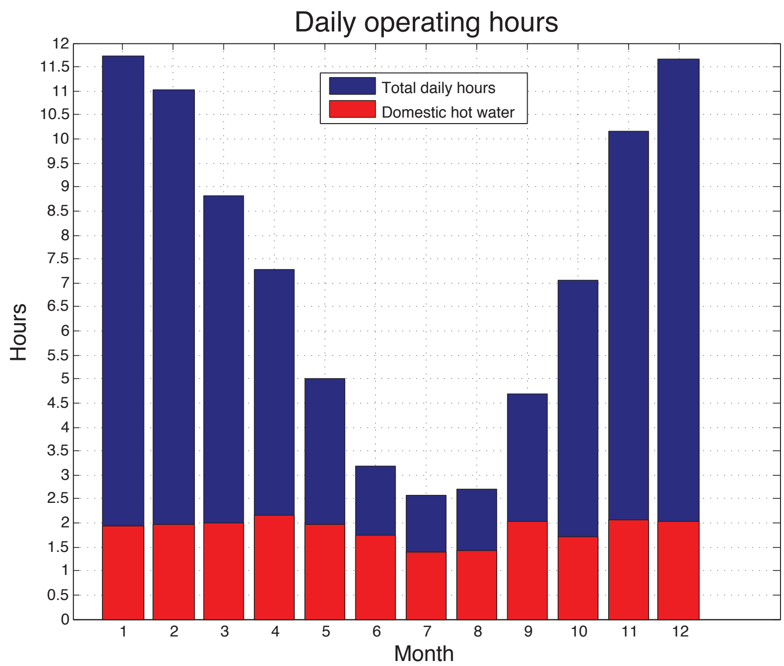


***Figure 25.*** *Daily required operation hours for each month*

In January and December over eleven and half hours daily operation was required. In contrast, in July and August two and half hours daily operation is enough. A number of daily operation hours to cover domestic hot water heat demand was almost constant over year.

The relation of the heat losses to the thermal production of the CHP unit was investigated such as described in the low demand case. In Figure 26 the percentage of the heat losses from the monthly thermal production is presented.

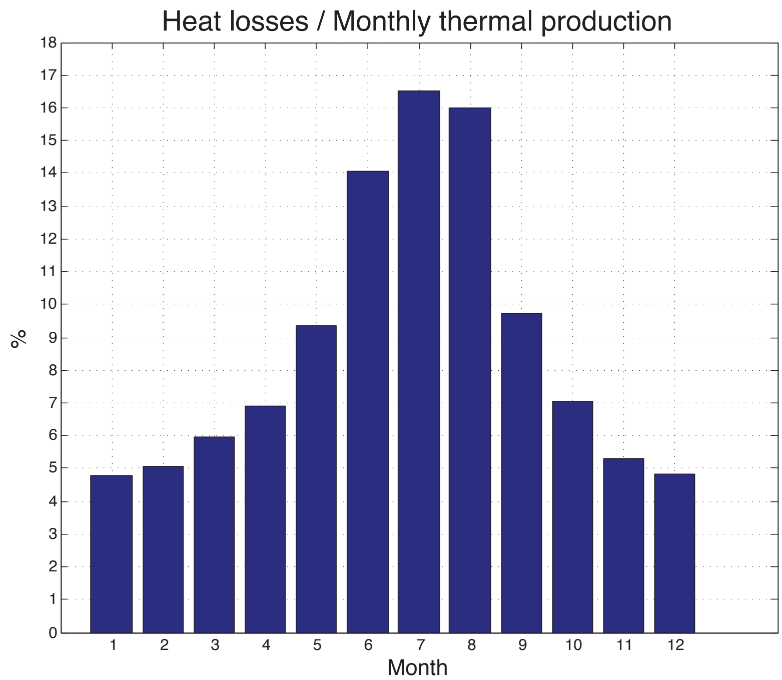


***Figure 26.*** *Percentage of heat losses from the monthly thermal production*

The percentage of the heat losses is marginally the largest in July due to the lowest heat demand. Additionally, in August the percentage is slightly over sixteen percent. In contrast to the high demand case in the low demand case the highest percentage was obviously only in August. However, in both cases the percentage increases distinctly in the summer months and is the smallest during the cold months due to high thermal production. In the high demand case the losses are definitely lower than in the low demand case. For example, in the high demand case the highest percentage is 16.5 % in July whereas in the low demand case the highest percentage is 28 %. During the high heat demand months the difference is not as significant, only 1.3 percentage point in January. This difference in heat losses can be explained by higher thermal production in the high demand case which makes the losses more insignificant.

In the high demand case the critical months for the CHP operation were January and July due to the highest and lowest heat demand. Thus, a week in January and July was investigated with the model in order to see the behavior of the temperature in the thermal storage considering and not considering the heat losses. Additionally, the corresponding data of the heat demand and the outside temperature during the week were investigated. The week from 4$^{th}$ until 10$^{th}$ January was selected to be the example of the behavior and is presented in Figure 27.

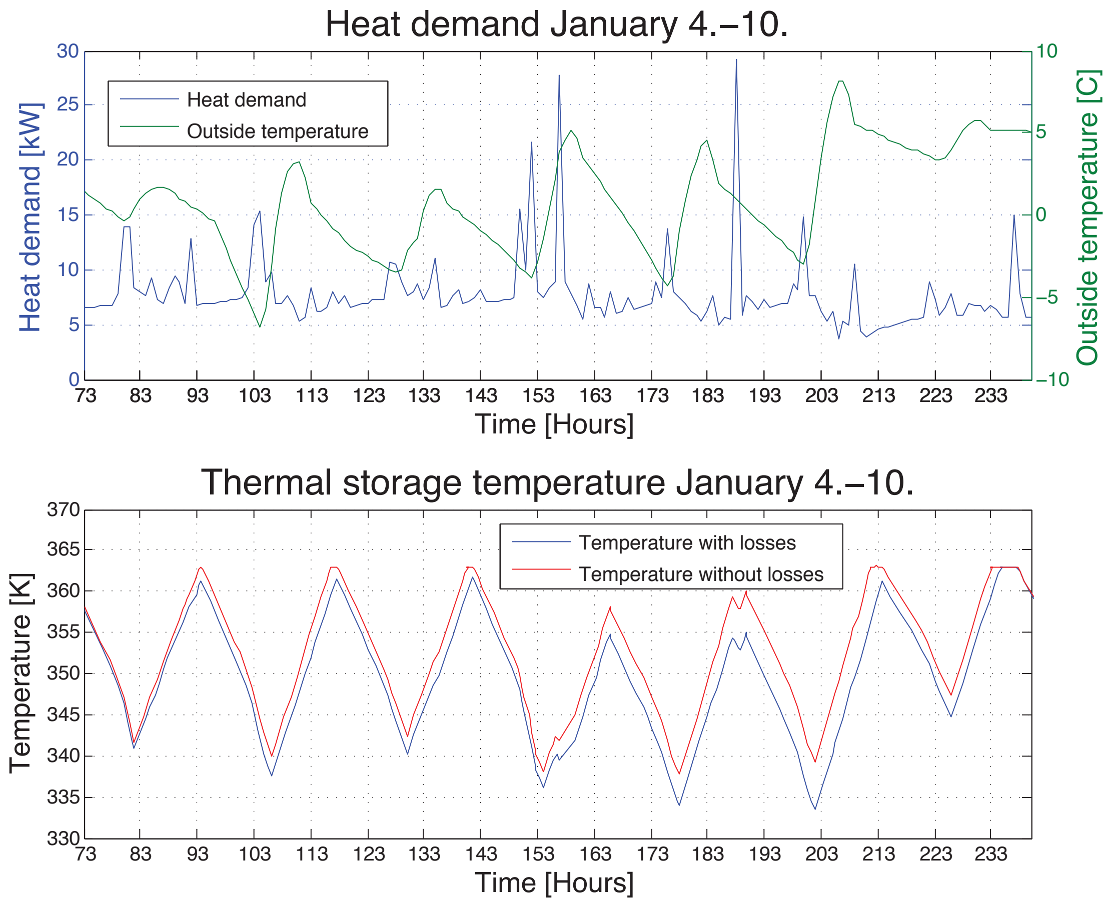


***Figure 27.*** *One week in January*

In Figure 27 can be seen that the outside temperature varies between plus and minus five Celsius degrees. However, the heat demand stay at the level of seven kilowatts due to the thermal capacity of the building which leads to thermal storage in the construction materials. At the end of the week the heat demand level is two kilowatts per hour lower because the outside temperature reaches the more stable conditions. The peak loads are caused by the intermittent domestic hot water consumption. The graph of the thermal storage temperature has a same shape than in the low demand case during the week of the coldest month. The charging period starts at ten o'clock and lasts eleven hours. Between hours of 153 and 163 the demand is higher than the production. This situation makes a small drop in the temperature during the charging period. In order to avoid this situation the optimal thermal power of a CHP unit should be more than the peak load. At the end of the week the thermal storage temperature reaches the maximum due to the lower heat demand.

The other critical month was July due to low heat demand. A week from 4th until 10th July is presented in Figure 28.

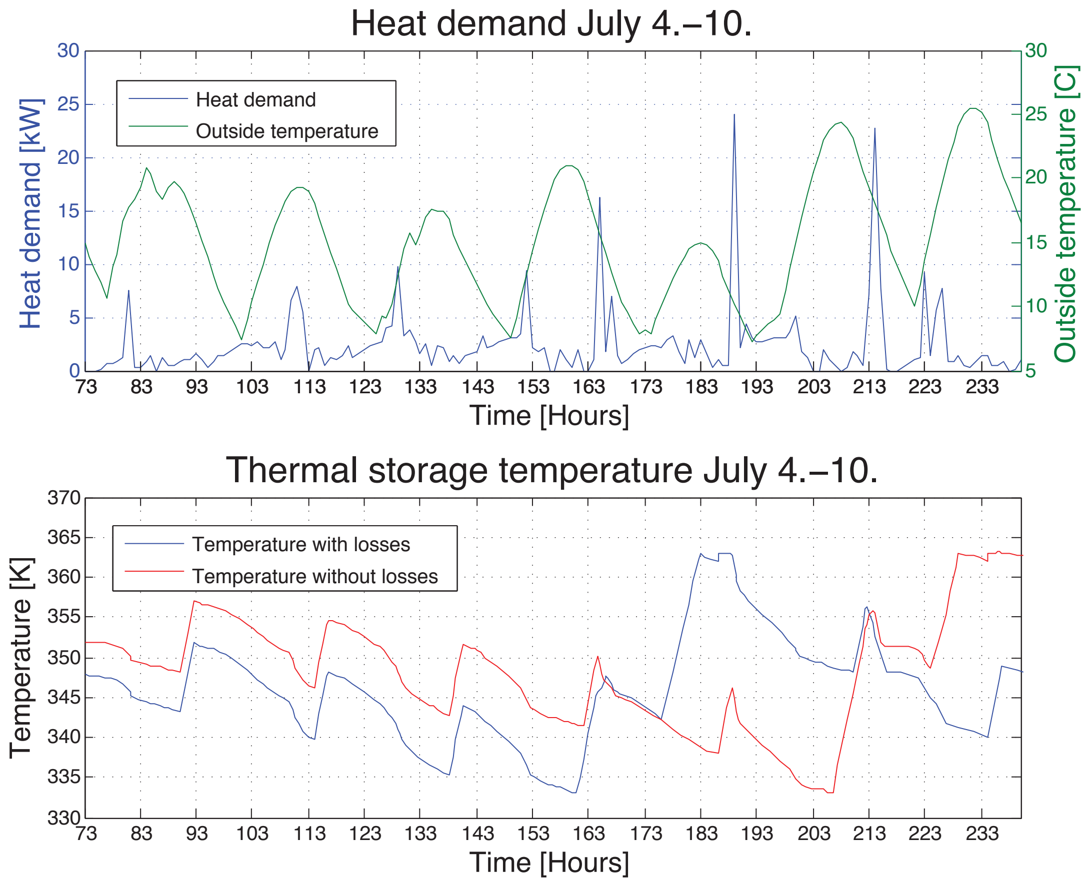


***Figure 28.*** *One week in July.*

The outside temperature is fluctuating between seven and 25 Celsius degrees. Due to this high temperature the heating demand is much lower than January. However, in case of the low temperature there is an increase in the heat demand. The thermal storage temperature is more stable than in January due to lower heat demand. Between hours 153 and 173 the temperature reaches the minimum temperature when the heat losses are taken into account. This situation starts the CHP unit in order to fulfill the storage. However, the customer does not allow the operation during the night and the unit stops for the night. This control priority was presented above in Figure 14. Next morning the unit starts again until it reaches the maximum temperature just before 183 hour because it did not reach the maximum the day before. Because of the high temperature in the storage the daily operating hours were not performed few hours later.

## 7.3 Exergy analysis

The exergy analysis was constructed in the Simulink model in order to calculate exergy efficiencies of a CHP unit and components. Additionally, the location of the highest exergy losses was intended to point out. The control volumes and components used in the analysis are presented in Figure 15. The results were assessed to be reasonable according to [19] and are presented in Table 17.

**Table 17.** Exergy efficiencies of the CHP unit and the components

| Component | Exergy efficiency |
|---|---|
| $\eta_{Ex\_ICE}$ | 70% |
| $\eta_{Ex\_EC\_HX}$ | 82% |
| $\eta_{Ex\_EG\_HX}$ | 21% |
| $\eta_{Ex\_CHP}$ | 40% |

The low exergy efficiency refers to the high entropy production and exergy losses. Due to this exergy efficiencies are used to define the magnitudes and locations of exergy losses and to find subject for improvements in the system. In this case the highest exergy losses occur in the exhaust gas heat exchanger. On the other hand, the engine cooling heat exchanger has the highest exergy efficiency. The improvements should be focused on heat exchange from the exhaust gasses.

## 7.4 Sensitivity analysis

The sensitivity analysis was carried out for the selected base case under the low and high demand cases in order to estimate the sensitivity of the net present value (NPV) to potential uncertainties in future cash flows. The relevant profitability parameters were set for the base case and they were varied systematically in order to see an influence to the net present value. The base case was normalized to one and the steepness of the graph indicates the sensitivity of the NPV to the varied parameter. In the low demand case the yearly operation hours were 1863 and in the high demand case 2606 hours. The results for each variation and both demand cases are presented as a Matlab 'm'-file code in Appendix B.

In the analysis the CHP system parameters were held as a constant and the six profitability parameters were varied systematically. These parameters were the operation and maintenance costs, discount rate, heat price, electricity price, fuel price and investment costs. The operation and maintenance costs can be varied between 0.02 and 0.05 CHF/kWh$_{el}$ depending on the size of a unit. The discount rate takes into account the risk associated with the investment. The higher discount rate the higher risk is related to the investment. With reference to the literature the discount rate can be varied from 5 % to 8 %. The investment costs of the unit excluding the heat store can have a range from 500 to 4000 CHF/kW$_{el}$ when the engine size is increasing. All profitability parameters were increased and decreased 10 % and 20 % from the base case value in order to see the influence of the change. In Table 18 the used base case is presented.

**Table 18.** The base case values

| | |
|---|---|
| **$P_{el}$, [kW]** | 9 |
| **$P_{th}$, [kW]** | 15.2 |
| **$\eta_{el}$, [%]** | 34.2 |
| **O&M costs, [CHF/kWh$_{el}$]** | 0.04 |
| **Discount rate, [%]** | 7.0 |
| **Heat price, [CHF/kWh$_{th}$]** | 0.10 |
| **Electricity price, [CHF/kWh$_{el}$]** | 0.20 |
| **Fuel price, [CHF/kWh gas]** | 0.086 |
| **Investment costs, [CHF/kW$_{el}$]** | 1500 |
| **Lifetime, [years]** | 20 |

The net present value is based on expectations of future cash flows over the lifetime which was set to be 20 years as a heating system should have. The monthly earnings before interest, taxes, depreciation and amortization (EBITDA) for the low and high demand cases are presented in Figure 29.

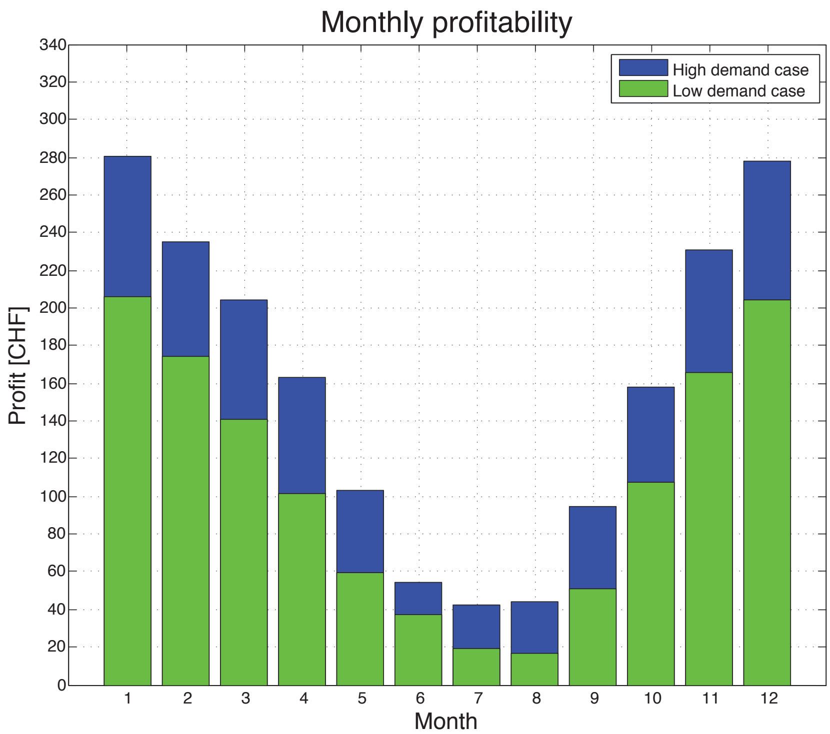


***Figure 29.*** *Monthly profitability*

The profit was higher in high demand case in each month due to a higher number of the operating hours and sold electricity and heat. The yearly profits in the high and low demand cases were 1892 CHF and 1280 CHF. These sums were expected to have each year over the lifetime in order to calculate the net present value as described in Section 6.4. The net present value of the base case with the high heat demand profile was 6503 CHF. On the other hand, with the low demand case the net present value was only 20 CHF. The difference between yearly operation hours was 743 hours. The payback period refers to a number of years required to pay the initial investment back and the value of NPV is equal to zero. This concept does not take into consideration the time value of money. In case of the higher yearly operation hours the payback period was 7.1 years and with lower yearly operation hours 10.5 years. On the other hand, the time value of money can be taken into account by the discount rate selected in the base case. Thus, the payback periods are 11 years and 20 years, respectively.

The sensitivity of the net present value to selected profitability parameters in the base case with low heat demand and less operation hours is presented in Figure 30.

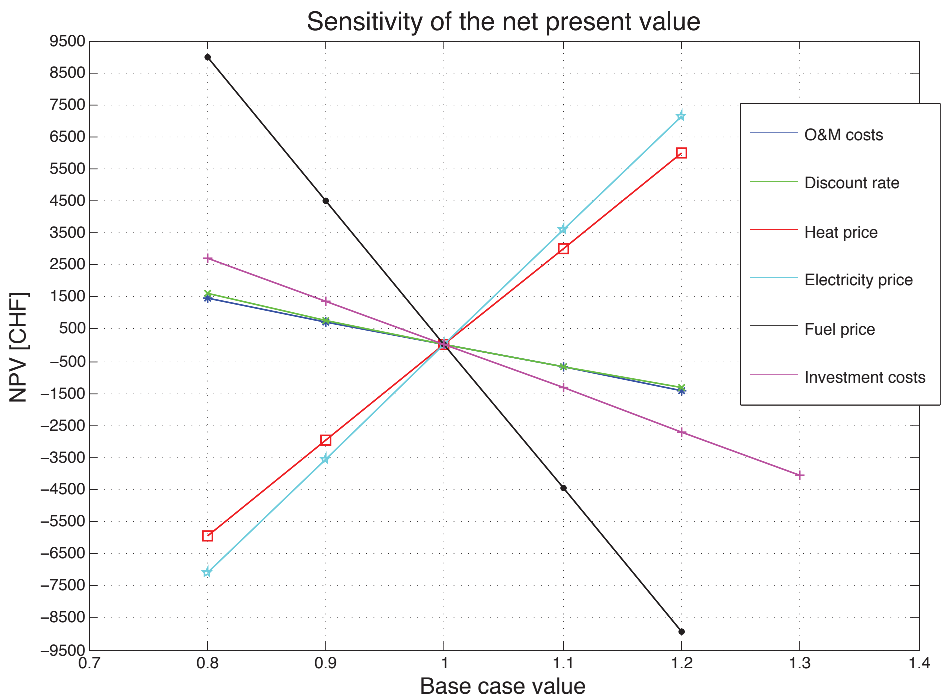


***Figure 30.*** *The sensitivity of the net present value in the low demand case*

The base case has the net present value of 20 CHF. The fuel price has the strongest influence on the NPV due to the steepest slope. If the fuel price decreases 10 % the NPV increases to 4499 CHF. On the other hand, if the fuel price increases 10 %, the NPV decreases to -4459 CHF from the base case value which is a signal of an unacceptable investment. This difference shows the significant sensitivity of the NPV to changes in the fuel price. Additionally, the heat and electricity have a high impact on the NPV. The other parameters do not influence this significantly to the net present value than the fuel, electricity and heat prices. The changes in the investment costs, discount rate and operation and maintenance costs have a lower impact on the NPV of which the discount rate and operation and maintenance cost have almost equal impact on the NPV. The revenue is earned from sold electricity and heat. If the refund from these energy forms changes 10 % or 20 %, the electricity price has a stronger influence on the NPV than the heat price.

The sensitivity of the net present value to selected parameters in the case of a higher amount of operation hours is presented in Figure 31.

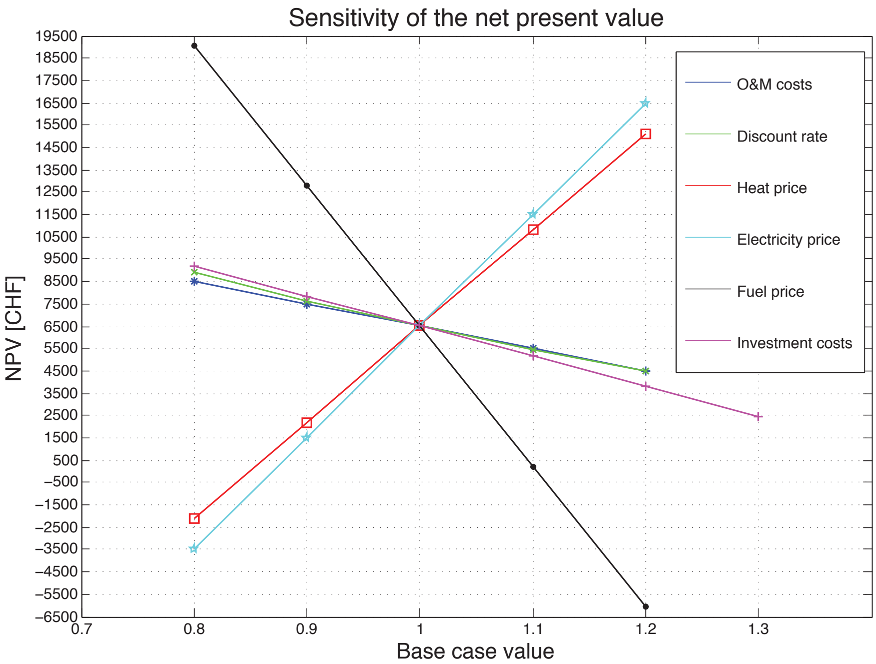


***Figure 31.*** *The sensitivity of the net present value in the high demand case*

In the high demand case a number of the yearly operating hours was 743 hours more and the net present value of the base case was 6503 CHF. The increase of the operating hours had an impact on the steepness of each graph except the investment costs. Thus, each parameter has a stronger influence to the net present value if the operating hours increase because the operating hours increase the costs in Equation 38. The investment costs are not related to a number of the operating hours. Due to this the steepness of the investment costs graph did not change compered to the low demand case.

As a conclusion of the sensitivity analysis the fuel price should be possible to keep as low as possible in order to have the higher net present value. The fuel, heat and electricity have the most important role in terms of the net present value.

# 8 OPTIMIZATION

An optimal size of a combined heat and power system maximizes a benefit for an electricity utility which is the contractor of the CHP unit. The benefit consists of revenue from sold electricity and heat. On the other hand, the revenue is reduced due to costs related to the system, such as initial investment, operation and maintenance, and fuel costs. When the electricity utility invests in the CHP system the net present value is used to assess the value of the initial investment after certain time period, such as the lifetime of the system. The net present value can be positive or negative of which the positive value presents an acceptable investment. The used optimization code is presented as a Matlab 'm'-file in Appendix C.

In order to find the optimal size of a combined heat and power system the net present value was maximized over the lifetime. The optimization was done for the given heat demand profile in the high demand case discussed before. The net present value is described as:

$$NPV = -S + \sum_t \frac{P_{yearly}}{(1-r)^t} \tag{40}$$

Where,

$$P_{yearly} = h_{op} P_e Pr_{Electricity} + E_{total\_heat\_demand} Pr_{th} - h_{op} P_e \left(Pr_{O\&M} + \frac{Pr_{Fuel}}{\eta_e}\right) \tag{41}$$

$$S = s_{CHP\_unit} P_e + s_{TS} V_{TS} \tag{42}$$

The initial investment costs were separated into the investment of the CHP unit and the thermal storage. These investments depend on the electrical power of the unit and a number of cubic meters in the storage. The specific investment costs of the CHP unit were estimated with the equalization function from [32].

$$s_{CHP\_unit} = 5783.5 * P_e^{-0.3875} \tag{43}$$

The operation and maintenance costs were estimated also with the equalization function from [32]. The euro was converted to Swiss Francs with a factor 1.2.

$$Pr_{O\&M} = (5.4452 * P_e^{-0.2613}) * 1.2/100 \tag{44}$$

In addition to the investment, and operating and maintenance costs, the main overhaul costs were taken into account with the equalization function. Two main overhaul were assumed to be required within the system's lifetime. According to [32] the main overhaul is required after 25 000–65 000 operating hours. However, the operating environment was defined to be residential and commercial buildings and produced electricity was used to support the grid during lunch- and dinnertime and renewable energy production. Due to this the duty cycle of the CHP unit increases and the main overhaul is required more frequently. In this case two main overhauls were assumed over the system's lifetime. The equalization function for the specific main overhaul costs is presented in [32] and described as:

$$c_{Main\_overhaul} = 719.45 * P_e^{-0.2933} \tag{45}$$

The optimization constraint for the maximum electric power was defined by the minimum hourly heat demand. Thus, the constraint of a five minutes operation to cover this minimum demand was used to define the maximum electric power in the optimization. On the other hand, the minimum electric power was defined by experience from the test cases. Hence, the minimum and maximum electric powers were 8 kW and 23 kW and variation was 1 kW for each simulation. The thermal storage volume was varied from 2000 liter to 5000 liter with a step of 200 liter. The electrical efficiency of the CHP unit was kept as a constant 35 %. The overall efficiency was expected to be 90 %.

The first optimization was done with two different economical situations in which economical parameters, such as energy prices, were constant over time and varied between the situations. The aim of the optimization was to find an optimal combination of the electrical power and thermal storage volume which maximizes the net present value. Thus, the electrical power and storage volume were varied systematically in order to see the NPV for each combination.

The second optimization was conducted after analyzing the result of the first optimization. Now, an electricity market price profile was generated so that it follow overall electricity demand fluctuation in Switzerland. Thus, the higher electricity price occurred during lunch- and dinnertime and during the night the price was significantly lower. In addition to this difference, solar power generation was taken into account in the electricity market price profile. The future assumption was that during the summer months the solar power generation can be expected to be such high that over lunchtime the electricity price will be lower than during the winter months. The thermal storage volume was maintained as a constant and the electric power of the CHP unit was varied within the same constraints than in the first optimization. In addition to the electric power, three levels for an electricity price threshold was appointed and varied. If the electricity price exceeded the threshold and the thermal storage temperature was below the upper temperature limit, the CHP unit was allowed to run.

## 8.1 Economical situation

The first optimization was done with two different economical situations in order to see how the net present value of different electric power and thermal storage volume combinations behaves. In the sensitivity analysis in Chapter 7 was seen that changes in the fuel, electricity and heat price had a strong impact on the net present value. Due to this impact these prices were changed between the economical situations. On the other hand, the discount rate had a low impact and was kept as a constant with the lifetime of the system. The initial investment, operation and maintenance, and main overhaul costs were varied depending on the electric power of the CHP unit. In Table 19 the used economical parameters are presented.

**Table 19.** Economical parameters of two economical situations

| | **Beneficial economical situation** | **Unfavorable economical situation** |
|---|---|---|
| **Fuel price, natural gas, [CHF/kg]** | 1.0 | 1.2 |
| **Electricity price, [CHF/kWh$_e$]** | 0.24 | 0.21 |
| **Heat price, [CHF/kWh$_{th}$]** | 0.11 | 0.10 |
| **Specific volume price, [CHF/m$^3$]** | 600 | 1200 |
| **Discount rate, [%]** | 7 | 7 |
| **Lifetime, [years]** | 20 | 20 |

The economical situations in Table 19 were simulated with the Simulink model. The electrical power and thermal storage volume were varied systematically.

### 8.1.1 Results and Discussion

The optimal electric power and thermal storage volume combination in the beneficial and unfavorable economical situations was the combination with the lowest initial investment costs. Thus, the smallest electric power and storage volume resulted in the highest net present value because of the lowest initial investment costs. Due to the constant electricity price over time the increasing electric power did not created significant benefit in a yearly profit. This insignificant increase in the profit was not able to cover the increasing initial investment costs. The behavior of the specific and initial investment costs are presented in Figure 32.

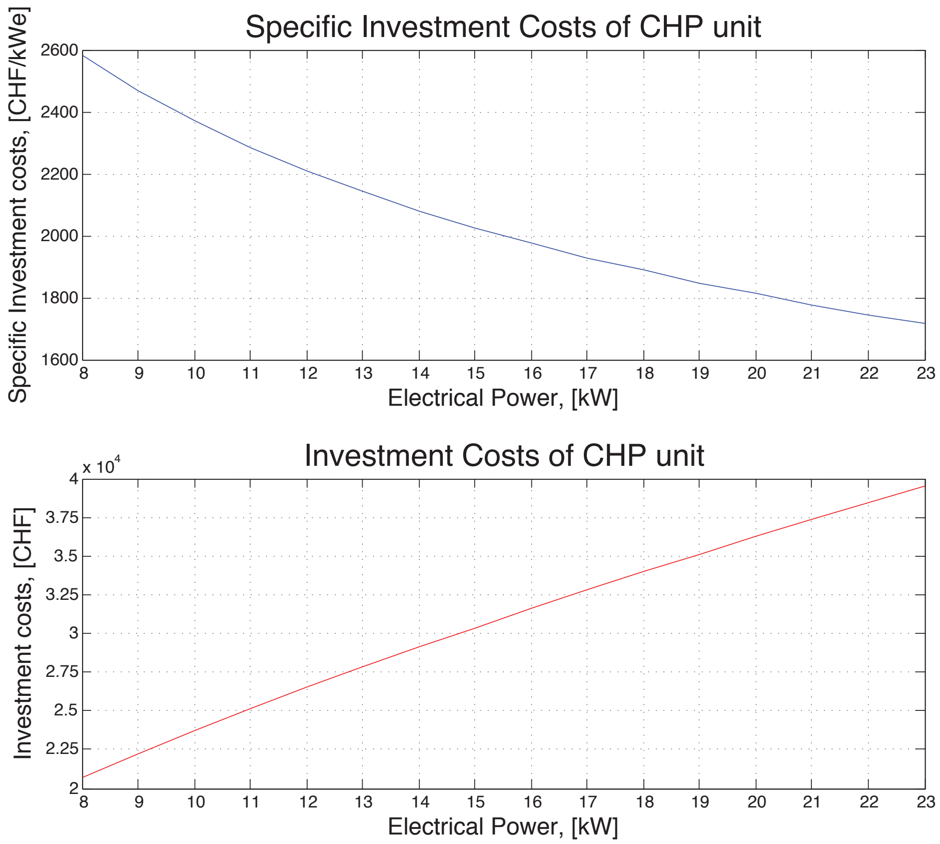


***Figure 32.*** *The specific and initial investment costs of a CHP unit*

The specific investment costs of the CHP unit are decreasing if the electric power increases. However, the initial investment costs increase strongly when the electric power increases. Due to this the larger CHP unit should generate significantly higher yearly profit than the smaller in order to cover the higher investment costs and to be the optimal solution in terms of the net present value. In addition to the prices and electrical efficiency, the yearly profit depends on the operating hours and electric power of the engine in Equation 38. In Figure 33 the behavior of the operating hours and yearly profit are presented in relation to the increasing electric power for the beneficial and unfavorable economical situations.

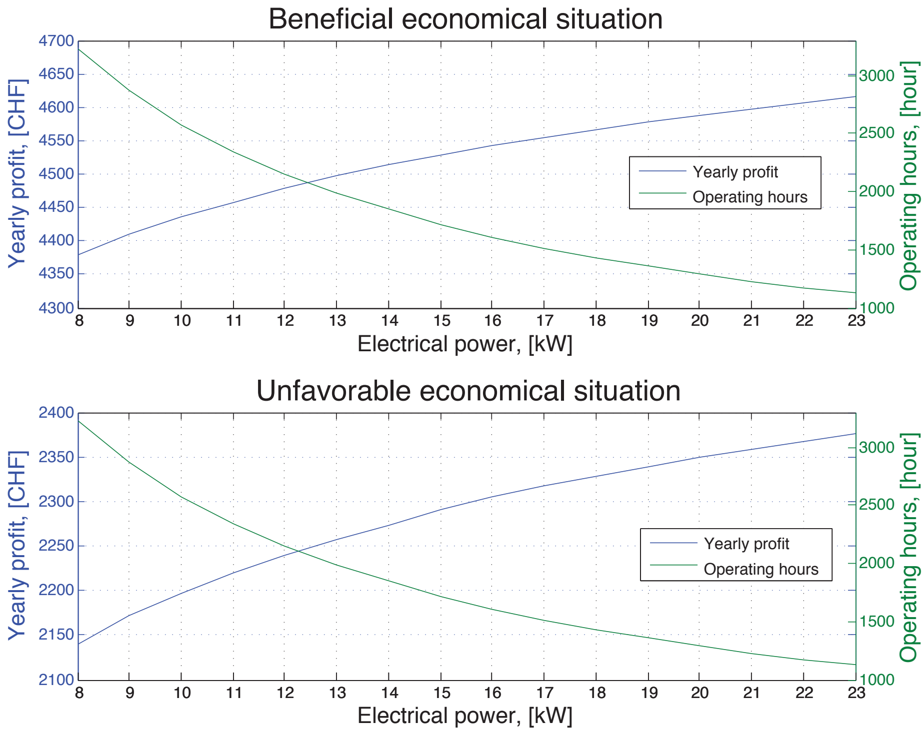


***Figure 33.*** *The relation of the yearly profit and operating hours to the electric power*

As can be assumed the unfavorable economical situation results in the lower yearly profit. In the beneficial economical situation the maximum yearly profit is 4616 CHF whereas in the unfavorable economical situation the maximum is 2376 CHF. In Figure 33 can be seen only small variation in yearly profit in both situations. On the other hand, if the electric power increases, the operating hours decreases and vice versa. This relation with constant electricity price led to only small variation in the yearly profit. Due to this small increase in the profit the investment costs were in a crucial role in terms of the optimal system combination and net present value. The net present value for different combinations and economical situations is presented as isolines or contour lines in Figure 34.

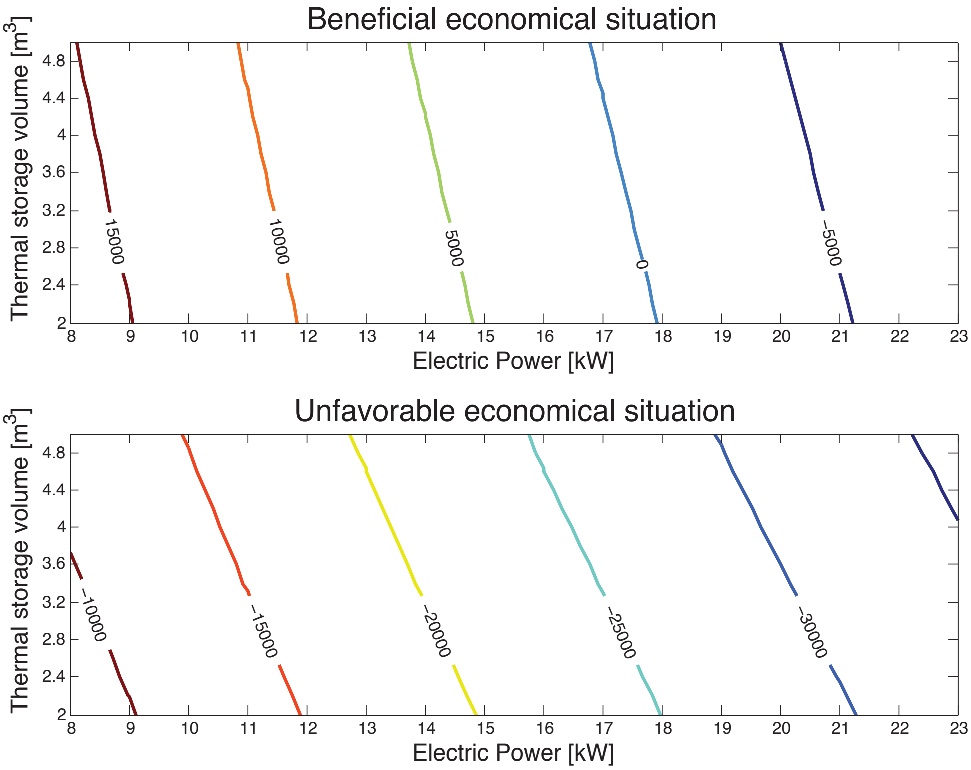


***Figure 34.*** The *contour lines of the net present value*

As can be seen in Figure 34 the highest net present value is reached, in both economical situations, with the combination of the smallest electrical power and thermal storage volume due to the lowest investment costs. In case of unfavorable economical situation the highest net present value is reached with the smaller range of combinations than in the beneficial economical situation. However, in case of the beneficial economical situation the positive net present value was reached with smaller electrical powers. With the larger engines the net present value was negative and the investment was not acceptable. The unfavorable economical situation led only to the negative net present value because of the lower yearly profit.

## 8.2 The electricity price profile

The electricity price profile was generated from general electricity demand profile with the assumption that the electricity price follows the demand. This price profile enabled to see an influence of the increasing electric power to the net present value. Now, the thermal storage volume was maintained as constant. In addition to the electric power, the electricity price threshold for the CHP operation was changed. The threshold was assumed with regard to a liberalized electricity market. The liberalized electricity market enables significant higher refund for generation of balancing energy. The CHP unit was allowed to run if the electricity price reaches or exceeds the certain threshold. The other switching on constraint was the thermal storage temperature limits. The lower limit was 60 Celsius degrees and the upper limit was set to 90 Celsius degrees. During lunchtime in the summer months high solar power generation was assumed as situation in the future generation portfolio. This leads to the lower electricity price during lunchtime. The summer months were June, July and August and the rest months were taken into account as winter months. The difference in the electricity price between a weekday and weekend was not taken into account. The profile of a winter and summer day are presented in Figure 35.

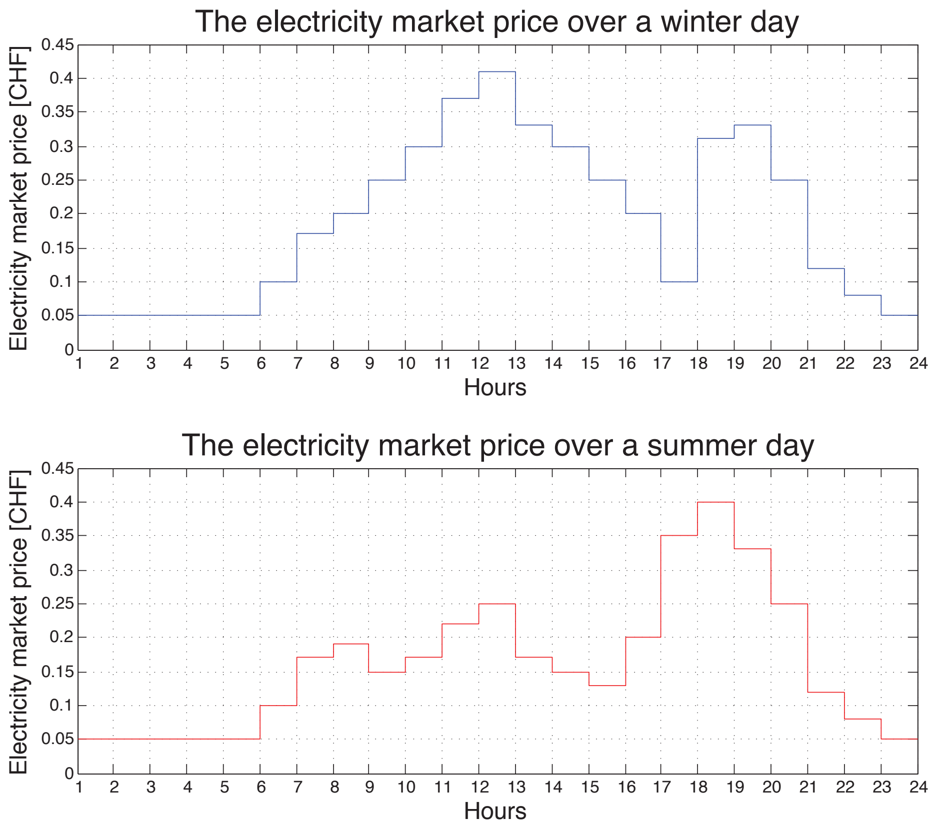


***Figure 35.*** *The electricity market price over a winter and summer day*

In this optimization problem the other economical parameters were maintained as constant. These values are presented in Table 20.

**Table 20.** Economical parameters in the optimization

| **Economical parameters** | |
|---|---|
| **Fuel price, natural gas, [CHF/kg]** | 1.2 |
| **Heat price, [CHF/kWh$_{th}$]** | 0.10 |
| **Specific volume price, [CHF/m$^3$]** | 1200 |
| **Discount rate, [%]** | 7 |
| **Lifetime, [years]** | 20 |

The optimization simulation was performed three times in order to see an influence of varying the thermal storage volume. The selected volumes were two, three and four cubic meters.

### 8.2.1 Results and Discussion

In terms of the net present value the optimal CHP unit size was not any more the one with the lowest initial investment costs. In addition to the thermal storage temperature limits the operation was controlled by the electricity price with three different thresholds. If the electricity price exceeds 20, 25 or 30 Rappen, the CHP unit was allowed to run. In the first case the thermal storage volume was four cubic meters. The behavior of the yearly profit and net present value is presented in Figure 36.

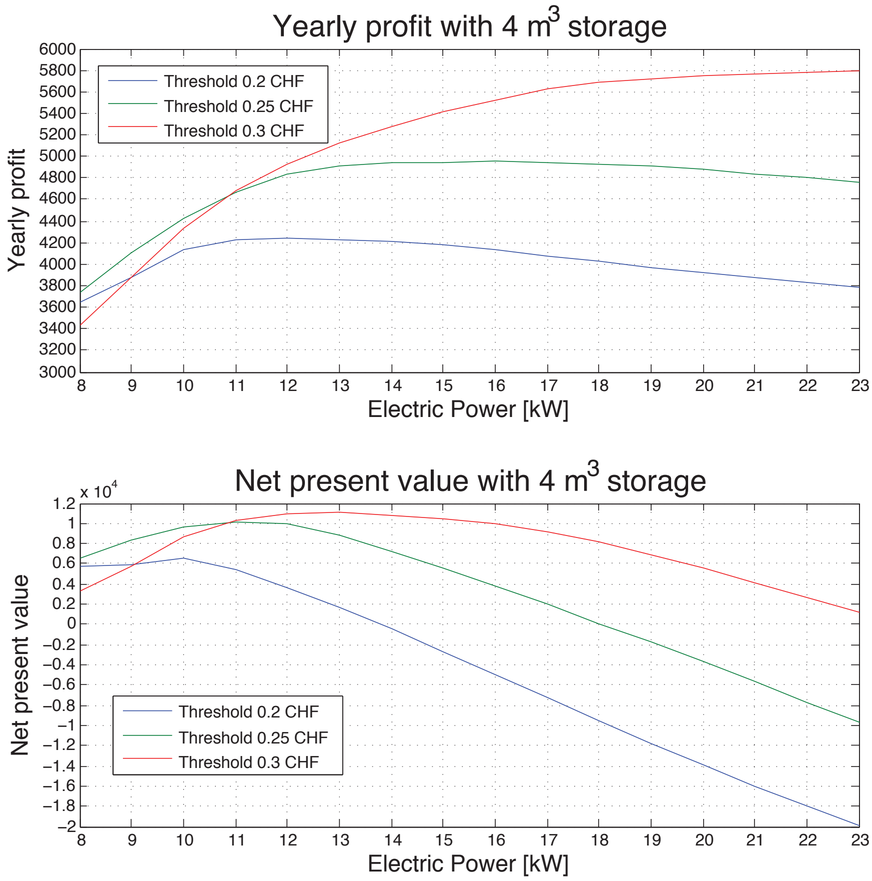


***Figure 36.*** *The yearly profit and net present value with the 4 m$^3$ thermal storage*

In Figure 36 can be seen that the optimal CHP size, in terms of the net present value, was not the smallest unit. Additionally, the optimal size was not the unit with the highest yearly profit due to the increasing initial investment costs when the electric power increases. If the threshold was increased, the maximum net present value was increased due to the operation at the higher price level. With the lower thresholds 20 and 25 Rappen the yearly profit decreases slowly after the highest point. This decrease occurs because the range of the allowed operation is relatively long and with the higher electric and thermal power the thermal storage temperature limit was reached faster than with the smaller unit. Due to this the smaller unit is allowed to run over the range of the higher price and the profit is higher even the operation is longer and the operation and maintenance are higher. On the other hand, the units before the highest point have smaller thermal power and they have to operate also during low price levels in order to cover the heat demand. However, there is not decrease in the yearly profit if the threshold is 30 Rappen because the allowed operation range is shorter and even a large unit can operate over the whole range because of the large thermal storage volume. Anyway, the net present value decreases due to increasing initial investment costs. In Table 21 the optimal CHP sizes for each threshold are presented.

**Table 21.** The optimization results with the 4 m$^3$ thermal storage

| Threshold | Optimal electric power | Net present value |
|---|---|---|
| 0.20 CHF | 10 kW$_e$ | 6590 CHF |
| 0.25 CHF | 11 kW$_e$ | 10130 CHF |
| 0.30 CHF | 13 kW$_e$ | 11055 CHF |

The optimal CHP size depends strongly on the electricity price profile. However, the optimization results in Table 20 present the trend of the optimal size. If the threshold is high and the allowed operation range shorter, the larger unit is the optimal and vice versa. However, the unit cannot be too large because of the increasing investment costs which can be seen in Figure 32.

In Figure 37 the isolines or contour lines of the net present value are presented. Now, the interpolation of the net present value is shown where the threshold increases 0.01 CHF.

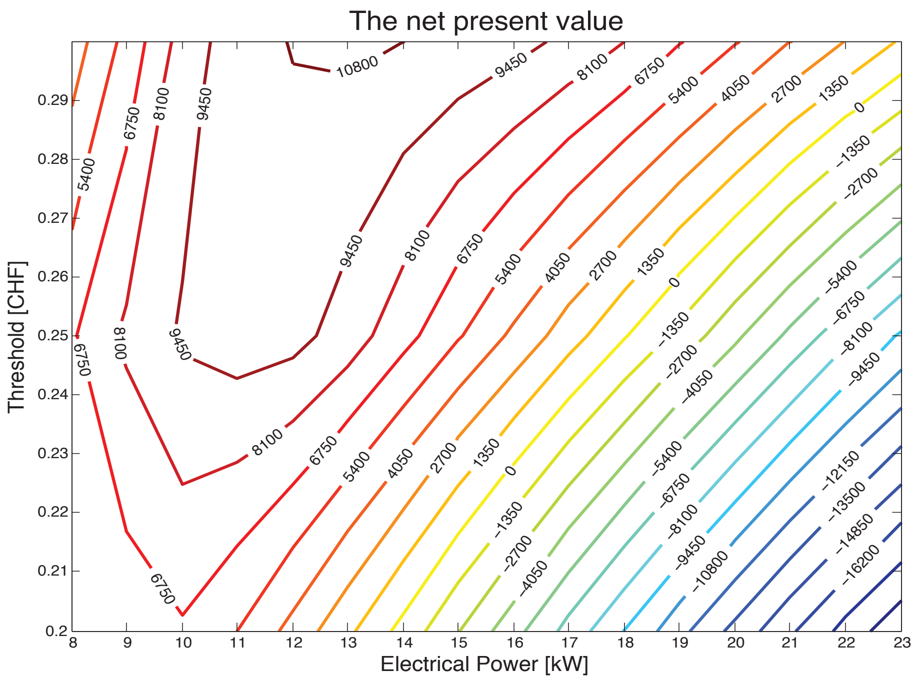


***Figure 37.*** *The contour lines of the net present value with the 4 m$^3$ storage*

In Figure 37 can be seen that the maximum net present value is reached with the electric power 13 kW$_e$ and the threshold 30 Rappen. With the largest electric powers the negative net present value is created and the line, of which value is zero, indicates limit for an application.

Next the thermal storage volume was decreased to three cubic meters in order to see an influence of the smaller storage capacity to the net present value and yearly profit. The smaller storage volume leads to a decrease in the initial investment costs which influence to the net present value positively. In Figure 38 the yearly profit and net present value is presented when the thermal storage volume is three cubic meters.

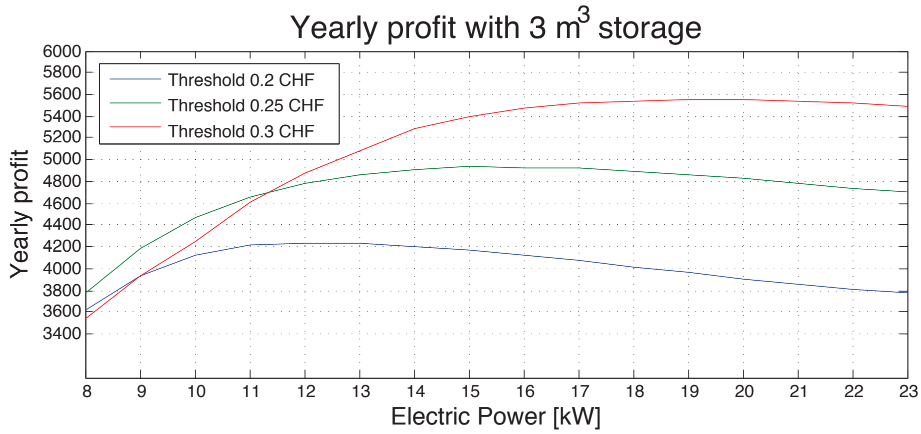


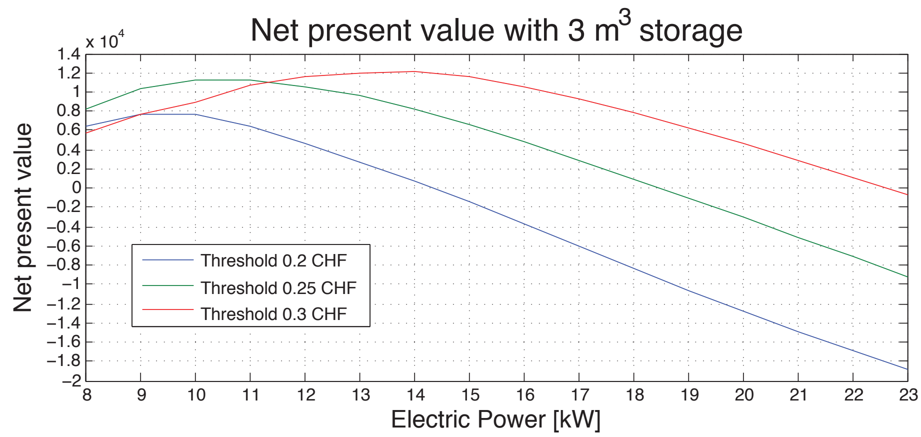


***Figure 38.*** *The yearly profit and net present value with the 3 m$^3$ thermal storage*

The trend of the graphs in Figure 38 is similar to the graphs in Figure 36. With the threshold of 20 Rappen the decrease of the volume does not influence to the yearly profit whereas with the other thresholds the profit decreases. Additionally, the yearly profit with the threshold of 30 Rappen has a decrease after the maximum point. These decreases in the yearly profit occur because of the decreased storage capacity and the temperature limits are reached faster. On the other hand, the decreases in the profit are relatively small compered to the decrease in the initial investment costs that the maximum net present values are higher with the smaller storage capacity. In Table 22 the optimal CHP sizes with the different thresholds are presented.

**Table 22.** The optimization results with the 3 $m^3$ thermal storage

| Threshold | Optimal electric power | Net present value |
|---|---|---|
| 0.20 CHF | 9 $kW_e$ | 7671 CHF |
| 0.25 CHF | 11 $kW_e$ | 11296 CHF |
| 0.30 CHF | 14 $kW_e$ | 12065 CHF |

There was no significant difference in the optimal CHP sizes compered to the case with the larger thermal storage. The net present value increased because of the lower initial investment costs. The isolines or contour lines of the net present value are presented in Figure 39.

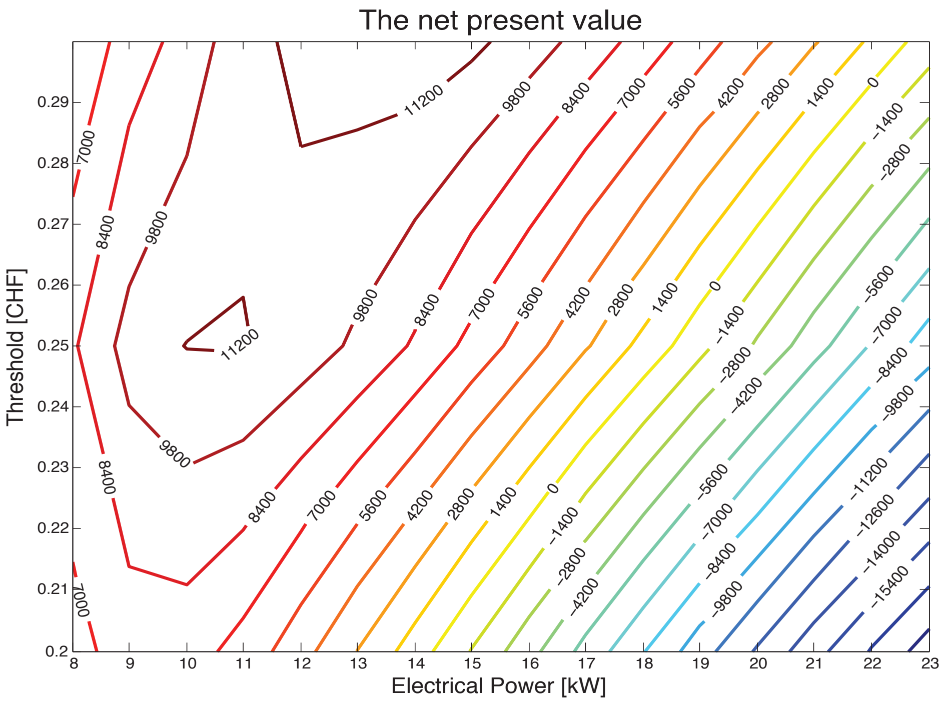


*Figure 39. The contour lines of the net present value with the 3 $m^3$ storage*

The contour lines present that a high net present value can be reached also with the lower threshold when the thermal storage volume is three cubic meters.

Finally, the thermal storage volume was decreased to two cubic meters in order to see an influence to the net present value and optimal CHP size. In Figure 40 the yearly profit and net present value are presented.

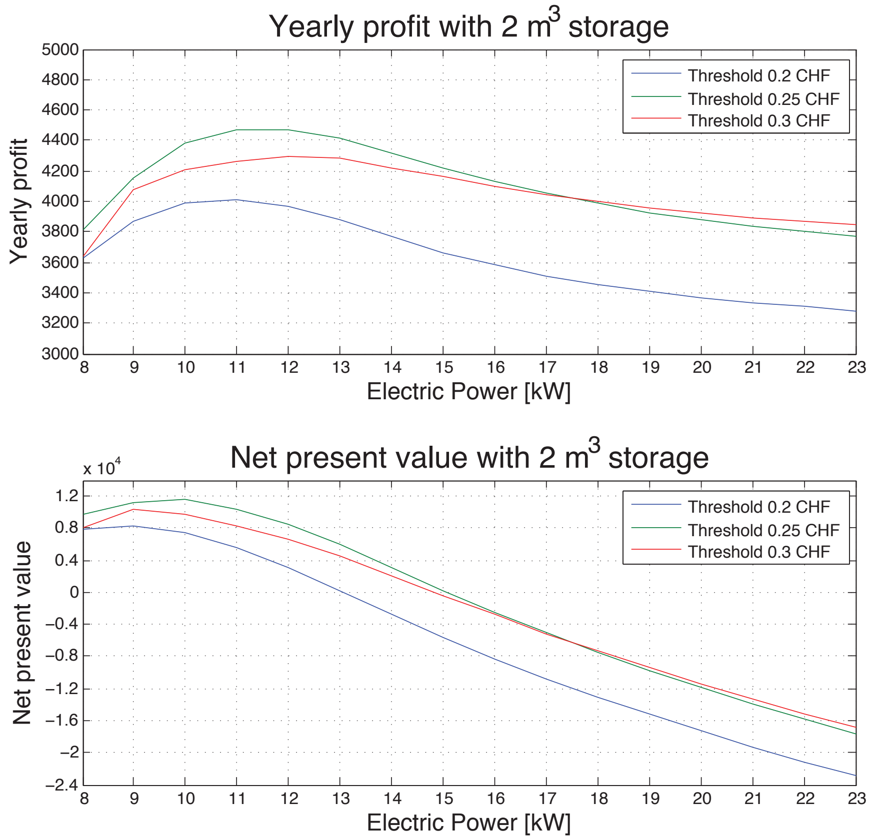


***Figure 40.*** *The yearly profit and net present value with the 2 $m^2$ thermal storage*

In case of the smallest thermal storage the yearly profit decreased with each threshold due to the lower storage capacity. This lower capacity leads to more operation time with the low electricity price because the thermal storage is full faster but also empty faster. Due to this the benefit of the operation during the highest electricity price is lost. If the storage capacity is large enough, it enables the operation only during the high electricity price because the capacity can provide heat for longer period. The maximum yearly profit and net present value with the threshold of 30 Rappen was lower than with the 20 Rappen threshold because the electricity price exceeds 30 Rappen less often. Due to this required storage time is longer in which case the minimum temperature limit is reached more often if the storage capacity is small. Thus, the operation during the low electricity price cannot be avoided.

The maximum reached net present value is lower than with the larger volume. Now, the lower yearly profit has a bigger influence to the net present value than the lower initial investment costs. In Table 22 the optimization results are presented for two cubic meters thermal storage.

**Table 22.** The optimization results with the 2 m$^3$ thermal storage

| Threshold | Optimal electric power | Net present value |
|---|---|---|
| 0.20 CHF | 9 kW$_e$ | 8238 CHF |
| 0.25 CHF | 10 kW$_e$ | 11558 CHF |
| 0.30 CHF | 10 kW$_e$ | 9711 CHF |

According to Table 22 the optimal CHP size decreased due to the decreased storage capacity. Additionally, the net present value decreased compered to the case with the volume of 3 m$^3$ even if the initial investment costs are lower in case of the smaller unit and thermal storage. The isolines or contour lines of the net present value in case of 2 m$^3$ thermal storage are presented in Figure 41.

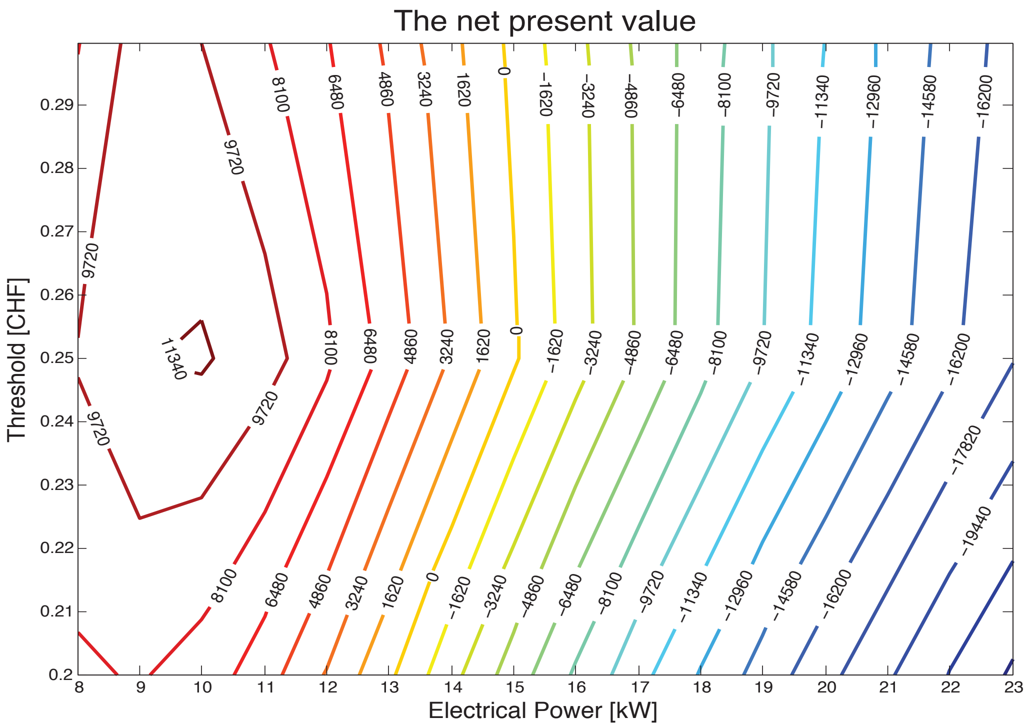


*__Figure 41.__ The contour lines of the net present value with the 2 m$^3$ heat storage*

In Figure 41 can be seen that the maximum net present value is reached only with the threshold of 25 Rappen.

### 8.2.2 Conclusion

The behavior of the net present value with three different thermal storage volumes and the varying electric power and switching on price thresholds was investigated. The aim was to find the optimal electric power and threshold combination in terms of the maximized net present value. Additionally, the impact of the decreasing thermal storage volume on the net present value was under the interest.

The optimal size of the CHP unit is highly influenced by the electricity market price profile. Additionally, in reality there is a really high fluctuation in the electricity market price even within minutes. Now, the price profile was generated hourly and was based on experience of peak load periods during a day. However, the trend of parameters' influences to the net present value can be assumed to be same than in these cases.

The optimization results indicate that the storage capacity has an influence to the net present value. If the capacity is large enough, the longer storage time and operation during the desired electricity price is enabled. On the other hand, if the volume is too large, the initial investment costs are unnecessarily high. These costs impact negatively on the net present value. In contrast, too small storage capacity leads to the lower initial investment costs but does not enable the operation during the desired electricity price.

The optimal size of the CHP unit was reached with three cubic meters thermal storage and 14 kW electric power. In this case the net present value was 12 065 CHF after 20 years lifetime. This size of the CHP unit leads to 1843 operating hours in year in order to cover the defined heat demand. The results indicate also that the unit, which generates the highest yearly profit, is not the optimal because of the increasing initial investment costs.

In each case the isolines of the net present value indicate the same kind of area where a high net present value can be reached. This area was reached with smaller electric powers and the higher thresholds. In each case the largest units had the negative net present value and the line, of which value was zero, indicates the limit for an application. The sensitivity of the electric power was also detected from the isolines. Already a one-kilowatt variation in the electric power had a significant effect to the net present value. This result indicates that an electricity supplier and unit manufacturer have to assess the electric power of a unit carefully in order to maximize the benefit.

Finally, these results present that small CHP operation can be profitable for the electricity utility under liberalized electricity market where the price can reach high peaks during a day. This CHP operation follows the electricity price but at the same time it has to cover the heat demand. This situation leads to power- and heat-driven system which is possible to realize with a large thermal storage volume. This volume enables long storage time when the occasional operation is possible if the CHP unit is large enough to cover an application specific heat demand.

# 9 OUTLOOK

The model of a combined heat and power system was constructed into the Matlab/Simulink environment. The model consists mainly of the physical model of co-generation unit and thermal storage, and techno-economical aspects of the system and operation. The third important part was the hourly heat demand profile as input for the model. The other important input parameters were the physical data on CHP unit and economical parameters of the system and operation. The enhancements for the future work can be divided into four parts the physical model, heat sinks, input profiles and optimization.

***The physical model***

The physical model should be enhanced with the start-up dynamics. The 3-way catalyst of an engine has to reach certain temperature in order to work perfectly. Thus, the start up process requires additionally energy input which could be taken from the thermal storage. The start-up process leads to the higher emissions than during the full operation. Finally, the process takes time until the engine is synchronized with the grid. Additionally, the thermal masses of all system components should be modeled except the thermal storage which is already taken into account. The CHP has to be warmed up before start which leads to additional losses. If the engine stops, it stays warm over certain time. The start-up characteristics influence to the maximum number of duty cycles, the start-up energy consumption and emissions.

The thermal storage model should be enhanced with stratified model. In this simple physical model the storage was modeled as a single node model. The stratification of the thermal storage can have a significant effect to the behavior of the system. Modeling the system losses could be enhanced. Now, the heat losses are modeled as heat transfer through the thermal storage and CHP block wall. Additionally, thermal and electric efficiencies of a CHP system could be modeled as function of size. The water mass flow between the storage and the CHP unit could be varied in order to have constant temperature out of the unit. In this case the engine cooling circuit runs constantly and has own temperature control. This requires a water mass flow controller into the model.

Additional CHP components could be added to the model in order to have combined cooling, heat and power system. Thermally activated cooling devices, such as absorption chiller and steam jet ejector, can increase the operating hours during the summer months when cooling is required. Additional electricity generators, such as the Rankine cycle and thermoelectric generator, could increase electric power of the system. This could lead better benefit during the high electricity price. The disadvantage is that the additional devices increase the initial investment costs of the system.

### *Heat sinks*

A weather depending building model could be included to the CHP model. Thus, weather forecast information could be used and an hourly heating demand profile is generated inside the model. Thus, an external building simulation is not required. Additionally, the better categories of the heat sinks should be made, such as single- and multi-family houses, office buildings and small industry. The categories should define both typical hourly heating demand and domestic hot water consumption profiles. Hence, the optimal CHP system size for each category, which maximizes the benefit, should be found. Micro-CHP systems could be also used within new buildings in which a heat pump is used. In this case CHP unit could produce domestic hot water and electricity during the high electricity price.

### *Input profiles*

An on-site electricity demand profile of a building was not investigated. All generated electricity was assumed to feed into the electric grid. This profile could be added to the model and only surplus electricity is fed into the grid. Thus, the transmission and distribution capacity of the grid can be released during peak loads.

The expected real electricity price profile on the liberalized electricity market could be interesting to have in the model. In order to have better economical analysis and optimization results. Additionally, the sensitivity of the fuel price to the optimization should be investigated. The fuel price can change significantly over time and between locations. The changes in the fuel price influence also to the heat price. If the fuel price increases, the heat price can be increased as well. Furthermore, in the sensitivity analysis was seen that the fuel price has the highest impact to the net present value and can change the optimal solution.

### *Optimization*

The optimization was carried out with two systematically varied parameters that were combinations of electric power and storage volume, and electric power and price threshold. For the future work more parameters should be varied at the same time because it is not anymore a solution to simulate a number of possible cases. This multivariable optimization requires the better optimization algorithm which could be a genetic algorithm or direct search in the Matlab global optimization toolbox.

# SOURCES


[1] Kraft-Wärme-Kopplung Change für Wirtschaft und Umwelt-Broschure. The German Association of Combined Heat and Power. 2009, [referred 13.4.2012]. Available: http://www.bkwk.de/aktuelles/Broschur/Broschur_Internet.pdf

[2] Steve N. Spentzas. Benefits and Applications of Small-scale and Micro-CHP Systems. 30 Dec 2009, Cogeneration & Distributed Generation Journal. 34 pgs.

[3] Jeremy Harrison. Micro CHP the big picture. July 2010, Big Picture Publishing. 294 pgs.

[4] Dr. Fabrizio Noembrini. Renewable energy technologies, Cogeneration. Spring semester 2011, ETHZ. 38 pgs.

[5] Robert Beith. Small- and micro combined heat and power (CHP) systems: advanced design, performance, materials and applications. 2011, Woodhead Publishing. 528 pgs.

[6] The European parliament and the Council of the European Union. DIRECTIVE 2004/8/EC OF THE EUROPEAN PARLIAMENT AND OF THE COUNCIL. 21.2.2004, Official Journal of the European Union. [referred 20.4.2012]. Available: http://eurlex.europa.eu/LexUriServ/LexUriServ.do?uri=OJ:L:2004:052:0050:0060:EN:PDF

[7] Martin Pehnt, Michael Colijn. Micro cogeneration: towards decentralized energy systems. 2006, Springer. 346 pgs.

[8] Denny Beyer, Nick Kelly. Modeling the behavior of domestic micro-cogeneration under different operating regimes and with variable thermal buffering. 2008, Energy Systems Research Unit, University of Strathclyde, Glasgow, UK.

[9] Gianfranco Chicco, Pierluigi Mancarella. Distributed multi-generation: A comprehensive view. 11 September 2007, Dipartimento di Ingegneria Elettrica, Politecnico di Torino. April 2009, Renewable and Sustainable Energy Reviews, Pages 535–551.

[10] Jeremy Harrison. Micro combined heat and power [WWW]. 12th February 2012, [referred 31.5.2012]. Available: http://www.microchap.info/INDEX.HTM

[11] Baxi Innotech. Gamma 1.0 [WWW]. [referred 11.4.2012]. Available: http://www.baxi-innotech.de/

[12] Hexis. Galileo Intelligent Wärme. Sauberer strom. [WWW]. [referred 11.4.2012]. Available: http://www.hexis.com/

[13] Ian Knight, Ismet Ugursal. Residential cogeneration systems: review of the current technology. 7 June 2005, International Energy Agency Annex 42. 79 pgs

[14] James Worth Bagley College of Engineering. micro-Cooling, Heating, and Power (m-CHP) Instructional Module. December 2005, Mississippi State University.

[15] A. F. Mills. Basic Heat & Mass Transfer. 1999, Prentice Hall, Inc. 1000 pgs.

[16] Vollrad Kuhn, Jiri Klemes, Igor Bulatov. MicroCHP: Overview of selected technologies, products and field test results. Nowember 2008, Applied Thermal Engineering, pgs. 2039-2048.

[17] Energy Solutions. Plate heat exchangers for energy conservation [WWW]. Engineer Live. [referred 5.6.2012]. Available: http://www.engineerlive.com/Energy-Solutions/Heat_Recovery/Plate_heat_exchangers_for_energy_conservation/22778/

[18] Chris Haslego. Specifying a liquid heat exchanger [WWW]. 7 November 2010, [referred 5.6.2012]. Available: http://www.cheresources.com/content/articles/heat-transfer/specifying-a-liquid-liquid-heat-exchanger

[19] Ekin Bingöl, Birol Kılkıs, Cahit Eralp. Exergy based performance analysis of high efficiency poly-generation systems for sustainable building applications. 29 July 2011, Energy and Buildings 43 (2011).

[20] Hot water association. Performance Specification for Thermal Stores. 21.03.2010. 78 pgs.

[21] Margaret Rouse. Seebeck effect [WWW]. SearchNetworking. December 2008, [referred 6.6.2012]. Available: http://searchnetworking.techtarget.com/definition/Seebeck-effect

[22] International Energy Agency. District Cooling, Balancing the production and demand in CHP. 1999, Novem. 184 pgs.

[23] G. Angrisani, A. Rosato, C. Roselli, M. Sasso, S. Sibilio. Experimental results of a micro-trigeneration installation. 14 January 2012, Aplied Thermal Engineering 38 (2012), pgs 78–90.

[24] Mike Dennis. Solar cooling using ejectors [WWW]. College of Engineering and Computer Science, The Australian National University. 22 December 2009, [referred 6.6.2012]. Available: http://solar-thermal.anu.edu.au/low-temperature/solar-cooling-using-ejectors/

[25] IEA Energy Conservation in Buildings & Community Systems. Annex 42 The Simulation of Building-Integrated Fuel Cell and Other Cogeneration Systems (COGEN-SIM) [WWW]. [referred 1.7.2012]. Available: http://www.ecbcs.org/annexes/annex42.htm

[26] Christoph Zürcher, Thomas Frank. Bauphysik Bau und Energie. 2004, vdf Hochschulverlag AG. 245 pgs.

[27] C.Koroneos, M.Tsarouhis. Exergy analysis and life cycle assessment of solar heating and cooling systems in the building environment. 21 March 2012, Journal of Cleaner Production, September 2012, Pages 52-60.

[28] E4tech. Overview [WWW]. 2010, [referred 31.7.2012]. Available: http://www.e4tech.com/

[29] Lesosai 7.1 software. User guide.

[30] Ralf Dott, Michel Haller, Jorn Ruschenburg, Fabian Ochs, Jacques Bony. Reference Buildings Description of the IEA SHC Task 44/ HPP Annex 38, Subtask

C – Working Group Boundary Conditions. Solar heating & cooling programme, International Energy Agency. 15.12.2011. 32 pgs.

[31] Jérôme Henri Kämpf. On the Modelling and Optimisation of Urban Energy Fluxes [WWW]. Appendix A. Programme doctoral en environnement, ́ECOLE POLYTECHNIQUE FÉDÉRALE DE LAUSANNE. 2009, [referred 31.7.2012]. Available: http://library.epfl.ch/theses/?nr=4548

[32] Arbeitsgemeinschaft für sparsamen und umweltfreundlichen Energieverbrauch E.V.. BHKW – Kenndaten 2001.

[33] Wolfgang Streicher, Richard Heimrath. Structure of the Reference Buildings of Task 26. Solar Combisystems, International Energy Agency. April 2003. 12 pgs.

[34] V. Dorer, Andreas Weber. Energy and $CO_2$ emissions performance assessment of residential micro-generation systems with dynamic whole-building simulation programs. 2009.

[35] Philipp Kräuchi, Viktor Dorer. Energetic and environmental performance evaluation of micro-polygeneration systems for small office buildings. Swiss Federal Laboratories for Materials Testing and Research. April 28 2008.

[36] V. Dorer, R. Weber, A. Weber. Performance assessment of fuel cell micro-cogeneration systems for residential buildings

[37] Stephane Thiers, Bernard Aoun, Bruno Peuportier. Experimental characterization, modelling and simulation of a wood pellet micro-combined heat and power unit used as a heat source for a residential building. Energy and Buildings 42. 25 December 2009.

[38] Ferdinand F. O. Daminabo. A novel 2 $kW_e$ biomass-organic Rankine cycle micro cogeneration system. April 2009.

[39] Christian Nellen, Konstantinos Boulouchos. Natural Gas Engines for Cogeneration: Highest Efficiency and Near-Zero_emissions through Turbocharging, EGR and 3-Way Catalytic Converter. I.C. Engines and Combustion Laboratory, Swiss Federal Institute of Technology ETH Zurich. October 2000.

# APPENDIX A

## A.1 The List of The Model Parameters

The list of the model parameters was set up in order to perform the simulations with physical data on CHP unit.

```
% The list of parameters of the CHP-model

load HeatDemandCase1; % Low heat demand case
load HeatDemandCase2; % High heat demand case
load Exergy;          % Enthalpy and entropy data for look up tables
                      % in exergy analysis
load PES;             % Data for primary energy saving calculation

%% Control
x = 1;                      % Contract driven system ON[1]/OFF[0]
t_period_supplier = 24;     % Time between starts of two intervals [h]
t_running = 11;             % Running time in hours
t_ON_supplier = 80/31/24*100; % Time interval of operation in
                            % percentage of t_period_supplier [h]
t_start_supplier = 18;      % Start time of the first operation
                            % interval [h]
t_period_user = 24;         % Time between starts of two intervals [h]
t_ON_user = 14;             % Sample based for yearly operation
t_ON_user = 58.33;          % Time interval of operation in percentage
                            % of t_period_user [h]
t_start_user = 8;           % Start time of the first operation
                            % interval [h]

%%% PHYSICAL MODEL PARAMETERS
%% Thermal storage
rhoo = 1000;                % [kg/m3] Density of water
c_p_W = 4186;               % [J/kg/K] Specific heat capasity of water
T_upper = 363;              % Upper limit of the thermal storage
V = 4;                      % Thermal storage volume
m_HS = V*rhoo;              % [kg] The mass of water in the thermal
                            % storage
x0=2;                       % Initial value for the height of
                            % the thermal storage
h = fminsearch(@high,x0);   % Minimaze heigh of the thermal
                            % storage in order to calculate minimazed
                            % thermal storage area.

%% Heat losses
T_ambient = 288;            % [K] The temperature in the basement
T_CHP_inside = 333;         % [K] The temperature in the CHP unit 60 C
U_HS = 0.30;                % [W/m2/K] U-value for the thermal
                            % storage surface, 1/U = 1/1000+0.02/15...
                            % ...+0.12/0.038+0.02/15+1/10
                            % --> U = 0.2065
U_CHP = 0.7;                % [W/m2/K] U-value for the CHP unit
```

```
                            % surface, 1/U = 1/25+0.01/15+...
                            % ...0.055/0.038+0.02/15+1/25
                            % --> U = 0.50588
A_CHP = 8.86;               % [m2] Area of the CHP unit (Lichtblick)
A_HS = 2*V/h+pi*h*sqrt(4*V/(h*pi)); % Minimazed thermal storage area

%% The engine
P_mech = 34200000;          % 9.5kW [J]
myy_mech = 0.36;            % Mechanical efficiency of the engine
myy_g = 0.95;               % Efficiency of the generator
myy_e = 0.342;              % Electrical efficiency of the engine

%% Engine cooling heat exchanger
Q_dot_engine = 21600000;    % [J] 6 kW Needed cooling power of
                            % the engine from GT Power simulation
T_EC_out = 365;             % [K] 92 C, the temperature out of the
                            % engine cooling
m_dot_W = 2000;             % kg/h the water mass flow between
                            % the thermal storage and the CHP unit
m_dot_c = 1500;             % kg/h the cooling mass flow of the engine
c_p_c = 4186;               % [J/kgK] Specific heat capacity of
                            % the cooling mass flow
T_EC = 365;                 % [K] 92 C, the temperature out
                            % of the engine cooling
T_EC_in = T_EC_out-Q_dot_engine/((m_dot_c)*c_p_c); % Engine cooling
                            % inlet temperature for exergy analysis

%% Exhaust gas heat exchanger
T_EG = 1053;                % [K] 780 C, The temperature of
                            % the exhaust gas
m_dot_EG = 52;              % [kg/h] The mass flow of the exhaust gas
c_p_EG = 1200;              % [J/kg/K] Specific heat capacity of
                            % the exhaust gas
e_EG_HX = 0.9;              % The efectiveness of the heat exchanger
T_EG_out = 361;             % [K] Exhaust gas temperature after
                            % HX and EGR

%% Economic parameters
LHV = 50100000;             % Lower heating value of natural gas
[J/kg]
Pr_NG = 1.2;                % Natural gas price [CHF/kg]
Pr_BG = 2.2;                % Biogas price [CHF/kg]
Refund = 0.20;              % Refund of electricity [rp/kWh]
OM = 0.04;                  % Operation and maintenance costs
                            % 0.02-0.05 [CHF/kWh]
Pr_Heat = 0.10;             % Contracted heat price [CHF/kWh]
Investment = 1500*P_mech*myy_g; %Investmnet costs
r = 0.07;                   % Discount rate

%% Exergy analysis
W_dot_aux = 0.120;          % [kW] Auxiliary electricity demand of
                            % CHP from the Dachs
T_0 = 303;                  % [K] Environment temperature inside
                            % the CHP
Ex_ratio = 1.04;            % Ratio of standar natural gas fuel
                            % exergy (52.1 MJ/kg) and lower heating
                            % value of natural gas
T_0_environment = 288;      % [K] Temperature of a basement
```

## A.2 CHP model in the Simulink

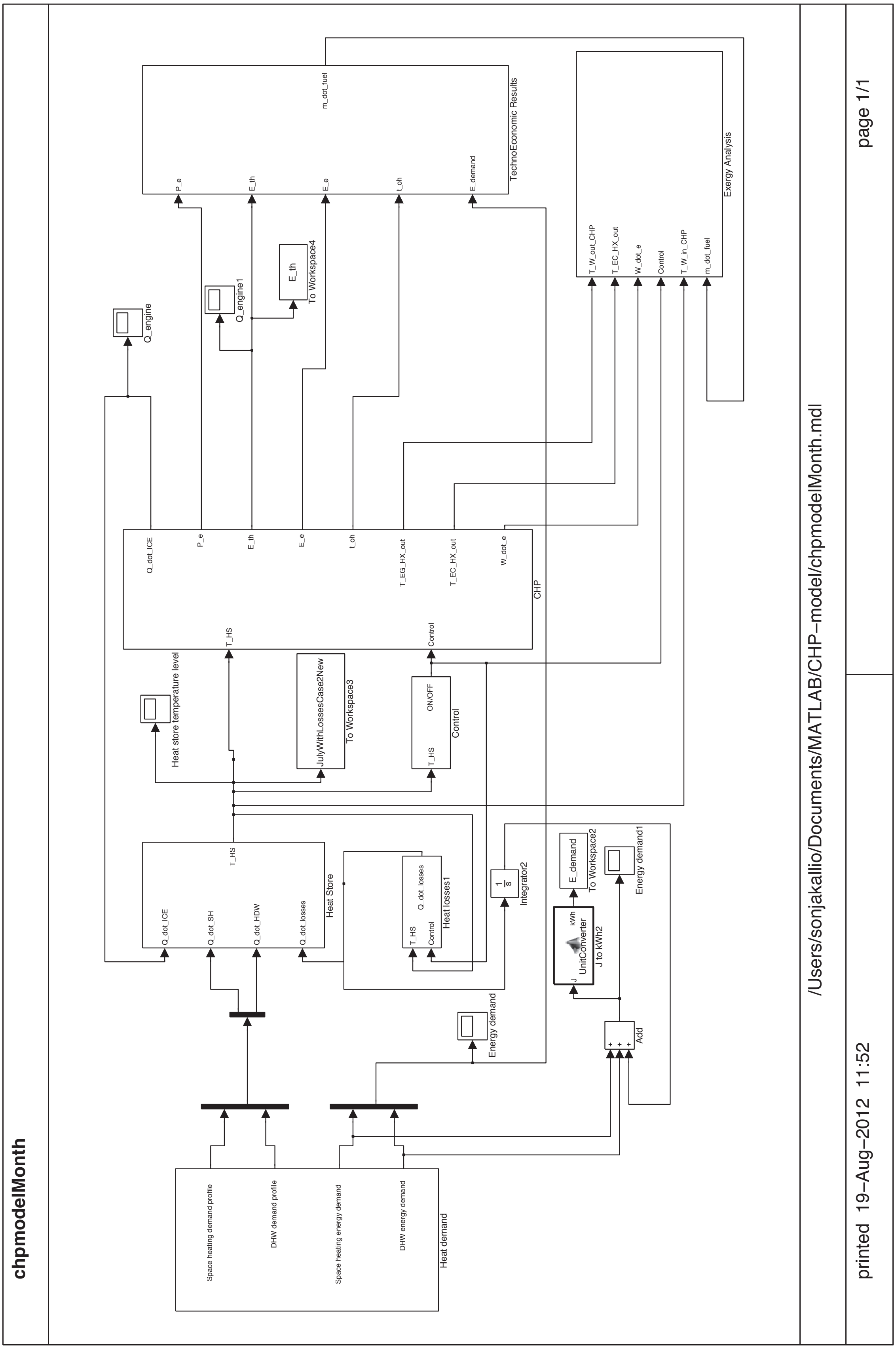


***Figure 1.*** *Overview of CHP model in the SIMULINK*

# APPENDIX B

## Sensitivity analysis

### B.1 Low heat demand case

```
load T_runningNew

% Base case, NPV = 19.911 CHF, Yearly profit = 1279.7 CHF, h_op = 1863
    % Base case:
    % P_mech = 9.5;       % kW
    % P_el = 9.5*0.95;        % kW
    % myy_mech = 0.36
    % myy_e = 0.342
    % P_th = 16.88;       % kW
    % OM = 0.04;          % CHF/kWh_el
    % r = 0.07;           % %
    % Heat_Price = 0.10;  % CHF/kWh_th
    % El_Price = 0.20;        % CHF/kWh_el
    % C_fuel = 0.086;         % CHF/kWh_th
    % I = 1500*P_el;      % CHF
    % Lifetime = 20;      % years

% Sensitivity of OM costs: -20%, -10%, +10%, +20% CHF/kWh_el
%   0.032: NPV = 1444.9 CHF, Yearly profit = 1414.2 CHF
%   0.036: NPV = 732.4 CHF, Yearly profit = 1347 CHF
%   0.044: NPV = -692.57 CHF, Yearly profit = 1212.5 CHF
%   0.048: NPV = -1405.1 CHF, Yearly profit = 1145.2 CHF

% Sensitivity of discount rate r: -20%, -10%, +10%, +20%
%   0.056: NPV = 1629.6 CHF, Yearly profit = 1279.7 CHF
%   0.063: NPV = 789.94 CHF, Yearly profit = 1279.7 CHF
%   0.077: NPV = -687.45 CHF, Yearly profit = 1279.7 CHF
%   0.084: NPV = -1338.3 CHF, Yearly profit = 1279.7 CHF

% Sensitivity of Heat price:
%   +20%, 0.12: NPV = 5989.7 CHF, Yearly profit = 1843.2 CHF
%   +10%, 0.11: NPV = 3004.8 CHF, Yearly profit = 1561.5 CHF
%   -10%, 0.09: NPV = -2965 CHF, Yearly profit = 997.97 CHF
%   -20%, 0.08: NPV = -5949.8 CHF, Yearly profit = 716.22 CHF

% Sensitivity of electricity price:
%   +20%, 0.24: NPV = 7144.8 CHF, Yearly profit = 1952.3 CHF
%   +10%, 0.22: NPV = 3582.3 CHF, Yearly profit = 1616 CHF
%   -10%, 0.18: NPV = -3542.5 CHF, Yearly profit = 943.46 CHF
%   -20%, 0.16: NPV = -7104.9 CHF, Yearly profit = 607.19 CHF

% Sensitivity of fuel price:
%   +20%, 0.1032: NPV = -8938.2 CHF, Yearly profit = 434.14 CHF
%   +10%, 0.0946: NPV = -4459.2 CHF, Yearly profit = 856.93 CHF
%   -10%, 0.0774: NPV = 4499 CHF, Yearly profit = 1702.5 CHF
%   -20%, 0.0688: NPV = 8978.1 CHF, Yearly profit = 2125.3 CHF
```

```
% Sensitivity of investment:
%   1200: NPV = 2727.4 CHF, Yearly profit = 1279.7 CHF
%   1350: NPV = 1373.7 CHF, Yearly profit = 1279.7 CHF
%   1650: NPV = -1333.8 CHF, Yearly profit = 1279.7 CHF
%   1800: NPV = -2687.6 CHF, Yearly profit = 1279.7 CHF
%   1950: NPV = -4041.3 CHF, Yearly profit = 1279.7 CHF

%   4000: NPV = -22543 CHF, Yearly profit = 1279.7 CHF


% Systematically varied parameters
P_mech = 9.5;     %kW
P_el = 9.5*0.95;      %kW
OM = 0.04;            %CHF/kWh_el
r = 0.07;
Heat_Price = 0.10;    % CHF/kWh_th
El_Price = 0.20;      % CHF/kWh_el
C_fuel = 0.086;       % CHF/kWh_th
I = 1500*P_el;        %CHF
Lifetime = 20;        %years

h_op = sum(T_runningNew(1:12,17));

YearlyProfit =h_op*(P_el*El_Price)+28175.1020422*...
    Heat_Price-(h_op*(P_el*OM)+h_op*(P_el/0.342)*C_fuel);

profit = [];

for i = 1:Lifetime
     profit(i,1) = YearlyProfit/(1+r)^i;
end

NPV = -I+sum(profit);
```

## B.2 High heat demand case

```
load T_runningCase2

% Base case, NPV = 6503.6 CHF, Yearly profit = 1891.7 CHF, h_op =
2606.2
    % Base case:
    % P_mech = 9.5;   % kW
    % P_el = 9.5*0.95;   % kW
    % P_th = 16.88;   % kW
    % OM = 0.04;      % CHF/kWh_el
    % r = 0.07;
    % Heat_Price = 0.10;% CHF/kWh_th
    % El_Price = 0.20;   % CHF/kWh_el
    % C_fuel = 0.086;    % CHF/kWh_th
    % I = 1500*P_el;  % CHF
    % Lifetime = 20;  % years

% Sensitivity of OM costs: -20%, -10%, +10%, +20% CHF/kWh_el
%   0.032: NPV = 8497 CHF, Yearly profit = 2079.9 CHF
%   0.036: NPV = 7500.3 CHF, Yearly profit = 1985.8 CHF
%   0.044: NPV = 5506.9 CHF, Yearly profit = 1797.7 CHF
%   0.048: NPV = 4510.2 CHF, Yearly profit = 1703.6 CHF
```

```
% Sensitivity of discount rate r: -20%, -10%, +10%, +20%
%   0.056: NPV = 8883.1 CHF, Yearly profit = 1891.7 CHF
%   0.063: NPV = 7641.9 CHF, Yearly profit = 1891.7 CHF
%   0.077: NPV = 5458 CHF, Yearly profit = 1891.7 CHF
%   0.084: NPV = 4495.8 CHF, Yearly profit = 1891.7 CHF

% Sensitivity of Heat price:
%   +20%, 0.12: NPV = 15103 CHF, Yearly profit = 15103 CHF
%   +10%, 0.11: NPV = 10803 CHF, Yearly profit = 2297.6 CHF
%   -10%, 0.09: NPV = 2203.9 CHF, Yearly profit = 1485.9 CHF
%   -20%, 0.08: NPV = -2095.8 CHF, Yearly profit = 1080 CHF

% Sensitivity of electricity price:
%   +20%, 0.24: NPV = 16471 CHF, Yearly profit = 2832.6 CHF
%   +10%, 0.22: NPV = 11487 CHF, Yearly profit = 2362.2 CHF
%   -10%, 0.18: NPV = 1520.1 CHF, Yearly profit = 1421.3 CHF
%   -20%, 0.16: NPV = -3463.5 CHF, Yearly profit = 950.91 CHF

% Sensitivity of fuel price:
%   +20%, 0.103473: NPV = -6061.2 CHF, Yearly profit = 705.71 CHF
%   +10%, 0.094850: NPV = 221.38 CHF, Yearly profit = 1298.7 CHF
%   -10%, 0.077605: NPV = 12786 CHF, Yearly profit = 2484.7 CHF
%   -20%, 0.068982: NPV = 19069 CHF, Yearly profit = 3077.8 CHF

% Sensitivity of investment:
%   1200: NPV = 9211.1 CHF, Yearly profit = 1891.7 CHF
%   1350: NPV = 7857.4 CHF, Yearly profit = 1891.7 CHF
%   1650: NPV = 5149.9 CHF, Yearly profit = 1891.7 CHF
%   1800: NPV = 3796.1 CHF, Yearly profit = 1891.7 CHF
%   1950: NPV = 2442.4 CHF, Yearly profit = 1891.7 CHF

%   4000: NPV = -16059 CHF, Yearly profit = 1891.7 CHF


% Systematically varied parameters

P_mech = 9.5;      % kW
P_el = 9.5*0.95;       % kW
OM = 0.04;             % CHF/kWh_el
r = 0.07;          % %
Heat_Price = 0.10;     % CHF/kWh_th
El_Price = 0.20;       % CHF/kWh_el
C_fuel = 0.086;        % CHF/kWh_th
I = 4000*P_el;         % CHF
Lifetime = 20;         % years

h_op = sum(T_runningCase2(1:12,19));

YearlyProfit =h_op*(P_el*El_Price)+40586.2774533333...
    *Heat_Price-(h_op*(P_el*OM)+h_op*(P_el/0.342)*C_fuel);

profit = [];

for i = 1:Lifetime
     profit(i,1) = YearlyProfit/(1+r)^i;
end

NPV = -I+sum(profit);
```

# APPENDIX C

## Optimization

```
load HeatDemandCase2
load TotalHeatDailyCase2
load PES;

%% System parameters
x = 1;            % Contract driven system ON[1]/OFF[0]
rhoo = 1000;                % [kg/m3] Density of water
c_p_W = 4186;               % [J/kg/K] Specific heat capacity of water
T_upper = 363;              % Upper limit of the storage
myy_e = 0.35;             % Electric efficiency

%% Economic parameters
LHV = 50100000;             % Lower heating value, natural gas [J/kg]
Pr_NG = 1.2;                % Natural gas price [CHF/kg]
Pr_Heat = 0.10;             % Contracted heat price [CHF/kWh]
r = 0.07;                   % Discount rate

%% Constraints

MaxDailyDemand = max(TotalHeatDailyCase2);
Pth_min = MaxDailyDemand/10;
B = TotalHeatDailyCase2;
B (B == 0)=NaN;
MinDailyDemand = min(B);
Pth_max = MinDailyDemand/(5/60);
NPValue = [];

% Systematically varied parameters
for P_el = 8:1:23
    for i = 20:5:30 % or i = 2000:200:5000

        Threshold = i/100;
        V = 3;             % The storage volume
        m_TS = V*1000;
        Investment = (5783.5*P_el^(-0.3875))*P_el+...
            1200*V+2*((719.45*P_el^(-0.2933))*P_el)*1.2;
        OM = (5.4452*P_el^(-0.2613)*1.2)/100;
        P_th = P_el/myy_e*0.55;

        sim 'chpmodelOptimalFinal.mdl';
        NPV(i, P_el) =  max(NPV1);
        h_operation(P_el,i) = max(h_op);
        ProfitYearly(P_el,i) = max(ProfitY);
    end

end
```